MASTER THESIS

TITLE: Fiber-based Orthogonal Frequency Division Multiplexing Transmission Systems

MASTER DEGREE: Master in Science in Telecommunication Engineering & Management

AUTHOR: Eduardo Heras Miguel

DIRECTOR: Concepción Santos Blanco

DATE: October 27th 2010

Title: Fiber-based Orthogonal Frequency Division Multiplexing Transmission Systems

Author: Eduardo Heras Miguel

Director: Concepción Santos Blanco

Date: October, 26th 2010

Overview

Orthogonal frequency division multiplexing (OFDM) is a modulation technique which is now used in most new and emerging broadband wired and wireless communication systems, because it is an effective solution to intersymbol interference caused by a dispersive channel.

Very recently a number of researches have shown that OFDM is also a promising technology for optical communications, though its application in real optical systems is still under study

In this work, an optical OFDM transmission is simulated in a scenario created by means of *Virtual Photonics Integrated* (VPI) software, which allows the design of many configurations regarding optical communications. The programming of the OFDM coder and decoder has been done with Matlab software, and custom modules have been created in VPI to perform the functions implemented in the codes.

Before that, the basic theoretical concepts of OFDM and the requirements implied by its adaptation to the optical field are explained, along with a brief description of the main VPI modules that have been used in the simulations.

INDEX

INTRODUCTION

Orthogonal frequency division multiplexing (OFDM) is a widely used modulation and multiplexing technology, which is now the basis of many telecommunications standards including wireless local area networks (LANs), digital terrestrial television (DTT) and digital radio broadcasting in much of the world. OFDM is also the basis of most DSL standards, though in this context it is usually called discrete multitone (DMT) because of some minor peculiarities.

Despite the important advantages that OFDM provides and its widespread use in wireless communications, it is only during the last years that it has been considered for optical communications [P1]. The lack of interest in optical OFDM in the past is partly because of the fact that the silicon signal processing power had not reached the point at which sophisticated OFDM signal processing could be performed in a CMOS integrated circuit, and partly because the demand for increased data rates across long fibre distances is quite recent.

Another important obstacle has been the fundamental differences between conventional OFDM systems and conventional optical systems. Table 1 summarizes these differences:

Table 1 Typical OFDM system vs. typical Optical system [P1]

Typical OFDM system	Bipolar	Info carried on electrical field	LO at receiver	Coherent reception
Typical Optical system	Unipolar	Info carried on optical intensity	No LO (laser) at receiver	Direct detection

In typical (non optical) OFDM system, the information is carried on the electrical field and the signal can have both positive and negative values (bipolar). At the receiver there is a local oscillator (LO) and coherent detection is used. In contrast in a typical optical transmission system, the information is carried on the intensity of the optical signal and therefore it can only be positive (unipolar). Generally, no laser is used at the receiver acting as a local oscillator and direct detection rather than coherent detection is used.

An initiative towards the application of OFDM modulation in optical networks is the Accordance (*A Novel OFDMA-PON Paradigm for Ultra-High Capacity Converged Wireline-Wireless Access Networks*), a European research project in which UPC takes part along with other universities and companies from around the continent. Within this collaboration, a new communications system is being developed based on OFDM access technology and protocols.

UPC is in charge of performing simulations and feasibility studies for this low-cost, high-capacity hybrid communications system where optical fibre is used as the transmission channel.

The results described in this Master Thesis will add to the UPC collaboration within the Accordance project.

The goal in this Master Thesis is to study the basis of OFDM systems applied to fibre optic networks, both from an analytical point of view and from a simulation software environment, using the Virtual Photonics Inc. (VPI) software.

The starting point will be the main theoretical concepts that distinguish OFDM from other modulations, making special emphasis in the peculiarities of its implementation in optical fibre systems. Then, the main optical OFDM characteristics are studied and simulated through built-in demonstrations available at VPI software.

These demos provide a convenient way to study some basic features of OFDM optical transmission systems, but their use is limited to specific scenarios.

In order to obtain a flexible platform for tests and exploration of optical OFDM systems a new setup will be built by exploiting the VPI Cosimulation functionality, which allows the use of other simulation software to operate as specific modules within VPI.

Thus, in this Master Thesis two VPI modules have been created based on Matlab programs to perform the OFDM modulator and demodulator inside the VPI optical OFDM transmission system simulation setup.

While VPI's built-in demonstrations are quite rigid in terms of configuring different simulation setups, the use of the Matlab code in the customized simulations allows the user to perform different configurations for the transmission scenario which are impossible to obtain from the demos.

The document is organized as follows: In Chapter I, the basic concepts of OFDM are described, so it can be understood how an OFDM system works and which is the role of each of its parts. After that, the most typical optical configurations in which OFDM can be implemented are listed in Chapter II, giving emphasis to those related with the simulations performed in the last part.

In Chapter III, the basic parameters of VPI software are introduced, and the required steps to create a new simulation are described. Moreover, two optical OFDM demonstration scenarios provided by VPI are analyzed in detail, so it can be seen how the concepts explained in the previous chapters are applied to a simulation environment.

The VPI built-in demos studied in Chapter III will serve as the base for the customized simulations in Chapter IV, where an insight is given into the main modules created in VPI for the customized demos. The resulting scenarios will perform the same functions as the built-in demos in VPI, though this time the user will be able to change any parameter of the simulation in order to see its effect on the transmission results. Also, some improvements have been added to the original functions in the demos, allowing a better understanding of each of the simulation stages and results.

Conclusions and future lines are developed in Chapter V. This work will set the basis for upcoming optical OFDM simulations studies, hoping to serve as a source of inspiration to other contributions to the subject. For this purpose, propositions to improve the current work as well as the study of other available optical OFDM techniques to explore are given as a future possibility.

Furthermore, 4 Annexes are attached, which are referred along the work. They contain complementary theoretical information, as well as secondary configurations for possible simulated scenarios. The last of them shows the Matlab code used in the simulations.

CHAPTER I - OFDM BASICS

I.1. General idea

Frequency Division Multiplexing (FDM) is a technique where the main signal to be transmitted is divided into a set of independent signals, which are called subcarriers in the frequency domain. Thus, the original data stream is divided into many parallel streams (or channels), one for each subcarrier. Each subcarrier is then modulated with a conventional modulation scheme, and then they are combined together to create the FDM signal.

In an FDM transmission, the receiver needs to be able to independently recover each of the subcarriers and therefore these signals need to fulfil certain conditions. For instance, they can have nonoverlapping spectra so that a bank of filters tuned to each of the different subcarriers can recover each of them independently. However, practical filters require guard bands between the subcarrier bands and therefore the resulting spectral efficiency is low.

If the subcarrier signals fulfil the orthogonality condition (which will be introduced by expression I.2) their spectrum can overlap, improving the spectral efficiency. This technique is known as orthogonal FDM or OFDM.

To see the main advantages offered by OFDM, it is useful to think about a set of packets which are transported in a truck. The whole set of packets can either be carried by one big truck or by several smaller ones, as shown in Figure I.1:

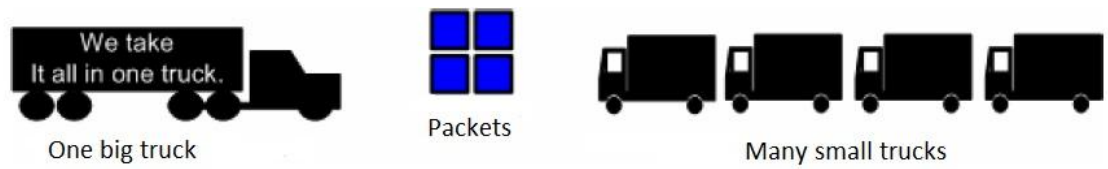

Fig. I.1 Data transported as a set of packets [P18]

Suppose that each small truck uses a different road, where every available path has the same length and all the trucks drive at the same speed. If an accident happens in one of the roads and it gets blocked, part of the packets will not be received with the rest at the destination. On the other hand, if all the packets are transported by a big truck that drives on the same road where the accident happens, the whole shipment will get stuck and will not arrive to destination.

For an OFDM signal transmission, each small truck represents a subcarrier, and the roads where data is going to be carried are an analogy of the different frequencies at which each subcarrier is going to be transmitted. Moreover, each packet containing goods represents the modulated portion of data to be carried by a subcarrier, which is called an information symbol.

Then, continuing with the analogy, it should be more difficult to drive a big truck than a smaller one, meaning that transmission impairments will have a bigger impact on the single carrier signal since, in the transmission case, it will have to be transmitted at a higher data rate.

On the other hand, for a transport company it is more expensive to contract N small trucks than a big one. In the transmission case, this is equivalent to the difference between using N emitter-receiver sets and using a single one.

Figure I.2 shows the OFDM modulation idea schematically. A bit sequence with rate R is parallelized into N different channels, each with a different frequency. The total bitrate is distributed in equal parts over each channel at a rate R/N. The data in each channel will be mapped to represent an information symbol and then multiplied by its corresponding frequency. The summation of these parallel information symbols will form one OFDM symbol.

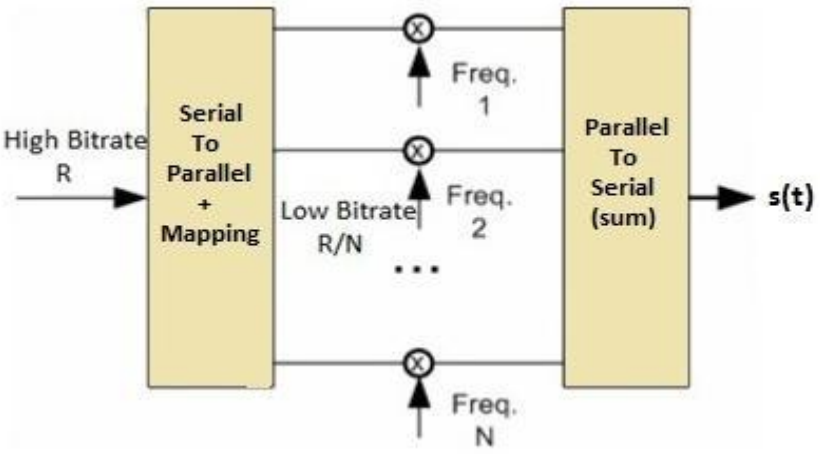

Fig. I.2 Frequency division multiplex: Analogue transmitter

Each OFDM symbol has thus a duration $T_s = N/R$. Hence, the OFDM signal in the time domain s(t) can be expressed as a summation of each information symbol $c_{i,k}$ being carried in the *k*th subcarrier within the *i*th OFDM symbol. Depending on the modulation used for the subcarriers, this superposition of subcarriers forming s(t) can result in complex values, though this case will not be taken into account yet. Then, with the OFDM symbol having a period T_s:

$$s(t) = \Re\left\{\sum_{i=-\infty}^{\infty}\sum_{k=0}^{N-1} c_{i,k}\, e^{j2\pi f_k t}\cdot P(t - iT_s)\right\} \qquad \textbf{(I.1)}$$

Where P(t) is an ideal square pulse of length T_s, the number of subcarriers is represented by N and f_k is the subcarrier frequency. This frequency has to fulfil the orthogonality condition:

$$f_k = k\frac{1}{T_s} \qquad \textbf{(I.2)}$$

This means that each subcarrier must be separated from its neighbours by exactly 1/T_s, so each subcarrier within an OFDM symbol has exactly an integer number of cycles in the interval T_s, and the number of cycles differs by exactly one, as depicted in Figure I.3. This way, orthogonality between subcarriers is achieved. This property can be explained for any couple of subcarriers by the following expression:

$$\int_{-T/2}^{T/2} \cos\left(\frac{2\pi nt}{T}\right) \cos\left(\frac{2\pi mt}{T}\right) dt = 0 \quad , \quad m \neq n \qquad \textbf{(I.3)}$$

If m and n are different natural numbers, the area under this product over one period is zero. The frequencies of these waves are called harmonics and for them the orthogonality condition is always fulfilled.

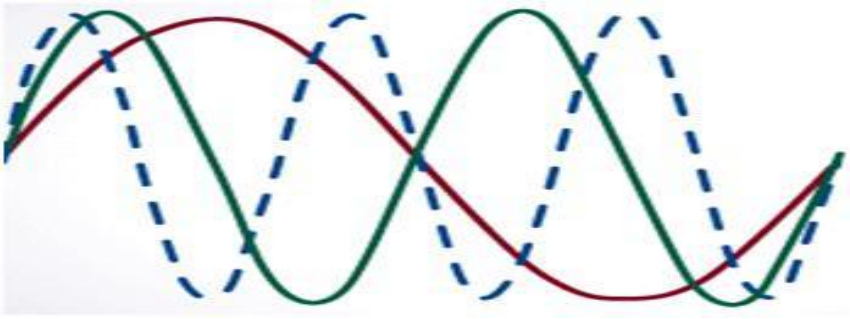

Fig. I.3 Time domain subcarriers within an OFDM symbol [W2]

Figure I.3 shows three subcarriers from one OFDM symbol in a time domain representation. In this example, all subcarriers have the same phase and amplitude, but in practice the amplitudes and phases may be modulated differently for each subcarrier.

In expression (1.1) the OFDM symbol is ideally multiplied by a square pulse P(t), which is one for a T_s-second period and zero otherwise. The amplitude spectrum of that square pulse has a form $sinc(\pi ft)$, which has zeros for all frequencies *f* that are an integer multiple of 1/T_s. Then, as shown in Figure I.4, an OFDM symbol spectrum consists of overlapping sinc functions, each one representing a subcarrier, where at the frequency of the k*th* subcarrier all other subcarriers have zeros.

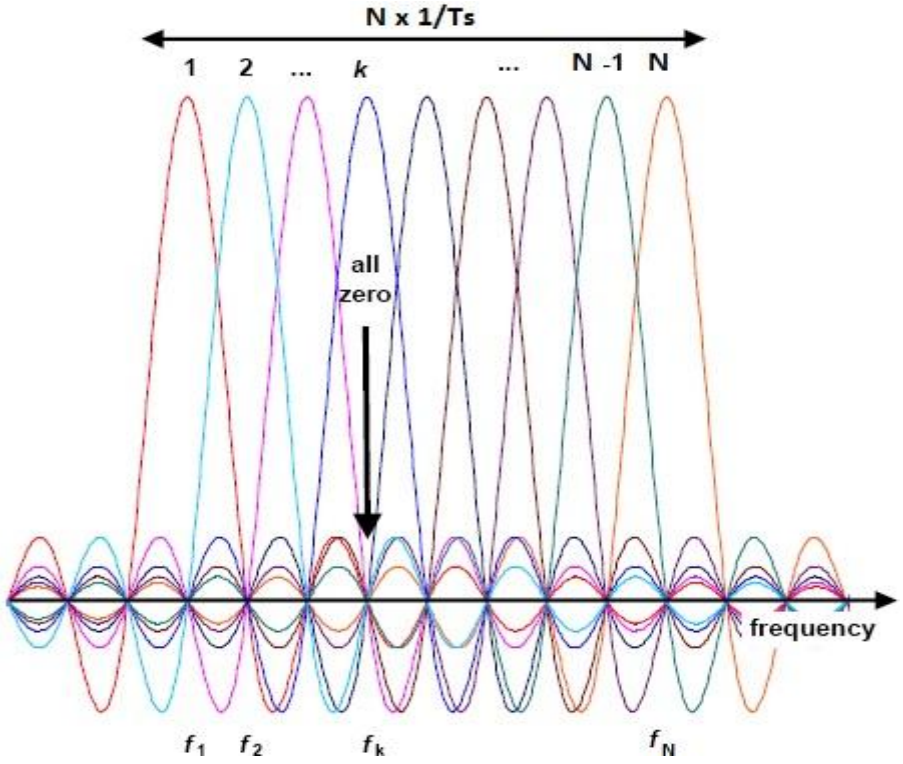

Fig. I.4 Spectrum of an OFDM symbol with overlapping subcarriers [P2]

Note that each subcarrier is centred at f_k and separated by 1/Ts from its neighbours. When this happens, the orthogonality condition is being fulfilled so a great spectral efficiency for the transmission is achieved. This way, the subcarriers can be recovered at the receiver without intercarrier interference (ICI) despite strong signal spectral overlapping, by means of the orthogonality condition (1.3) using a bank of oscillators and low-pass filtering for each subcarrier, as shown in Figure I.5

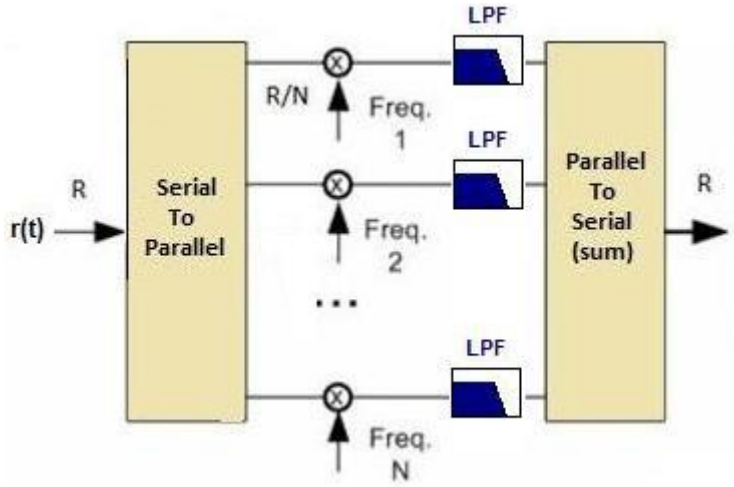

Fig. I.5 Frequency division multiplex: Analogue receiver

Note that many analogue components are needed in case of using a large number of subcarriers. This factor gives rise to a tradeoff between the desire to

use as many subcarriers as possible to make the OFDM signal stronger against transmission impairments, and the system complexity associated to the use of analogue components, especially when many of them are needed.

In single carrier systems, the symbol period is given by the reciprocal baud rate 1/R. Since in multicarrier systems such as OFDM the symbol period is N times longer, the effect of channel dispersion is typically lower and the inter-symbol interference (ISI) decreases. Moreover, as it will be seen in the next section, ISI can be almost eliminated by introducing a guard time in every OFDM symbol such that most of the dispersion caused by a multipath channel remains within the guard interval.

It will also be explained later that in the guard time, the OFDM symbol is cyclically extended to avoid generating ICI. In single-carrier systems ISI occurs and can only be compensated by using complex equalizers at the receiver. In a multicarrier system, no equalization to overcome ISI is required and only the amplitude and phase of each subcarrier need to be corrected according to the channel frequency response. This is simply done by one complex-valued multiplication per subcarrier, which is in fact a single-tap equalization.

I.2. Digital generation of subcarriers

I.2.1. Fast Fourier Transform

Following the last section's analogy, the more trucks are used to transport the load, the fewer packets are going to be carried by each one, the easier it is for each truck to complete the journey, and the less load is going to be lost in case of an accident. Then, it can be said that in an OFDM transmission a large number of subcarriers is desirable so that the minimum possible quantity of data is lost in case of any non-ideality occurring in the transmission channel. This effect is shown in Figure I.6:

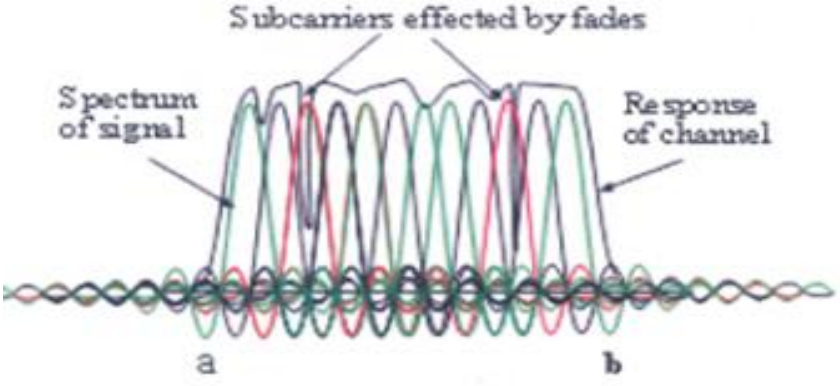

Fig. I.6 OFDM subcarriers affected by a fading channel [P18]

However, creating an OFDM signal with a large number of subcarriers following the analogue method presented before leads to an extremely complex

architecture involving many oscillators and filters at both the transmit and receive ends. In present-day OFDM transmissions, though, this complexity is reduced by transferring it from the analogue to the digital domain.

To see this, take Equation (I.4), where just one OFDM symbol of the signal s(t) in (I.1) is sampled at an interval of T_s/N. Then, the n_{th} sample of s(t) becomes:

$$s(nT_s/N) = \sum_{k=0}^{N-1} c_k \, e^{\frac{j2\pi f_k n T_s}{N}} = \sum_{k=0}^{N-1} c_k \, e^{\frac{j2\pi kn}{N}} = \mathcal{F}^{-1}\{c_k\} \qquad \textbf{(I.4)}$$

Where $\mathcal{F}$ is the Fourier transform, and n ∈ [1,N]. Thus, it can be said that the discrete value of the transmitted OFDM signal s(t) is merely a simple N-point inverse discrete Fourier transform (IDFT) of the information symbol c_k. The same case can be applied at the receiver, where the received information symbol will be a simple N-point discrete Fourier transform (DFT) of the received sampled signal.

This superposition of independent modulated subcarriers is typically performed by the inverse fast Fourier transform (IFFT) where the input channels are spaced equivalently according to Expression I.2. In fact, IFFT/FFT blocks in an OFDM system are mathematically equivalent versions of an IDFT and a DFT of the transmitted and received OFDM signal, with the advantage of providing lower computational implementation.

Because of the orthogonality property, as long as the channel is linear, the OFDM receiver will calculate the spectrum values at those points corresponding to the maximum of individual subcarriers. Then, the received subcarriers can be demodulated through an FFT operation without interference and without the need for analogue filtering to separate them, which makes OFDM not only efficient but also easy to implement in practical transmission systems.

Hence, it can be said that the modulated OFDM signal can be obtained by performing the IFFT operation to the symbols to transmit and then using a DAC to convert the digital signal into an analogue signal at a sampling rate *Ts*.

Ideally, this D/A conversion should convolve each temporal sample by a sinc function. This ideal shaping is translated into a perfectly rectangular filter that removes the alias in the frequency domain, as shown in Figure I.7:

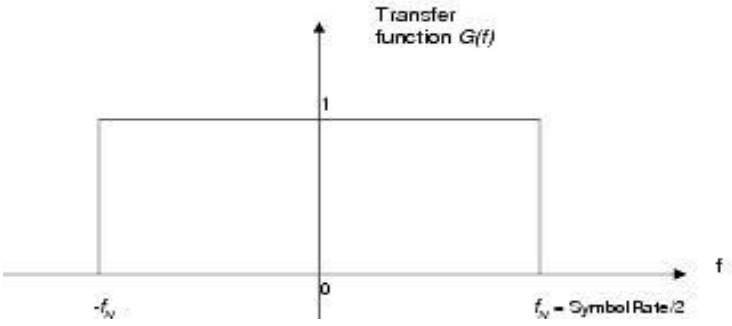

Fig. I.7 Ideal filter at the DAC [VPI]

Where f_N is the Nyquist frequency, which will be the highest frequency component of the OFDM signal. This ideal filter will remove the alias generated due to the sampling process, leaving the fundamental signal untouched.

The contribution of the different sinc pulses at each of the samples of the OFDM symbol results in a perfect square pulse of the OFDM symbol, and each of the subcarriers would be represented by a perfect sinc function in the frequency domain.

Figure I.8 shows a very basic schematic for an OFDM transmitter where subcarriers are modulated in the digital domain by means of an IFFT. The transformed symbols at the output of the IFFT block are then serialized and converted into an analogue signal before transmitting them to the channel. For simplicity, some other blocks have been omitted, though they are going to be described during this chapter.

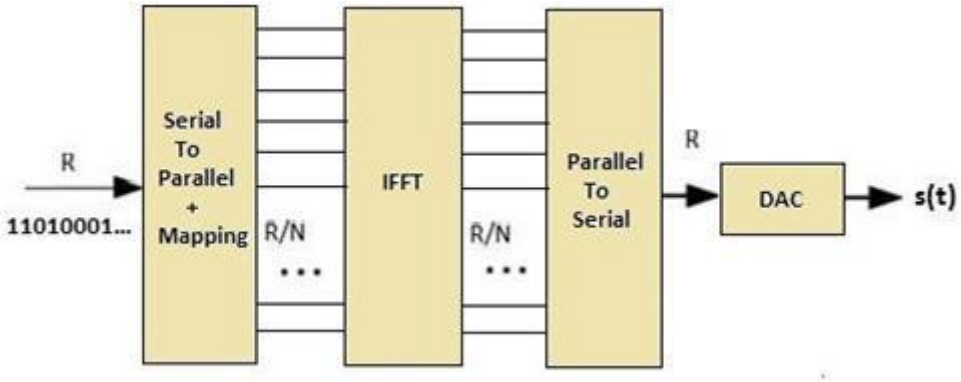

Fig. I.8 Use of an IFFT block to modulate an OFDM signal

In a similar way, the subcarriers forming the received signal r(t) are demodulated by an FFT operation after being analogue to digital (A/D) converted and parallelized to form the FFT block inputs, as shown below.

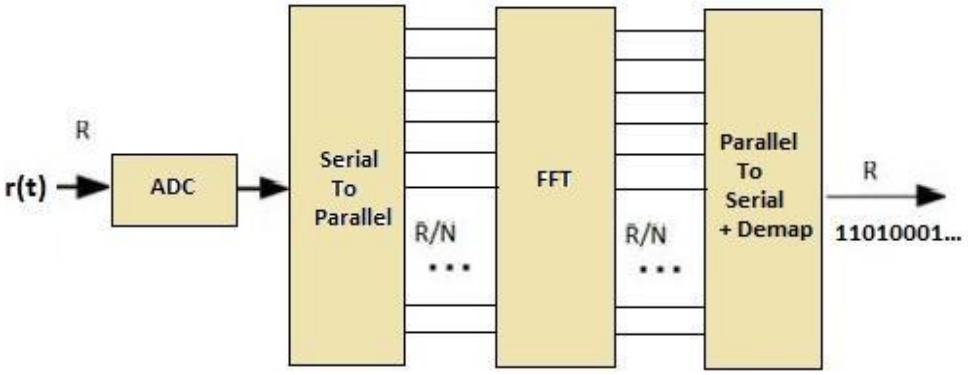

Fig. I.9 Use of an FFT block to demodulate an OFDM signal

In order to understand the concepts that are going to be explained in the next sections, it is useful to know which frequencies of an OFDM signal are represented in each branch of an IFFT operation. Figure I.10 shows a schematic of the IFFT block, where $x_1 \ldots x_N$ are the input sequence symbols from subcarrier 1 to the total number of subcarriers N, and $y_1 \ldots y_N$ is the corresponding output sequence. Moreover, the frequency domain OFDM symbol generated at the IFFT output is depicted. The inverse procedure can be applied to the FFT block at the receiver end.

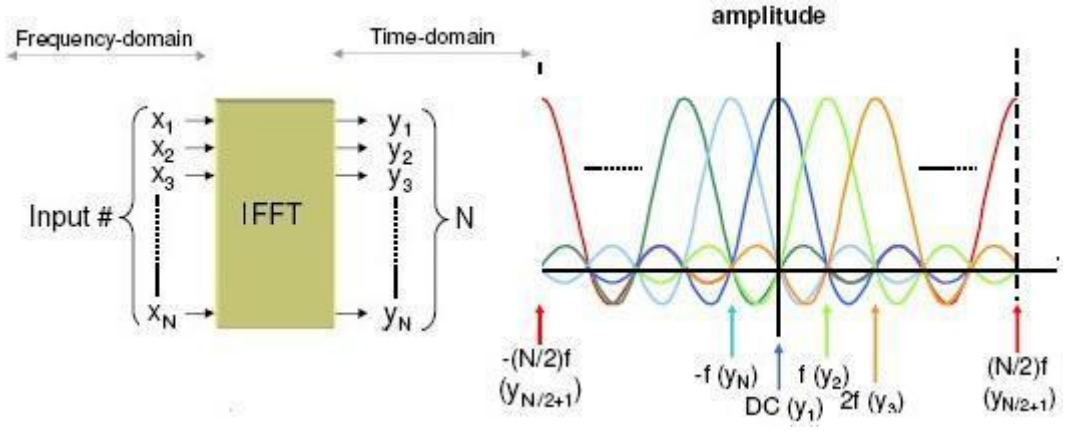

Fig. I.10 IFFT block and the frequency domain OFDM symbol at its output [P4]

The first output channel (y_1) is located at DC, so it is not used for modulation because carrier leakage of the modulator disturbs the quality of this channel and it would put stringent requirements on the low-pass characteristics of all electronic (and also optic) components.

Furthermore, in a complex valued IFFT the first half of the rows corresponds to the positive frequencies while the last half corresponds to negative frequencies. Thus, the so called "Nyquist channel" is located at $y_{Nc/2+1}$, which corresponds to the highest frequency that the subsequent digital-to-analogue converter can modulate: the Nyquist frequency (f_N), or half the sampling frequency f_s according to the sampling theorem.

In a practical system, if the superposition of subcarriers results in complex valued time domain signals, two D/A converters may be applied in parallel for conversion of the real and imaginary IFFT output, though other techniques like the imposition of Hermitian symmetry among samples can be applied in order to have a perfect real IFFT output, as explained in Annex A.

I.2.2. D/A and A/D conversion

As it can be seen from figures I.8 and I.9, a digital-to-analogue converter (DAC) is needed to convert the discrete value of s_n (n_{th} sample) to the continuous analogue value of s(t), and an analogue-to-digital converter (ADC) is needed to convert the continuous received signal r(t) to discrete sample r_m.

In order to build a real system, the fact of being able to use commercial off-the-shelf converters at both ends of the transmission scheme becomes one of the main issues. This is why many techniques are available to take advantage from the digital signal processing stages and simplify the analogue processing, lowering the requirements for both the DAC and the ADC.

I.2.2.1 Pulse shaping

Inside the DAC, symbols are applied to a transmit filter, which produces a continuous-time signal for transmission over the continuous-time channel. A simple transmit filter has a rectangular impulse response, shown in figure I.11, where a symbol sequence using 2 bits per symbol and its corresponding continuous-time signal are also represented.

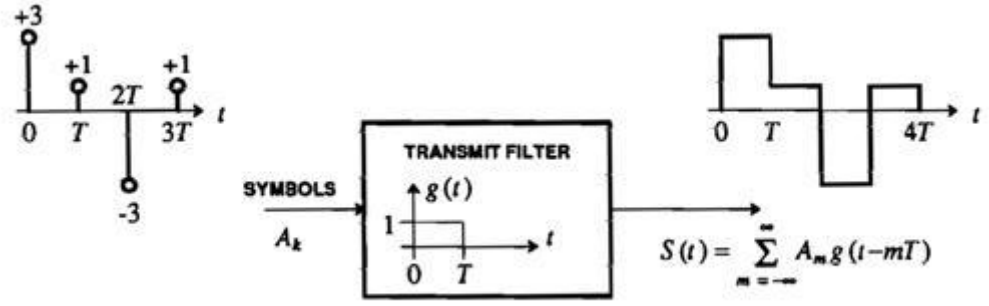

Fig. I.11 Rectangular impulse response [B6]

The impulse response *g(t)* of the transmit filter is called the pulse shape. The output of this filter is the convolution of the pulse shape with the symbol sequence, so the resulting signal can be interpreted as a sequence of possibly overlapped pulses with the amplitude of each determined by a symbol.

An ideal low-pass filter as the one represented in Figure I.7 has a sinc function impulse response with equidistant zero-crossings at the sampling instants and hence no ISI. However, this ideal filter is not realizable.

A practical extension is a raised cosine characteristic fitted to the ideal low-pass filter, which is a commonly used pulse shape in OFDM. Its transfer function is given by expression I.5:

$$For\ \ 0 \le |f| \le \frac{1-\alpha}{2T_s} \ \rightarrow\ \ G(f) = 1$$

$$For\ \frac{(1-\alpha)}{2T_s} \le |f| \le \frac{(1+\alpha)}{2T_s} \ \rightarrow\ \ G(f) = 0.5 \cdot \left(1 - sin\left[\left(\frac{\pi T_s}{\alpha}\right) \cdot \left(|f| - \frac{1}{2T_s}\right)\right]\right) \quad \textbf{(I.5)}$$

Here, T_s is the symbol period and α is the roll-off factor, defined as the ratio of excess bandwidth above f_N. When α = 1 the bandwidth is doubled over the bandwidth when α = 0. The impulse response of the raised cosine filter used in

VPI for α = 0 and α = 0.5 is shown in figure I.12 Note that the length is reduced at the expense of increased bandwidth.

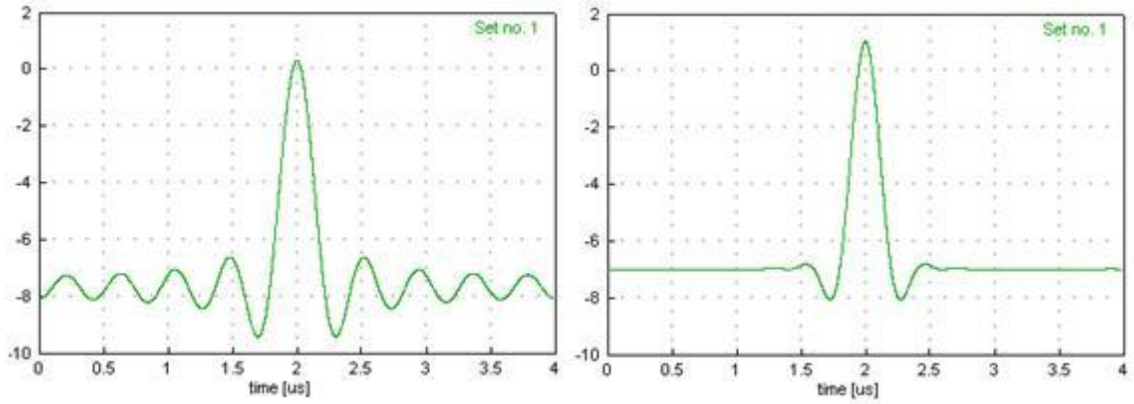

Fig. I.12 Impulse response for the raised cosine for α = 0 and α = 0.5 [VPI]

I.2.2.2 Oversampling by means of zero padding

Before giving the OFDM signal its corresponding shape, the values at the output of the IFFT representing the analogue signal to transmit have to be sampled by the DAC. By sampling them at a rate of $1/T_S$, the aliases produced by the sampling process would be right next to the main OFDM signal, making it impossible for any practical filter to separate them.

However, padding the correct positions of the IFFT input sequence with zeros can help to shift the aliases away from the OFDM signal, as shown in Figure I.13. This technique will be referred during this work as *oversampling* or *frequency zero padding*.

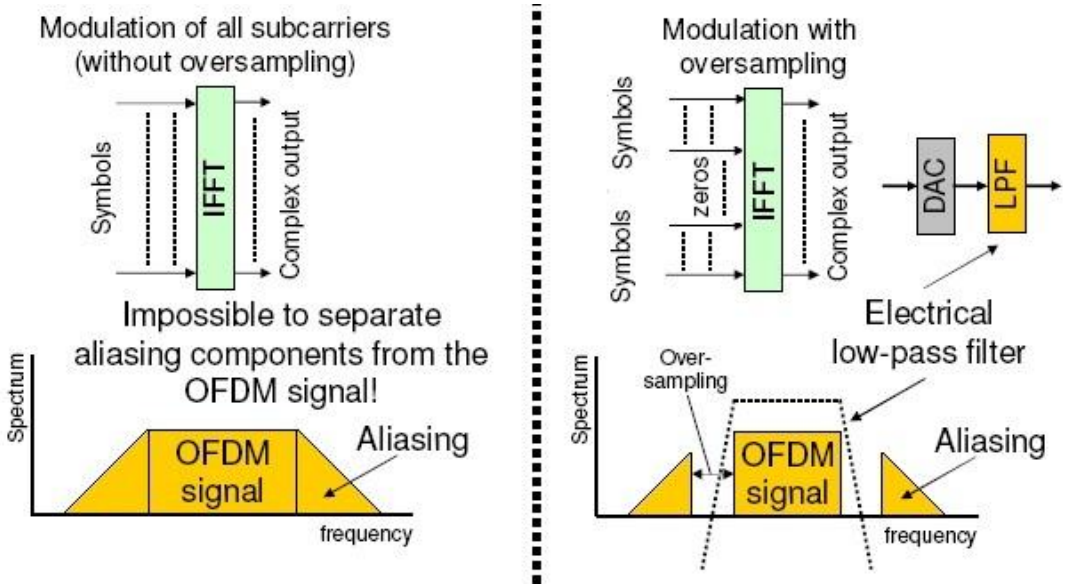

Fig. I.13 Oversampling used to shift aliases away [P4]

Note that the zero-padded frequencies are those around the Nyquist channel. This ensures the zero data values are mapped onto the highest positive frequencies and lowest negative frequencies (those around $\pm f_N$), while the nonzero data values are mapped onto the subcarriers around 0 Hz, preserving the main OFDM signal.

The reason why the aliases are shifted away from the OFDM signal can be understood by looking at Figure I.14. In the upper case no oversampling is applied, while the lower case represents a typical *2xoversampling* transmission, where half of the IFFT inputs (those in the centre around the Nyquist frequency) have been used for zero padding in the same way as in Figure I.13. In this case, the number of IFFT inputs has to be doubled in order to allocate the same number of OFDM subcarriers as before.

The input sequences of the IFFT are represented in the left side. After performing the IFFT operation, the sampled signal is obtained (centre figures). Note that twice the number of samples is used to represent that signal in the case of using oversampling. The D/A conversion carried out in the DAC is understood as temporal extrapolation / frequency-alias filtering of this sampled signal.

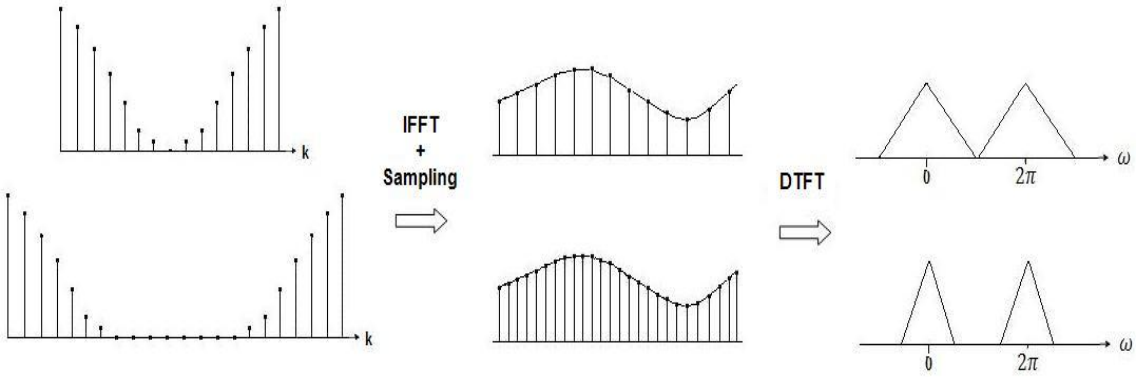

Fig. I.14 Aliases moving away due to zero padding

If the spectrums of these analogue signals are represented by applying the Discrete-time Fourier transform (DTFT), it can be seen how the oversampled signal spectrum becomes narrower.

This narrowing effect is produced because the high frequencies are zero padded, though the same quantity of information is still being added over the same bandwidth, so the spacing between subcarriers is decreased.

This will cause a frequency separation between the maximum frequency of the OFDM signal and the minimum frequency of the subsequent alias. Thus, the requirements of the filter needed to recover the original signal will not be too high, enabling the choice of a non-expensive DAC for the system.

This technique will be applied in the simulations performed in chapter IV by using the same number of IFFT inputs for information symbols and for zeros.

For instance, a 128 IFFT/FFT size will be used to apply the oversampling technique when the information is coded into 64 OFDM subcarriers.

I.2.3. Cyclic Prefix

As mentioned before, by dividing the data stream into N subcarriers, the symbol period is made N times longer, which also reduces the delay spread or chromatic dispersion relative to the symbol time. To avoid interferences between OFDM symbols (meaning null ISI) and also eliminate ICI, a guard time is introduced for each OFDM symbol after the IFFT, which is cyclically extended within this guard time, as shown in Figure I.15. This cyclical extension is called the cyclic prefix (CP).

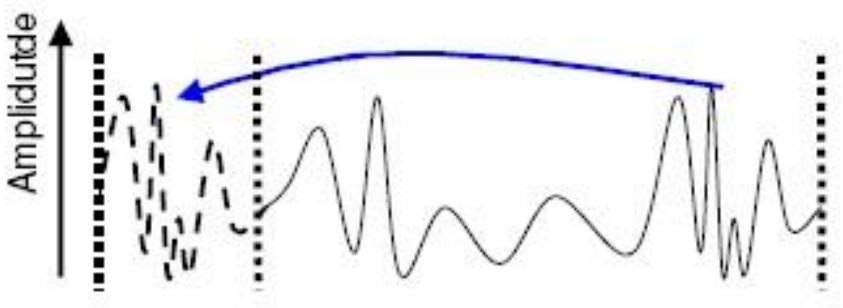

Fig. I.15 Cyclic prefix in an OFDM symbol (time domain sequence) [P4]

Due to the insertion of this prefix, the symbol duration is extended without transmission of additional data, leading to a reduction of the net bitrate by a factor of $^{T_s}/_{T_s + t_{CP}}$, where t_{CP} is the extension of the symbol period due to the cyclic prefix . However, the simple equalization resulting from the elimination of both ISI and ICI from the received signal is a major advantage which deserves giving up a bit of transmission efficiency.

As long as the cyclic prefix duration is equal or longer than the maximum delay caused by the channel impairments, the effect of one symbol over its neighbours will be limited to its cyclic prefix corruption, without damaging the information part. The effect of a cyclic prefix length shorter than the drift caused by chromatic dispersion in optical OFDM is shown in Figure I.16, where an OFDM signal is represented with different colours for each subcarrier:

It is true that null ISI could be achieved with the introduction of any temporal guard interval, but only the cyclic prefix can guarantee null ICI. This fact is mathematically demonstrated in [P1].

It is important to mention that the introduction of cyclic prefix entails the loss of orthogonality in the transmitted symbols, though this will not be a problem, as this cyclic extension will be eliminated in the receiver recovering the original orthogonality [B7].

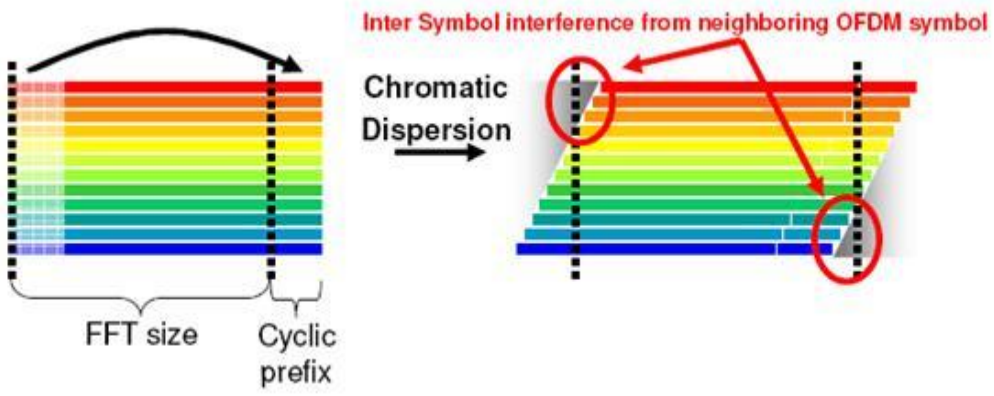

Fig. I.16 ISI because an insufficiently large CP [P4]

Another interesting effect can be observed in the OFDM signal spectrum: when the temporal duration of the OFDM symbol is increased due to the CP insertion, the corresponding sincs are narrower in frequency than before, so their maximums don't match up exactly with their neighbours' nulls and the resulting spectrum is not plain any more, but it suffers from rippling. This effect is dealt with in Annex B, where the consequences of adding a CP on the signal spectrum are discussed.

In the simulations performed with VPI, the cyclic prefix parameter will be determined by a percentage of the total number of symbols at the output of the IFFT block. The typical values for a cyclic prefix in an OFDM system range from 10 to 20%.

In view of all the above, the final schematic for the OFDM signal generation could be represented by the one in Figure I.17, where oversampling by means of frequency zero padding and a temporal cyclic prefix are added in the following order:

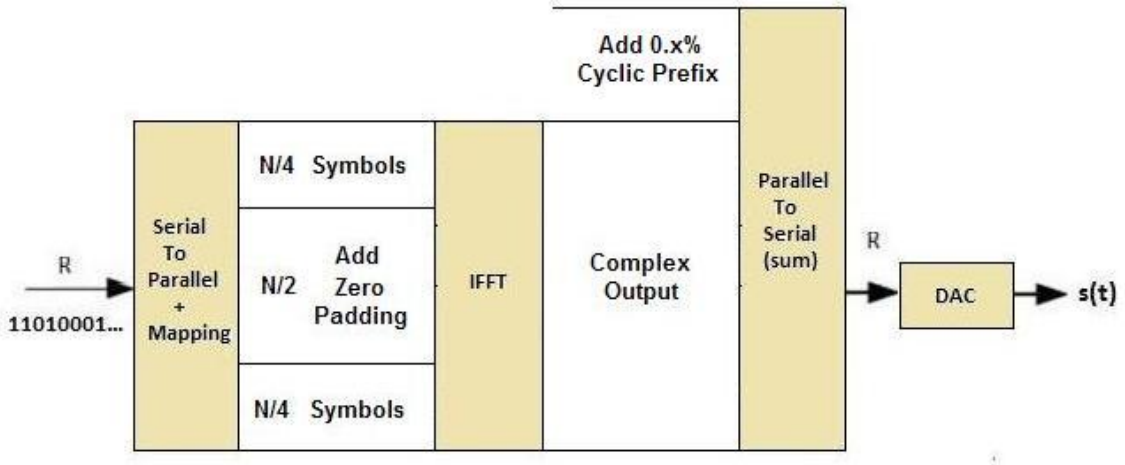

Fig. I.17 OFDM signal generation schematic

At the receiver end, zero padding and cyclic prefix are extracted in the opposite order in which they were inserted at the transmitter, as shown in Figure I.18:

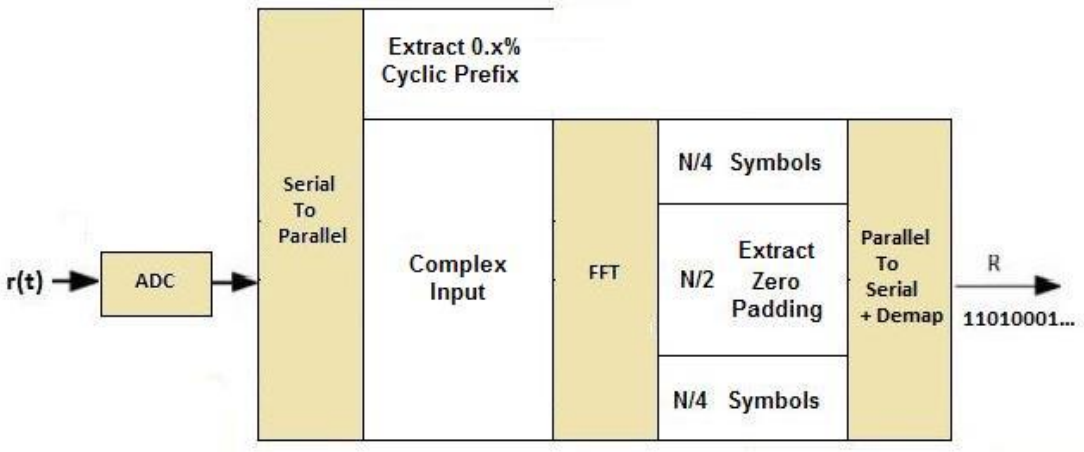

Fig. I.18 OFDM signal reception schematic

Now that the electrical OFDM signal is ready to be transmitted, it needs to be re-modulated over an optical carrier to be transmitted through an optical channel. For this purpose, different methods of optical modulation and detection are presented in Chapter II, but before that, Section I.3 will serve as an introduction to the used method in the optical OFDM simulations.

I.2.4. Mapping and demapping

It has been said before that the bit stream coming from the signal source needs to be converted into many parallel data pipes, each mapped onto corresponding information symbols for the subcarriers within one OFDM symbol.

The incoming bits to send have to be packed and mapped to a symbol generally using a complex modulation format such as for example M-QAM or QPSK.

For the 4-QAM modulation used in this work's simulations, the incoming serial data uses two bits to create each of the 4 possible complex-valued QAM symbols (or information symbols), as it can be seen from Figure I.19:

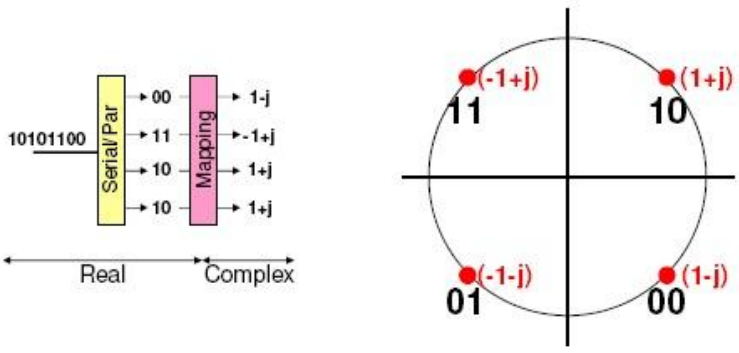

Fig. I.19 4-QAM mapping [P4]

The inverse procedure will take place at the receiver side: each complex-valued received symbol will be demapped and the obtained symbol sequence will be serialized to (ideally) obtain the original bit stream from the transmitter. However, because data is not going to be transmitted over an ideal channel, a decision of which constellation point is received has to taken before demapping. This process is called slicing, and it is depicted in Figure I.20:

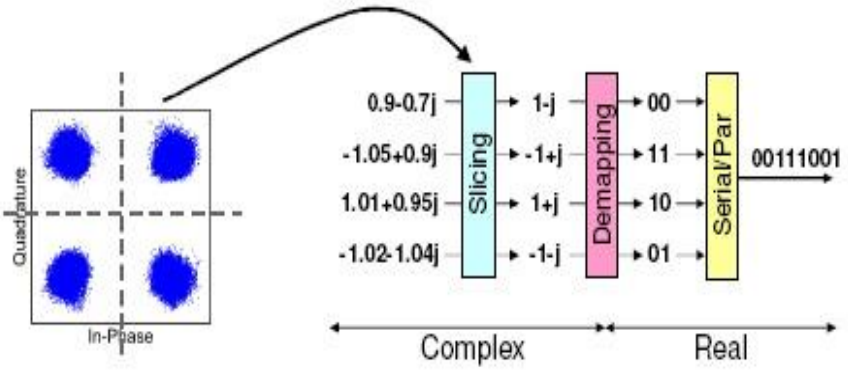

Fig. I.20 4-QAM slicing and demapping [P4]

The most commonly used method for slicing is a hard decision threshold, though many other methods have been introduced to perform it with soft decision thresholds at a cost of an increased system complexity.

I.3. Gap generation

As it can be seen in Chapter II, when the conventional opto-electrical direct-detection technique is used in the receiver, due to the square-law characteristic unwanted mixing products among the subcarriers may interfere with other subcarriers in the electrical domain.

Also, when using the conventional intensity modulation technique, replicas of the signal appear on the optical spectrum. In order for these replicas not to overlap with the OFDM signal, guard bands with respect to the optical carrier are also required. This is described in more detail in Chapter II.

To prevent these interferences a frequency gap may be allocated between the optical carrier and the OFDM spectrum, which width at least equals that of the signal's bandwidth.

In this section two strategies to create a spectral gap between the carrier and the OFDM spectrum are described, namely the RF upconversion and the low-frequency zero padding.

I.3.1. RF upconversion

In the RF upconversion technique, the complex baseband OFDM signal s(t) generated with QAM subcarrier modulation as depicted in Figure I.17 is upconverted into a passband signal centred at an intermediate frequency (IF), as shown in Figure I.21.

Note that the cyclic prefix stage has been omitted in this schematic, though it will be used in the simulation. Also, note that two DACs are used to process the real and imaginary parts of the signal after the IFFT operation.

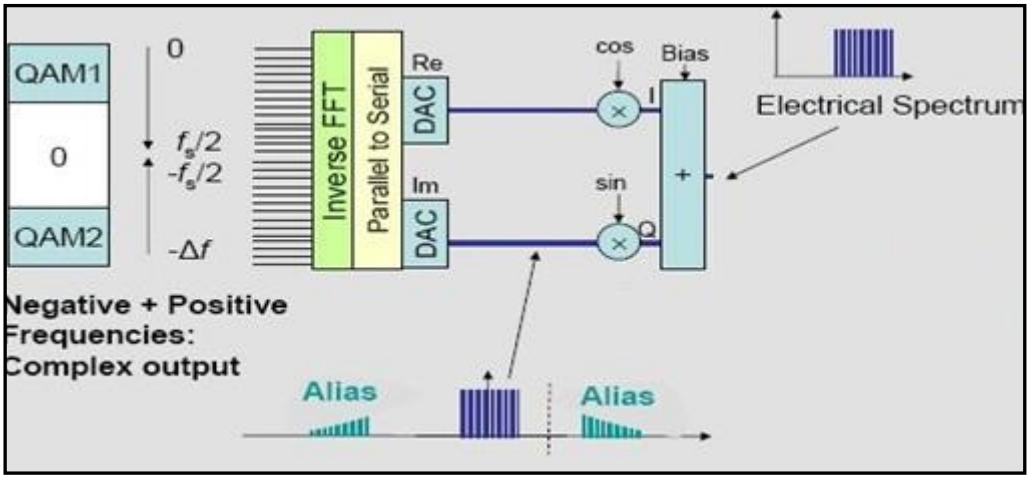

Fig. I.21 RF upconversion [P6]

In this schematic, oversampling is first used to shift the alias away from the OFDM signal, and then the frequency upconversion is done to create a gap in the electrical spectrum. The real and imaginary parts of the signal are separated after the IFFT stage, and after its conversion to the analogue domain the complex baseband signal is obtained (lower inset of the figure).

The real and imaginary parts corresponding to the in-phase (I) and quadrature (Q) components of the signal are then passed through an electrical IQ mixer for its upconversion to an IF, namely f_c. For this purpose, there must be a 90º phase shift between the locally generated carrier at IF frequency that multiplies the in-phase component and the one multiplying the quadrature component.

Despite the increase in complexity of the analogue part entailed by the use of an RF upconversion stage, the IFFT/FFT size and the DAC bandwidths could be fully used to process useful data in order to lower the DAC requirements. Alternatives exist to this configuration, sometimes involving a tradeoff between reduced efficiency and lower complexity arrangements. The following subsection is good example.

At the receiver, the signal is downconverted by another IQ mixer with the opposite function, returning the OFDM signal to baseband before extracting the CP and performing the FFT operation.

I.3.2. Zero padding at the edges of the IFFT input sequence

This is another way to create a gap between the OFDM signal and the DC component which allows avoiding the problems carried by the use of analogue mixers and oscillators.

As shown in Figure I.22, zeros are added at the beginning and at the end of the IFFT input sequence. The more zeros are added, the larger will be the created gap, though the bitrate efficiency will decrease.

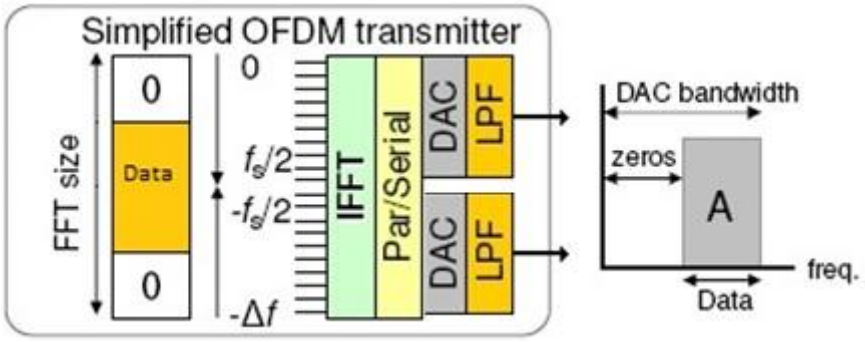

Fig. I.22 Gap created by zero padding [P4]

In the same way as in the RF upconversion case, this gap will serve as a guard band between the OFDM subcarriers and the optical carrier when optical modulation is applied. This will be used to avoid unwanted mixing products both in emission when using IM modulation and at the receiver when using DD.

This form of zero padding can be used at the same time as the oversampling method when creating the input sequence for the IFFT, obtaining a signal with remote aliases and a guard band close to DC, though it can result in quite a reduction of the spectral efficiency. Thus, this trade-off between low complexity of the receiver and spectral efficiency of the transmission will be decisive in the resulting configurations.

I.4. General system schematic

By putting together all the concepts explained until now, the final appearance of an OFDM system could be the one depicted in Figure I.23.

In order to correct the channel's response, a single-tap equalizer should be used at the receiver end to calculate any possible phase shift.

The optical modulation and demodulation stages, as well as the channel impairments affecting an OFDM transmission over optical fibre are explained in detail in the next chapter.

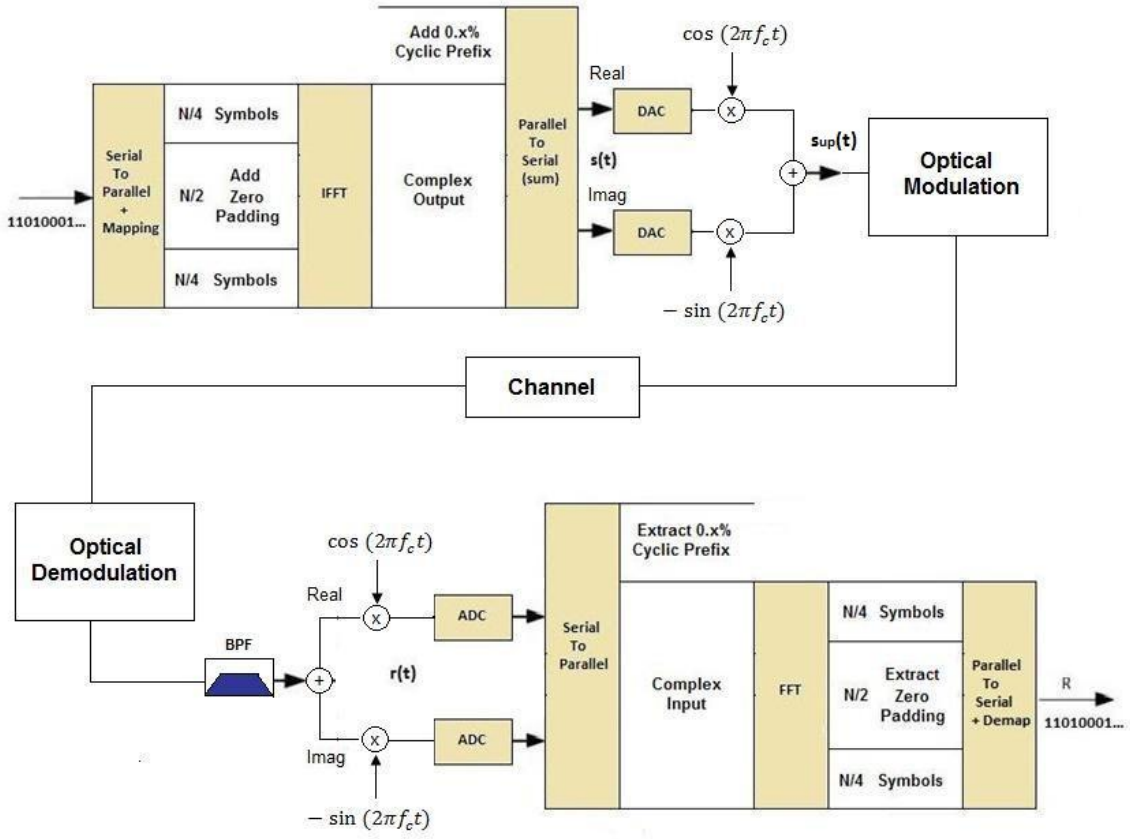

Fig. I.23 OFDM system schematic

Before the RF upconversion, s(t) is approximately bandlimited, consisting of sinusoids of the baseband subcarrier frequencies. For the simulations carried out in this work, the signal $s_{up}(t)$ after the RF mixer will form the electrical input to an optical modulator after being upconverted to the carrier frequency. Thus, the upconverted electrical OFDM signal at the output of the front end block is:

$$s_{up}(t) = \Re\{s(t)\}\cos(2\pi f_c t) - \Im\{s(t)\}\sin(2\pi f_c t) = \Re\{s(t)e^{2\pi f_c t}\} \qquad \textbf{(I.7)}$$

Where s(t) is the complex baseband OFDM signal as in (I.1). For wireless systems, this signal could be modulated by a complex IQ modulator and then transmitted. Otherwise, it would be necessary to transmit real quantities, which can be accomplished by first appending the complex conjugate to the original input block. See Annex A for a detailed description of the process.

CHAPTER II - OPTICAL OFDM

The growing interest for optical OFDM due to an increase of the demanded data rates has fostered the appearance of a large variety of solutions for different applications, so this chapter will deal with its classification into different categories. The preference for simple and low-cost solutions based on the use of direct detection photodiodes which operate according to the square-law detection technique and the requirement of a linear system between the transmitter IFFT input and the receiver FFT output are common in almost all of these solutions.

Moreover, basic concepts of optical communications will be described in order to make it easier to understand the simulations performed in the following chapters, such as the available types of optical modulation and demodulation and the main characteristics of an optical channel. Some of these concepts are not usually referred in the current bibliography of optical OFDM, though they are the basis for creative contributions to the subject.

II.1. The optical channel: Chromatic Dispersion

Chromatic dispersion is a deterministic distortion given by the design of the optical fibre. It leads to a frequency dependence of the rate at which the phase of the wave propagates in space (optical phase velocity) and its effect on the transmitted optical signal basically scales quadratically with the data rate [P2].

This frequency dependence of the phase can be easily identified by describing a pulse propagating through a monomode optical fibre in the frequency domain:

$$X_{out}(w) = X_{in}(w)e^{-j\beta(w)z} \quad \textbf{(II.1)}$$

Where $X_{in}(w)$ represents the Fourier transform of the transmitted signal, $X_{out}(w)$ is the Fourier transform of the received signal and $\beta(w)$ corresponds to the phase constant of the fundamental propagating mode.

Because of the frequency dependence of β, the main limiting effect considered in expression (II.1) will be chromatic dispersion. Other phenomena such as losses or nonlinearities will be not considered, though their effects in fibre propagation can be added afterwards. The consideration of dispersion as the main limiting effect in an optical transmission has been shown to be a good approach in a broad variety of practical applications, but more importantly allows the simplification of its study.

In an ideal case, the phase constant $e^{-j\beta(w)z}$ in (II.1) has a linear dependency with frequency, meaning that all the spectral components undergo the same phase delay, which is the same as saying that they travel at the same velocity.

At reception the same signal will be obtained without any distortion but with a constant delay.

On the other hand, in a dispersive channel the phase constant has a nonlinear dependency with frequency and as a consequence of the different arrival times of the frequency components, the recovered signal at the reception end will differ from the transmitted one.

Assuming a slow variation of the phase constant inside the signal's frequency bandwidth, it is possible to consider a Taylor expansion of the propagation constant about a central pulse frequency ω_0 as follows:

$$\begin{aligned}\beta(\omega) &\approx \beta(\omega_0)+(\omega-\omega_o)\frac{\partial\beta}{\partial\omega}+\frac{(\omega-\omega_o)^2}{2}\frac{\partial^2\beta}{\partial\omega^2}+\frac{(\omega-\omega_o)^3}{6}\frac{\partial^3\beta}{\partial\omega^3}+\dots \\ &= \beta_o+\Delta\omega\beta_1+\frac{\Delta\omega^2}{2}\beta_2+\frac{\Delta\omega^3}{6}\beta_3+\dots\end{aligned} \quad \textbf{(II.2)}$$

Where the third and higher order terms can be neglected if it is considered that $\Delta\omega = \omega - \omega_0 \ll \omega_0$, which enables the possibility to rewrite (II.2) as:

$$\beta(w) \approx \beta_0 + \Delta\omega\beta_1 + \frac{\Delta\omega^2}{2}\beta_2 \quad \textbf{(II.3)}$$

The coefficients in (II.3) are related to the following parameters:

- β_0 relates to the *Phase Velocity* v_{ph}, which verifies:

$$\beta_0 = \frac{\omega_0}{v_{ph}} \quad \textbf{(II.4)}$$

  And it can be defined as the velocity at which the phase of a pure tone at frequency ω_0 would propagate.

- β_1 is related to the *Group Velocity* v_g, of the pulse by:

$$\beta_1 = \frac{\partial\beta}{\partial\omega} = \frac{1}{v_g} = -\tau_g \quad \textbf{(II.5)}$$

  The group velocity can be defined as the rate with which changes in the envelope of the wave (amplitude) propagate. The Group Delay τ_g, given in (II.5) in seconds/fibre length, gives the delay experienced by an envelope centred at frequency ω_0, provided its bandwidth is not too large, as the Taylor expansion would no longer be valid. It can also be thought that this delay is a kind of average delay of all the frequencies in a small bandwidth around the carrier.

- β_2 is the *Group Delay Dispersion* (GDD) given by:

$$\beta_2 = \frac{\partial \beta_1}{\partial \omega} = -\frac{\partial \tau_g}{\partial \omega} \quad \textbf{(II.6)}$$

And thus it gives the frequency dependency of the group delay. The GDD can also be related to the chromatic dispersion parameter ($D = {}^{\partial \tau_g}/_{\partial \lambda}$) of an optical fibre by:

$$\beta_2 = -\frac{\lambda_o^2}{2\pi c} D = -\frac{c}{2\pi f_o^2} D \quad \textbf{(II.7)}$$

Being *c* the speed of light and λ_o the corresponding wavelength.

If the references for phase and time are set at a certain reference frequency (ω_{ref}) approximately located at the centre of the signal's bandwidth, the transfer function of the fibre can be expressed as:
:

$$H(\omega) = e^{j\chi(\omega-\omega_{ref})^2} \quad , \quad \chi = \frac{\beta_2}{2} L \quad \textbf{(II.8)}$$

Where L is the fibre length and ω_{ref} is the reference frequency for the fibre under study.

For the works carried out in this Master Thesis, it is important to understand how the simulator applies this fibre transfer function, and this is why section IV.3.4 is devoted to describe its relation with the chosen reference frequency.

II.2. Optical modulation techniques

In Chapter I, it has been described how to generate an electrical OFDM signal. In order to transmit this signal through an optical channel, optical modulation is required. For that purpose, many different methods could be applied, though just three of them have been chosen as the most representative for this work's purposes: those are the directly modulated laser and two versions of a Mach-Zehnder modulator (MZM): the "standard" mode and the IQ MZM.

II.2.1. Conventional Intensity Modulated / Direct Detection systems

In this case, a laser diode is directly modulated by an electrical signal through its bias current. Figure II.1 shows the characteristic curve of a laser diode, where a linear-behaviour zone can be identified. The slope of this zone is known as slope efficiency. Moreover, the schematic of a diode laser is also shown, where I_L and P_0 refer to the bias current and optical power, respectively.

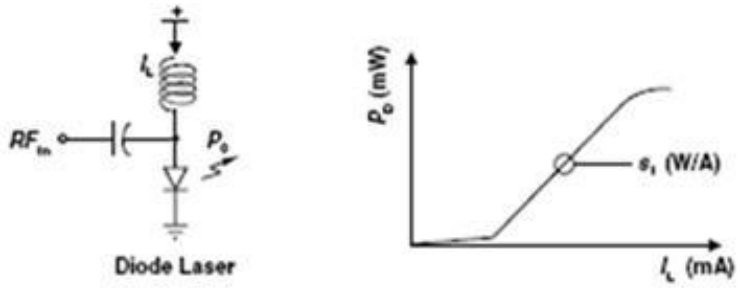

Fig. II.1 Schematic and characteristic curve of a laser diode

This is the most straight-forward method to send information through optical fibre, based on causing variations of the bias current of a diode laser above a given threshold.

These current variations (I_m) lead to proportional variations of the output optical power P_{out}, which are detected by a PIN diode at the receiver end, carrying out the reverse process to recover the sent information signal s(t), as:

$$P_{out} = P_o(1 + m \cdot s(t)) \quad \textbf{(II.9)}$$

Where P_o is the power associated to the laser bias and m is the used modulation index, which is also related to the laser bias current I_o as:

$$m = \frac{I_m}{I_o} \quad \textbf{(II.10)}$$

Finally, the total received intensity for an ideal channel is a function of the PIN diode's responsivity R and the different gains of the amplifier devices in reception (G):

$$I_R(t) = RGP_o(1 + m \cdot s(t)) \quad \textbf{(II.11)}$$

Figure II.2 shows an example of an electrical information signal s(t) being modulated over an optical carrier. At the emission stage, the signal is converted from the electrical into the optical domain (E/O), and vice versa at the reception stage (O/E). This kind of optical transmission is known as Intensity Modulation / Direct Detection (IM/DD).

Fig. II.2 Schematic of an Intensity Modulation and Direct Detection

The direct detection process is mathematically equivalent to applying the squared modulus:

$$I(t) \propto |s(t)|^2 \quad \textbf{(II.12)}$$

As this is a modulation of the optical power or intensity (not directly from the amplitude of the transmitted electrical field), its spectrum is composed by various sidebands, replicas from the one being modulated.

Mathematically, starting from expression (II.9) about the optical power at the laser output and applying the square root, the low-pass equivalent of the electrical field being transmitted on the fibre is obtained:

$$E_{out}(t) = \sqrt{P_o} \cdot \sqrt{1 + m \cdot s(t)} \quad \textbf{(II.13)}$$

In order to give an insight into the spectral content of the signal, the Taylor expansion of the previous expression is considered, obtaining expression (II.14) where it can be seen that the modulated signal is composed by the information signal and its corresponding harmonics:

$$E_{out}(t) = 1 + \frac{\mathrm{m}}{2} s(t) - \frac{\mathrm{m}^2}{8} s^2(t) + \frac{\mathrm{m}^3}{16} s^3(t) + \cdots \quad \textbf{(II.14)}$$

For a pure RF tone, that is, $s(t) = \cos(\omega t)$, if Intensity Modulation is used, each of the Taylor series terms will give rise to harmonics at multiples of frequency ω with amplitudes which decrease with the harmonic order, as the modulation order is smaller than 1. This will cause several sidebands separated at a distance $n \cdot \omega$, where n is the harmonic order. Figure II.3 represents the resulting spectrum for an intensity modulated optical signal.

Fig. II.3 Spectrum of an intensity modulated optical signal

II.2.2. Mach-Zehnder Modulator

II.2.2.1. Standard Mach-Zhender Modulator

The direct modulation of a laser is cheap and also easy to adapt to low cost applications for moderated distances or transmission rates. However, for advanced applications involving high data rates or long distance links, resorting to external modulation is a good solution.

The most typical external modulator is the Mach-Zehnder modulator (MZM), which modulates the light generated in a laser operating in continuous wave mode. The MZM has typically an RF input and another input for a DC bias, as it can be seen from Figure II.4:

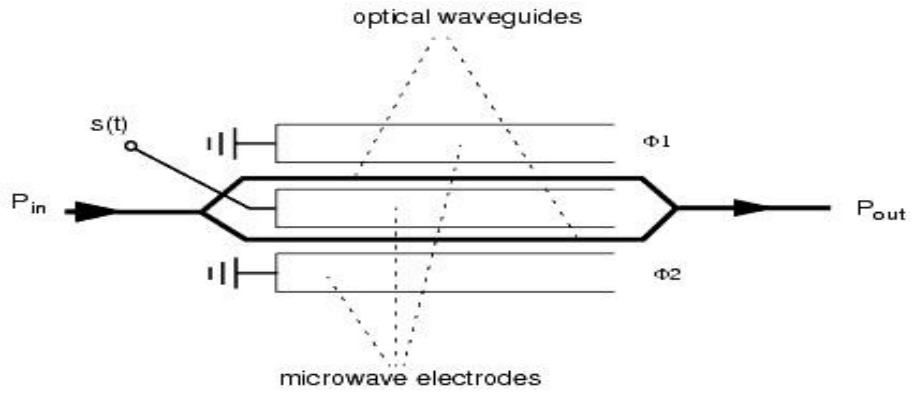

Fig. II.4 Mach-Zehnder modulator [VPI]

The material for the MZM has electrooptical properties by which the phase of the optical wave propagating inside it receives a phase modulation proportional to the applied electrical field. Therefore, the optical power P_{out} at the output of the MZM depends on the phase difference $\Delta\Phi$ between the two arms of the modulator, which can be changed by varying the bias of the MZM:

$$P_{out}(t) = P_{in}(t) \cdot d(t) = P_{in}(t)cos^2[\Delta\Phi(t)]\ ,\ \Delta\Phi(t) = \frac{\Delta\Phi_1(t) - \Delta\Phi_2(t)}{2} \quad \textbf{(II.15)}$$

Where d(t) is the MZM power transfer function and $\Delta\Phi_1(t)$ and $\Delta\Phi_2(t)$ are the phase changes in each arm caused by the applied modulation signal s(t).

Figure II.5 shows the Intensity Modulation schematic and transfer function for a MZM, where the bias point is situated in the linear zone of the transfer function in order to obtain a linear intensity-to-optical power relationship (IM). This point is known as the *quadrature point* and is the most used in combination with DD.

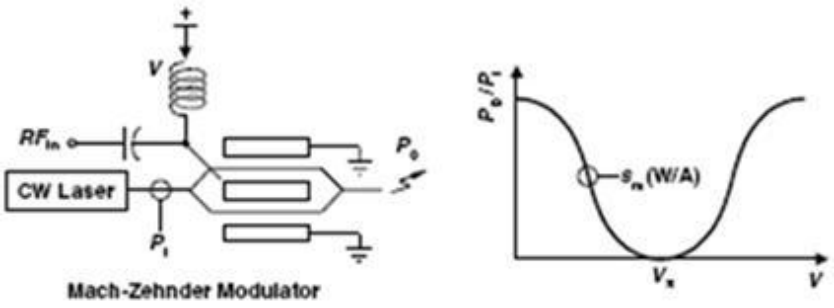

Fig. II.5 IM with Mach-Zehnder modulator

By changing the bias of the MZM, the phase of its two arms is shifted. Hence, the so called Optical Field Modulation mode can be achieved by setting the bias

of the MZM to the null point. This is shown in Figure II.6, where the transfer functions of the optical intensity and optical field are represented, and the drive voltage determines the type of modulation performed by the MZM:

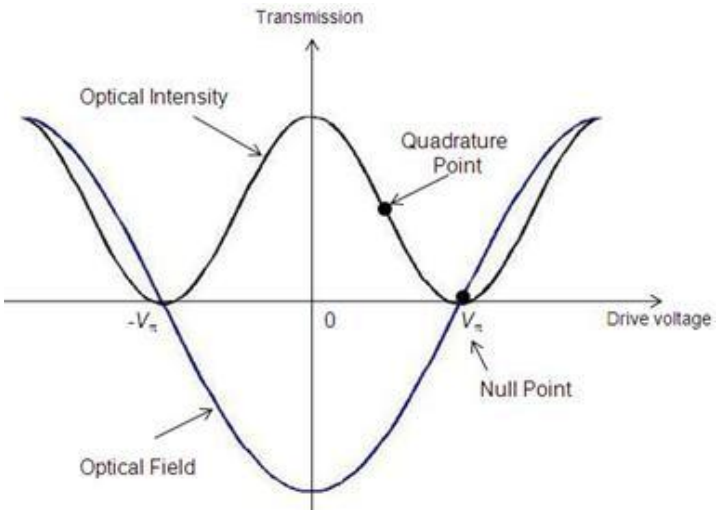

Fig. II.6 Transfer functions of the optical intensity and optical field

Either if the MZM is biased in the quadrature or null point, the signal produced by a standard MZM is a so called “double sideband”, as the OFDM signal is present symmetrically at both sides of the optical carrier. This is shown in Figure II.7, where A* is the complex conjugate of the main OFDM signal A.

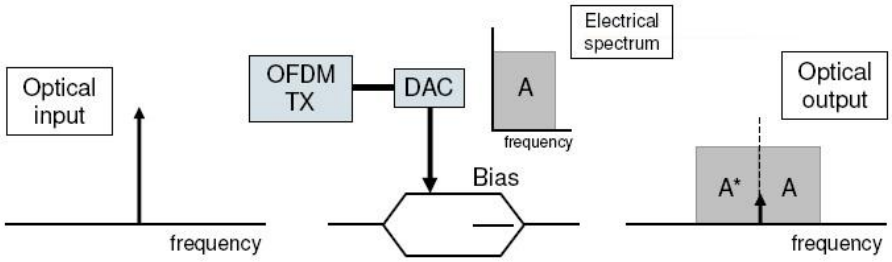

Fig. II.7 Optical OFDM modulation using a standard MZM [P4]

The duplicated sideband generated by the MZM entails some considerable disadvantages for optical OFDM systems, so it needs to be removed by an optical filter. Section II.3 describes this process.

II.2.2.3. IQ Mach-Zehnder Modulator

The previous solution does not make an efficient use of the spectrum and depends on the performance of the optical filters being used, so another option of modulating an electrical signal onto an optical carrier can be considered. This is the optical IQ modulation.

The IQ MZM basically consists of two null-biased standard MZ modulators arranged as in Figure II.8 with a 90º phase difference among them, consisting of one RF input for each component of the OFDM signal (I and Q).

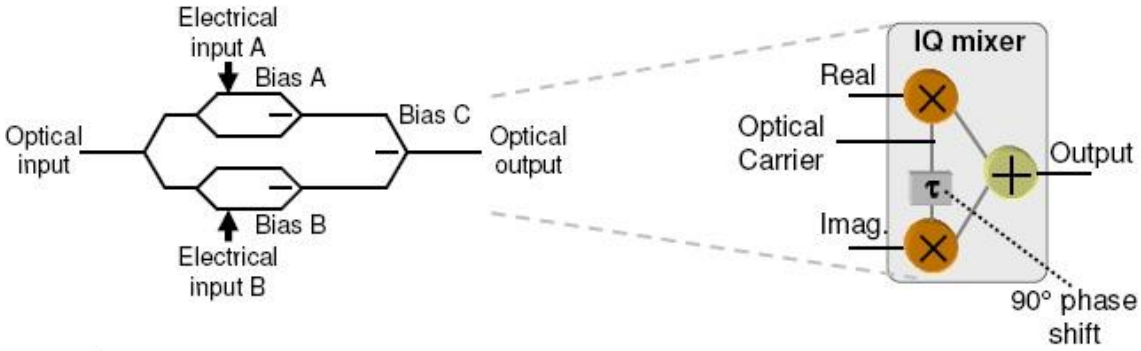

Fig. II.8 IQ Mach-Zehnder modulator [P4]

Thus, an IQ MZM in its bias null-point is used so that the envelope of the electrical field of the optical modulated signal is proportional to the information signal. The main disadvantage of this type of modulation is that the IQ MZM has three bias voltages that need to be precisely adjusted.

This way, the optical IQ signal is directly obtained. For a complex OFDM signal, the output results in just one optical band (see Figure II.9), overcoming the problems caused by the double sideband spectrums in the last configurations.

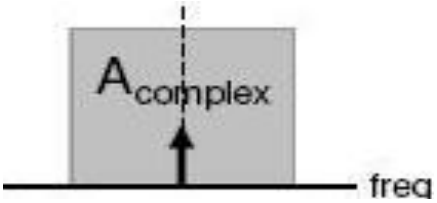

Fig. II.9 Complex signal at the output of an IQ MZM [P4]

II.3. Why optical single sideband?

The main disadvantages caused by the double sideband spectrum appearing at the output of a standard MZM are:

- For complex modulations, the information carried by the phase is lost
- For both direct and coherent detection, it reduces the obtainable spectral efficiency
- Specifically for direct detection, the duplicated sideband causes fading in presence of chromatic dispersion.

Thus, double sideband OFDM will only be considered for low cost applications where chromatic dispersion is not present, or at least is not a limiting factor, as in free-space communications or access networks.

In the case of optical OFDM applications, it will be necessary to remove the duplicated sideband by using an optical filter. This is because the phase shifts of the upper and lower sidebands always result in symbols allocated in the real axis, as shown in Figure II.10:

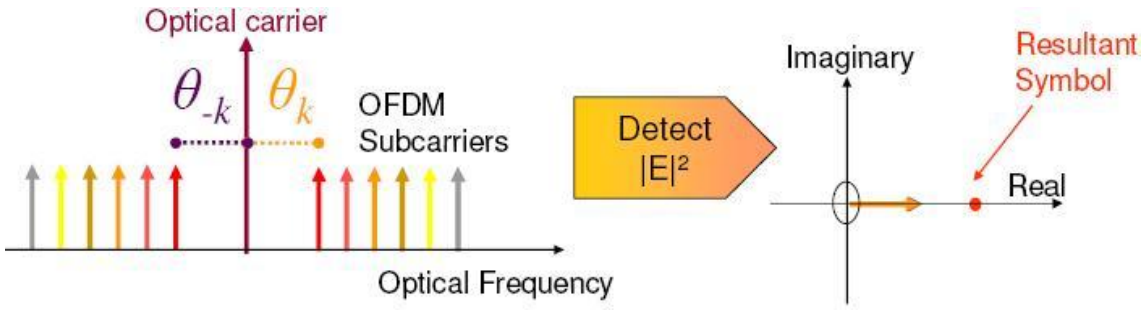

Fig. II.10 Detection of double sideband optical OFDM [P6]

This way, any phase shift of $(n+1)\pi/2$ will null the subcarrier power.

On the other hand, if the lower sideband is filtered out, there is only one photodetection component at each electrical frequency, so there is no nulling at certain frequencies. This situation is represented in the next figure:

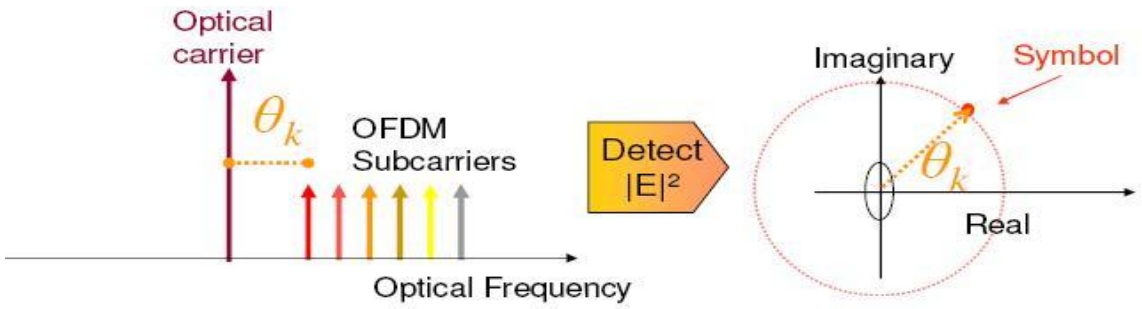

Fig. II.11 Detection of one optical OFDM band [P6]

The phase shift θ_k due to dispersion can be easily equalized in the electrical domain at the receiver.

II.4. Optical OFDM detection

Basically there are two techniques in which an optical OFDM signal can be detected at the receiver: direct detection (DD) and coherent detection (CO-D). All of the existing applications or designs concerning an optical OFDM receiver are variations of these two options.

Although the direct detection configuration is going to be explained in detail throughout this chapter, it is important to introduce its principle of operation prior to describing each optical OFDM system.

Despite coherent detection-based systems represent the best performance in receiver sensitivity, spectral efficiency and robustness against polarization dispersion, this work will be mainly focused on direct detection. This is because coherent detection-based systems require the highest complexity in the transmitter design, so just its main operation principle will be briefly introduced at the end of this chapter.

The square-law detection technique has been mentioned in this work as a typical solution for optical OFDM systems. As no other components than a single photodiode are required to detect the transmitted optical signal, this technique is usually known as direct detection.

The mathematical expression for the square-law technique and the study of the spectral components derived from it can be found in section II.5.2, but before that, an overview of its main repercussions within an optical transmission can be realized.

Because the optical signal is obtained in reception as the squared modulus of its electric field (square-law detectors), the signal mixes with itself, producing at the detector's output harmonics at frequencies multiples of the modulated frequency. Since usually in a transmission the conventional IM modulation is used, in an ideal case the spectral components of the signal would have the precise amplitudes and phases to cause each of the contributions between harmonics to cancel, as shown in Figure II.12:

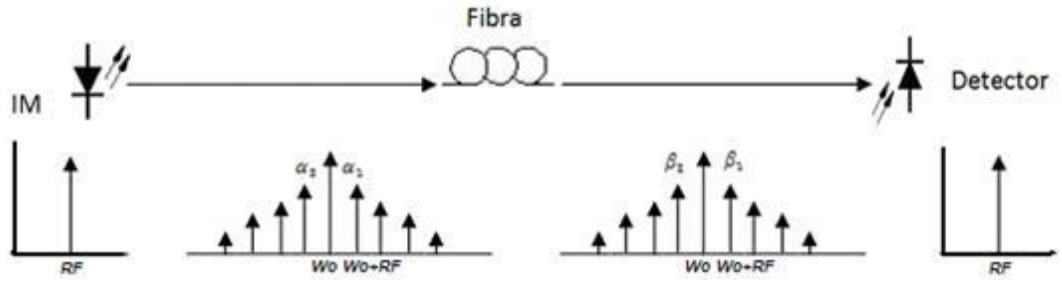

Fig. II.12 Conventional IM/DD transmission system with an ideal fibre

However, a monomode fibre will introduce variations over the transmitted optical signal due to chromatic dispersion, which will cause a different phase delay to each spectral component of the signal being transmitted through the fibre. Thus, these effects in direct detection configuration will not allow a complete cancellation of the harmonics and a nonlinear distortion will appear at the receiver end, as shown in Figure II.13.

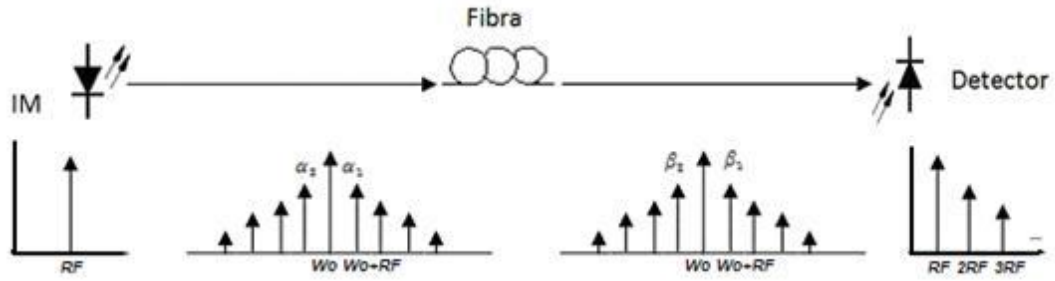

Fig. II.13 Transmission system for a dispersive fibre

In an intuitive mode, the nonlinear effect can be thought of as set of spectral components which spreads out at the transmitter end, and it is not able to fold back in the receiver end to just one spectral component because the spectral components are different and do not match up between them any more.

II.5. Optical OFDM transmission systems

One way to categorize OFDM generators would be to classify them depending on the type of subcarrier generation. This would give rise to two different transmitter categories: analogue and digital generation. While the first one requires a complex integrated modulation, the latter allows a simple optics design with flexible and adaptive constellations at the receiver side. Thus, the generation of subcarriers in the analogue domain is not of interest for the performed simulations in Chapter IV, and it will not be considered in this work.

At the same time, optical OFDM systems with subcarriers generated in the digital domain can be classified according to many other parameters. In order to understand the system simulated in VPI, the most important ones are the modulation technique used in the electrical to optical (e/o) conversion and the type of detection at the receiver.

Many system configurations will appear from the combinations of the modulation techniques and the type of detection at the receiver, though just one will be considered for the simulations in VPI. This will be seen in Chapter III.

II.5.1. Modulation techniques

The way in which data is allocated at the input sequence of the IFFT gives rise to many different transmitter configurations. Thus, different optical modulations should be applied depending on the type of electrical OFDM signal obtained at the transmitter output.

Here, two different configurations are emphasised, one using a standard MZM and the other based on an optical IQ modulation. Both of them avoid the

transmission impairments caused by dispersion by applying the optical single sideband technique, though they do it in different ways.

Other interesting transmitter configurations such as the *Real drive signal* (where a real OFDM signal is obtained by means of Hermitian symmetry) can be found in Annex A at the end of this work.

II.5.1.1. RF upconversion based on Intensity Modulation

It has been said that when performing optical modulation over a baseband OFDM signal with a standard MZM, one of the two resulting sidebands must be suppressed in presence of dispersion.

Thus, an optical band-pass filter can be used for the separation of both complex bands, requiring the allocation of a guard band with respect to the carrier. If the size of this guard band is equal to the OFDM signal's bandwidth, direct detection can be used at the receiver. To that effect, the baseband OFDM electrical signal can be first upconverted to a proper RF frequency, as depicted in Figure II.14.

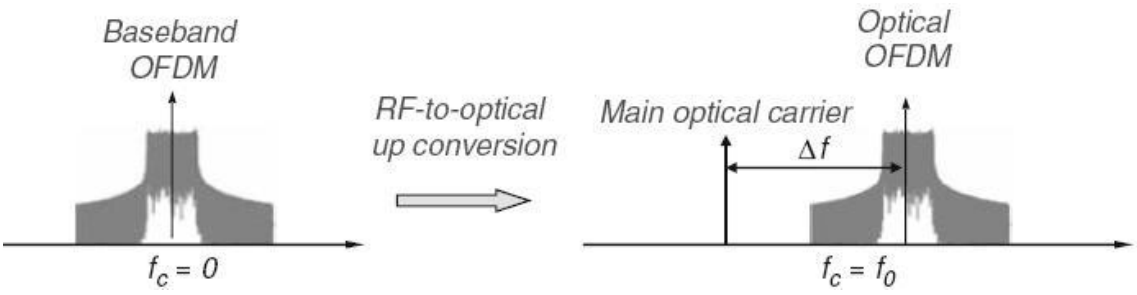

Fig. II.14 Electrical upconversion of the complex OFDM baseband signal [B1]

As shown above, the optical spectrum of the optical OFDM signal at the optical transmitter output is a linear copy of the RF OFDM spectrum plus an optical carrier that is usually 50% of the overall power. This is the technique used in the RF upconversion based on Intensity Modulation kind of optical OFDM, and Figure II.15 shows its schematic.

In this configuration, the whole input sequence of the IFFT is carrying data, though the zero padding oversampling method described in Chapter I can be applied for easier filtering of the electrical OFDM signal with respect to its aliases before the e/o conversion.

Two DAC's are used to convert the real and imaginary parts of the electrical OFDM signal from the digital to the analogue domain. Subsequently an analogue electrical IQ mixer allows both parts of the complex OFDM signal to be sent as inphase and quadrature signals over the RF frequency carrier, so that the signal can be modulated with a standard MZM.

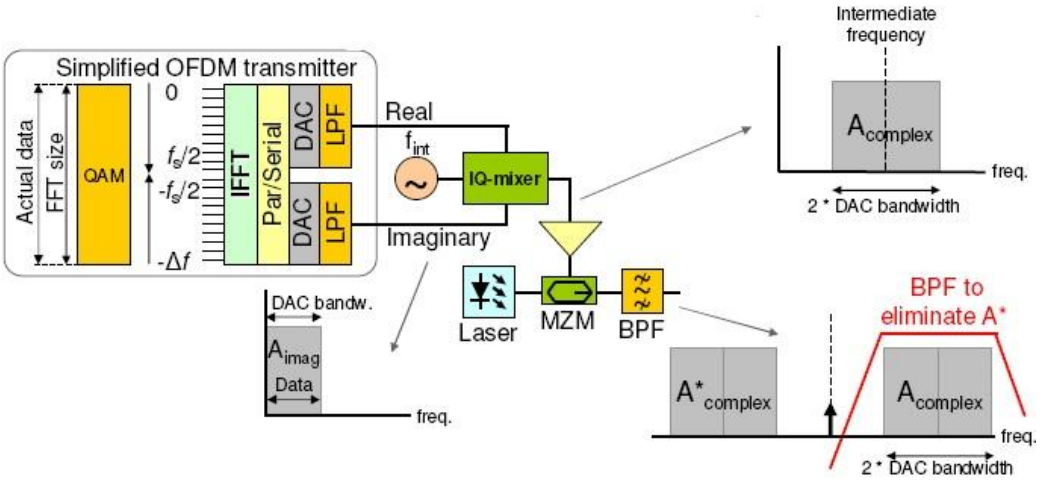

Fig. II.15 RF upconversion based on Intensity Modulation schematic [P4]

II.5.1.2. Optical IQ modulation

If an IQ MZM is used for the optical modulation of the electrical OFDM signal, only one complex optical OFDM band is obtained, so no optical filter is required at the transmitter end.

The resulting schematic for this technique is depicted in Figure II.16, where the real and imaginary components of the OFDM signal are directly fed to the IQ MZM. For simplicity, oversampling is neglected.

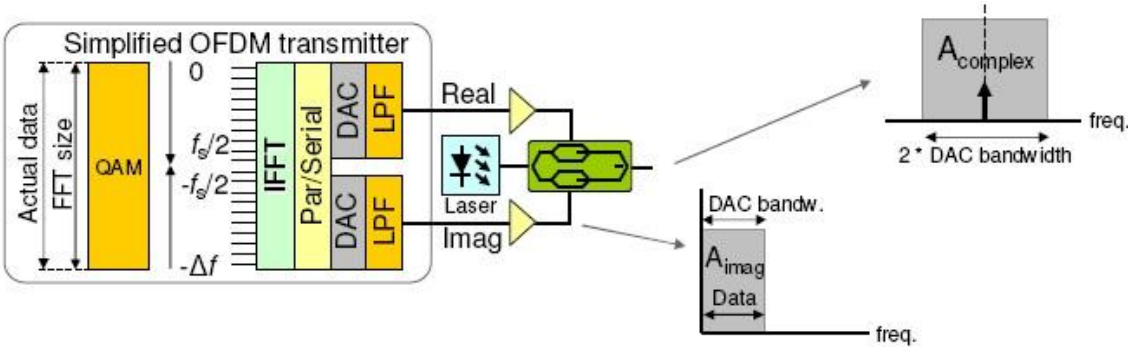

Fig. II.16 Optical IQ modulation schematic [P4]

This scheme provides the possibility of a full-data IFFT input sequence and the complete DAC bandwidths usage (when no oversampling is applied). Moreover, few electronic devices are needed for the implementation of this scheme, though two DACs are required and three bias voltages have to be adjusted for the IQ MZM.

II.5.2. Detection techniques

As said before, there are two basic kinds of techniques allowing the demodulation of an optical signal into the originally transmitted electrical signal: those are the direct and coherent detection.

Both techniques have its pros and cons, and this section describes them. As the simulated transmission scenarios within this work use direct detection, this technique will be described in more detail than coherent detection.

II.3.2.1. Direct Detection Optical OFDM

There are many publications in which different forms of direct detection methods are presented [P7], [P9], [P10], [P11], each with some advantages over the others. However, all of them share a very important characteristic, which is the use of a simple receiver. For instance, five different transmitter configurations using DD method at the receiver are presented in Annex C, where the use of different components such as IQ and e/o modulators varies depending on the input sequence of the IFFT.

The performed simulations in Chapter IV will use the RF upconversion based on IM technique with DD at the receiver. For this configuration, the optical OFDM signal s_{opt}(t) can be described as:

$$s_{opt}(t) = e^{j2\pi f_0 t} + \alpha e^{j2\pi (f_0+\Delta f)t} \cdot s(t) \qquad \textbf{(II.16)}$$

Where f_0 is the main optical carrier frequency, Δf is the guard band between the main optical carrier and the OFDM band (as in Figure II.16), and α is a scaling coefficient that describes the OFDM band strength related to the main carrier (ideally 1). The term $s(t)$ represents the baseband OFDM signal given in expression (1.1) in Chapter I.

Thus, the real valued electrical OFDM signal is available after upconversion and drives directly the e/o modulator. Figure II.17 shows the schematic designed by Lowery and Armstrong in [P12] for one of the first direct detection optical OFDM published simulations using VPI software, where the offset single sideband technique (OSSB) was used. It dates from year 2007, and it has been the basis of the system designed in this work.

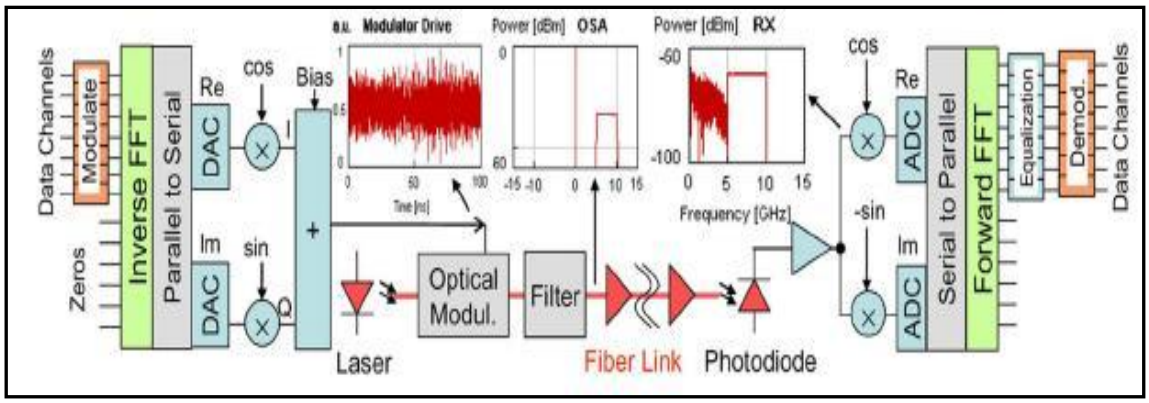

Fig. II.17 DDO-OFDM Long-haul optical communication system [P12]

After the signal passes through fibre link with chromatic dispersion, the OFDM signal can be approximated as

$$r(t) = e^{j(2\pi f_0 t + \Phi_D(-\Delta f) + \phi(t))} + \alpha e^{j(2\pi(f_0+\Delta f)t + \phi(t))} \cdot \sum_{k=-\frac{1}{2}N_c+1}^{\frac{1}{2}N_c} c_{ik} e^{(j2\pi f_k t + \Phi_D(f_k))}$$

$$\Phi_D = \pi c D_t f_k^2 / f_0^2 \qquad \textbf{(II.17)}$$

where $\Phi_D(f_k)$ is the phase delay due to chromatic dispersion for the k_{th} subcarrier, D_t is the accumulated chromatic dispersion in unit of picoseconds per picometer (ps/pm), f_0 is the centre frequency of O-OFDM spectrum, and *c* is the speed of light. At the receiver, only one photodetector is used, which can be modelled as the square law detector so the resultant photocurrent is

$$I(t) \propto |r(t)|^2 = 1 + 2\alpha\, Re\left\{ e^{j2\pi\Delta f t} \sum_{k=-\frac{1}{2}N_c+1}^{\frac{1}{2}N_c} c_{ik} e^{(j2\pi f_k t + \Phi_D(f_k) - \Phi_D(-\Delta f))} \right\} +$$

$$|\alpha^2| \sum_{k_1=-\frac{1}{2}N_c+1}^{\frac{1}{2}N_c} \sum_{k_2=-\frac{1}{2}N_c+1}^{\frac{1}{2}N_c} c_{k_2}^* c_{k_1} e^{(j2\pi(f_{k_1}-f_{k_2})t + \Phi_D(f_{k_1}) - \Phi_D(f_{k_2}))} \qquad \textbf{(II.18)}$$

The first term is a DC component that can be easily filtered out. The second term is the fundamental term consisting of linear OFDM subcarriers that are to be retrieved. The third term is the second-order nonlinearity term that needs to be removed.

Those terms will be easily identified in the next set of figures, which shows the contributions and results of the mixing products that appear at the receiver when the optical carrier mixes with the optical subcarriers to regenerate the electrical OFDM signal. First, the received optical spectrum for an OSSB O-OFDM transmission is depicted in Figure II.18, and then each of its components are analyzed in Figures II.19, II.20 and II.21:

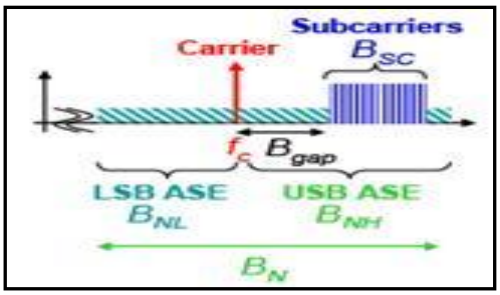

Fig. II.18 Received optical spectrum [P13]

The OFDM subcarriers have a bandwidth B_{sc} and there is a gap, B_{gap}, between the carrier and the subcarriers, which can be produced by RF upconversion of the electrical OFDM signal or by zero padding at the input IFFT sequence, as explained in Chapter I. The amplified spontaneous emission (ASE) inherent to the laser is unpolarized and is band-limited by an optical filter, extending from B_{NL} below the carrier f_c to B_{NH} above it, being present in both the lower and the upper sideband zones.

The useful components in the electrical spectra (that is, the OFDM subcarriers) are the different terms which result from the mixing of the OFDM sideband and the optical carrier. Figure II.19 shows the optical spectra of the contributions to this mixing and the resulting electrical spectra after downconversion.

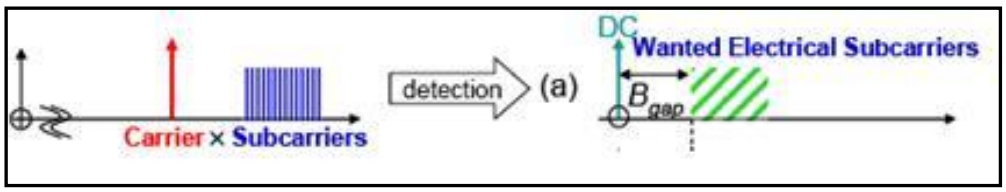

Fig. II.20 Useful components in the electrical spectra [P13]

When a frequency guard band is used ($B_{gap} > B_{sc}$) all of the results of the mixing products between OFDM subcarriers will fall out of band, not degrading performance. This way, the unwanted out of band noise will be avoided:

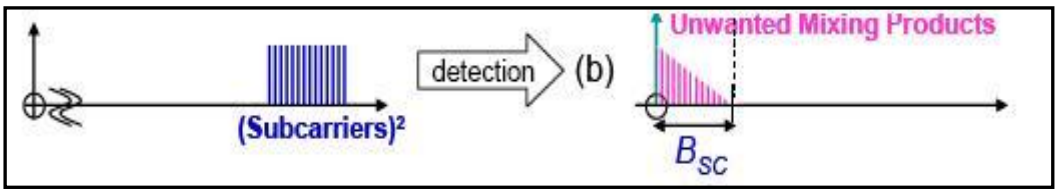

Fig. II.20 Unwanted out of band noise [P13]

However, other undesired mixing products resulting from the square law detection will fall inside the OFDM band. Those are called the unwanted inband terms, and correspond to the products resulting from *optical carrier x noise*, *OFDM signal x noise* and *noise x noise*, as depicted in Figure II.21. Noise from both sidebands will be detected unless a narrow optical filter is used.

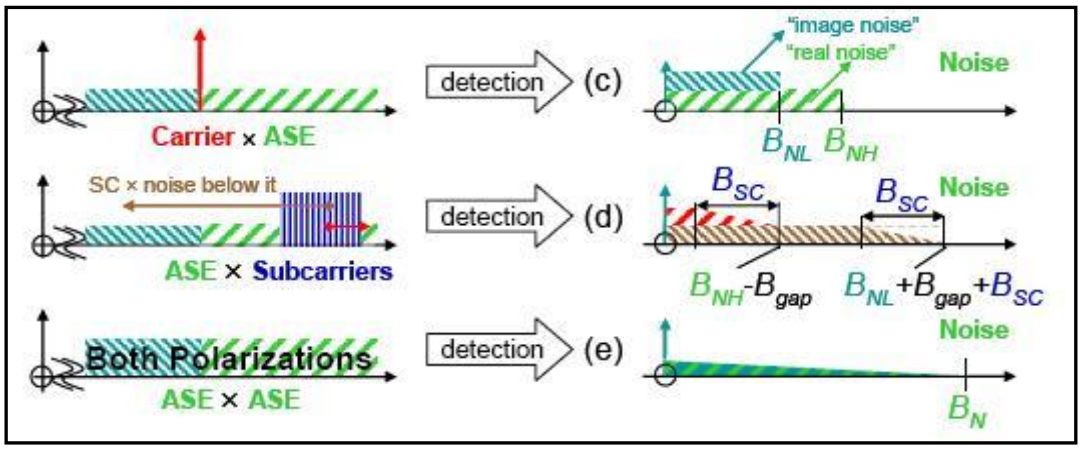

Fig. II.21 Unwanted inband terms [P13]

The single tap equalizer function in the OFDM receiver corrects for the amplitude distortions caused by frequency roll-off of the components and the phase distortions caused by CD and OFDM symbol timing offsets. It should be taken into account that there may be other mixing products because of nonlinearities in the system or I/Q imbalance in the transmitter.

Figure II.22 represents a typical DD receiver used in optical OFDM, where the optical and electrical spectrums before and after the photodetector are also represented.

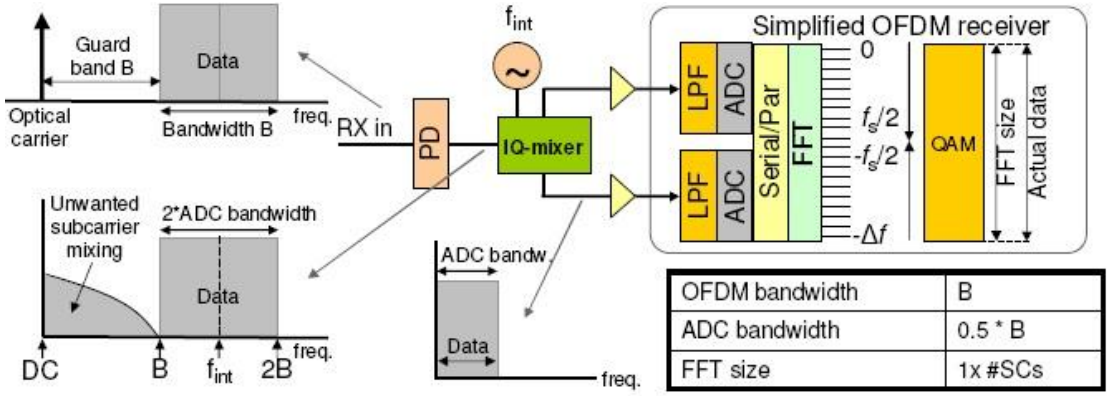

Fig. II.22 Direct detection at the receiver [P4]

It can be seen that the second-order intermodulation is located in the guard band from DC to the OFDM signal bandwidth B, whereas the OFDM spectrum spans from B to 2B. Then, the RF spectrum of the intermodulation does not overlap with the OFDM signal, meaning that the intermodulation does not cause detrimental effects after proper electrical filtering.

Once photodetected, the electrical signal is downconverted to baseband in the opposite way as it was done at the transmitter, before applying the FFT to ideally recover the original subcarriers.

Thus, if the optical OFDM band is located close to the optical carrier in the frequency domain, the intra mixing products are located in the same frequency range as the electrical OFDM signal leading to performance degradation.

Taking all this into account, it can be said that the optical bandwidth requirements for direct detection optical OFDM are determined both by the OFDM band and the gap between the OFDM band and the optical carrier, always omitting one optical sideband. Typically the width of gap is equal to the width of the OFDM band in minimum.

II.5.2.2. Coherent Optical OFDM

Coherent optical OFDM (CO-OFDM) represents the best performance in receiver sensitivity, spectral efficiency and robustness against polarization dispersion, but it requires the highest complexity in the transmitter design.

There are two main advantages coming from the combination of coherent optical communications and OFDM: OFDM brings coherent systems computation efficiency and ease of channel and phase estimation, and the coherent systems bring OFDM a much needed linearity in e/o upconversion and o/e downconversion, since a linear transformation is the key goal for the OFDM implementation. Moreover, there is no need to create a gap between the OFDM signal and the DC component as in the DD receiver setups.

The principle of coherent OFDM is depicted in Figure II.23:

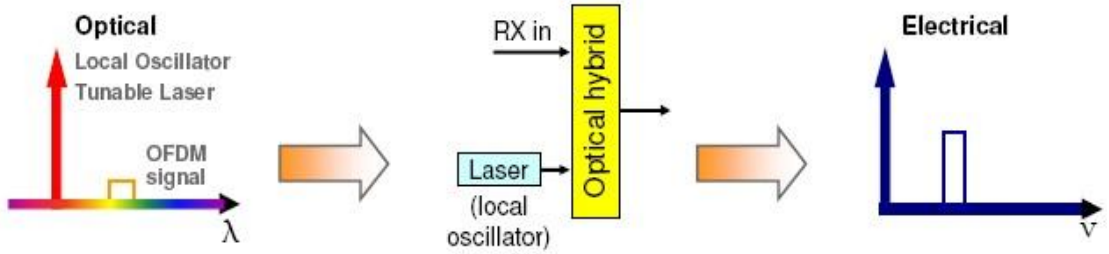

Fig. II.23 Principle of coherent OFDM receivers [P4]

In coherent OFDM systems, the optical carrier is not transmitted with the optical OFDM signal, but generated locally by a laser. This makes this kind of system to require less transmitted optical power than DD-OOFDM, though it is more sensitive to phase noise.

As shown above, a local oscillator (LO) is mixed with the OFDM signal by means of a 90º hybrid that performs the optical IQ detection. If both signals are

aligned in polarization, the mixing of the optical OFDM signal with the LO signal results in the desired electrical OFDM signal. In case of orthogonal polarizations there are no mixing products available.

There are two frequently used configurations regarding to coherent receivers for optical OFDM. Those are depicted in Figures II.24 and II.25, and are called homodyne and heterodyne, respectively.

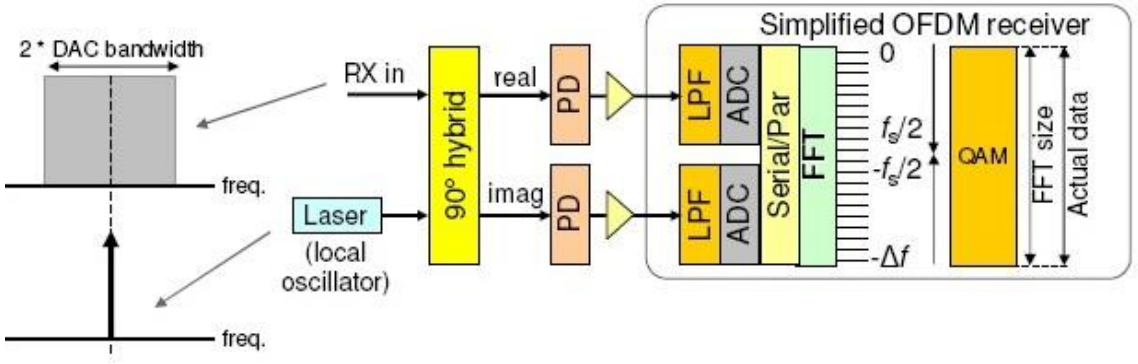

Fig. II.24 Homodyne CO-OFDM receiver [P4]

In this case, the local oscillator is placed in the middle of the OFDM signal. Essentially, this implementation is the reverse of the transmitter using the optical IQ mixer in Figure II.18. Thus, it shares the same advantages and disadvantages: the FFT size and ADC bandwidths can be used for data modulation (if no oversampling is applied) and few electronic components are used, though it requires two ADCs and the IQ MZM at the transmitter side has three bias voltages that need to be adjusted.

On the other hand, the heterodyne reception setup can be considered as a variant of the DD receiver in Figure II.22, where an electrical IQ mixer was used to process the real and imaginary parts of the OFDM signal. Here, the local oscillator is placed left or right of the OFDM signal, as depicted in Figure II.25:

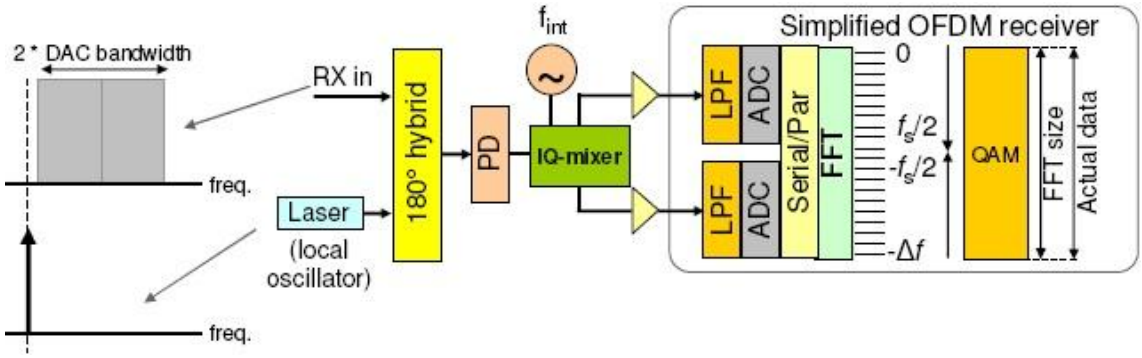

Fig. II.25 Heterodyne CO-OFDM receiver [P4]

This setup shares the same advantages and disadvantages with the homodyne one, so its use will depend on the chosen transmitter configuration.

As explained in Chapter I, the electrical IQ mixer at the receiver can be substituted by a larger FFT block to implement the required operations.

The optical bandwidth requirements for CO-OFDM are much lower compared to DD optical OFDM because there is no need to transmit an optical carrier with the required gap to the OFDM band in addition to the modulated subcarriers. This leads to a spectral efficiency of nearly twice the one in DD-OFDM for any type of subcarrier modulation.

II.6. Equalization

In order to obtain an OFDM signal without errors at the receiver, the use of cyclic prefix is essential. This will eliminate ISI when a temporal dispersion affects the channel. However, the effect of chromatic dispersion causes the information symbols to still be affected by amplitude and phase changes when arriving to the receiver, as shown in Figure II.26:

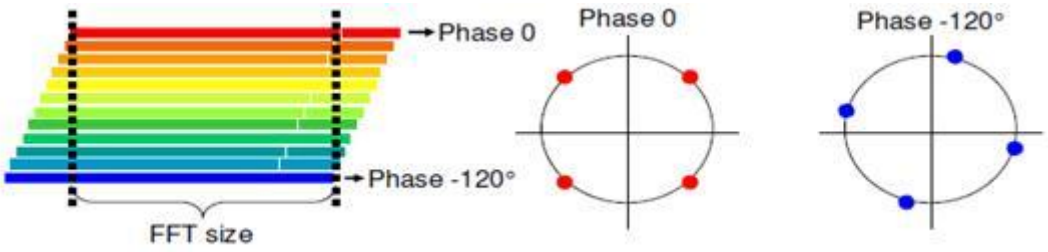

Fig. II.26 Phase distortions on the received constellation [P4]

Consequently, an N-level equalizing stage has to be introduced right after the FFT operation at the receiver in order to correct the phase and amplitude levels, where N is the number of received subcarriers.

The design parameters for this stage should be obtained through a channel estimation, which is usually performed with training sequences. These sequences are added by using pilot subcarriers in each OFDM symbol, so the channel transfer function can be approximated.

As the design of training sequences is beyond the scope of this work, the required phase compensation for each OFDM symbol will be calculated based on the dispersion model suffered by each subcarrier (see section II.X):

$$\varphi = \frac{1}{2}\beta_2 \omega^2 L \qquad \textbf{(II.19)}$$

Where L is the fibre length, ω is the subcarrier frequency, and β_2 is the second term order of the signal phase delay approximation in (II.7).

However, this equalization will be not enough to obtain the ideal received constellation, as a constant phase shift will still affect the received symbols due

to the choice of the reference frequency for the fibre. This issue will be dealt with in section IV.X.

CHAPTER III - VPI DEMOS

Virtual Photonics Integrated (VPI) is a powerful tool that allows to simulate a wide range of optical transmission designs, giving the possibility to create multiple configurations for a given transmission scenario. Specifically, the simulations described in this chapter are going to be performed by means of the *VPI Transmission Maker* application, though it will be simply referred as VPI during this work.

VPI contains two demonstration scenarios which are very interesting regarding this work's purposes. Those are the *OFDM Generation and Detection* demo (Optical Systems Demos/Modulation Multilevel/) and the *OFDM for Long-Haul Transmission* demo (Optical Systems Demos/Long Haul/).

These demos are going to be described in this chapter in order to get an idea of how to implement an optical OFDM transmission on a simulation environment. The first demo simply deals with the generation and detection of an electrical OFDM signal, so no optical transmission is considered at all, while in the second one some of the concepts explained in the previous chapter are applied so the signal can be optically modulated, transmitted through optical fibre and detected at the receiver end, where the transmission quality is assessed in presence of various transmission impairments.

The simulation results presented in this chapter, as well as the ones in Chapter IV, have been displayed by means of the *VPI Photonics Analyzer* tool, which is automatically executed after the simulation is run when using in the setup any of the analyzer modules provided by VPI.

In order to understand VPI's simulation environment, Section III.1 describes its basic structure and the most important settings to take into account when creating a simulation. For more information about it, see the VPI Transmission Maker user's manual in [W6].

III.1. VPI Transmission Maker as a simulation tool

III.1.1. Graphical User Interface

When starting VPI, the basic screen layout is similar to other simulation programs based on interconnection of modules to create, design and simulate the operational characteristics of determined systems.

Figure III.1 shows VPI's graphical user interface (GUI), where some numbers have been added in order to identify each of the parts which are going to be mentioned during this section.

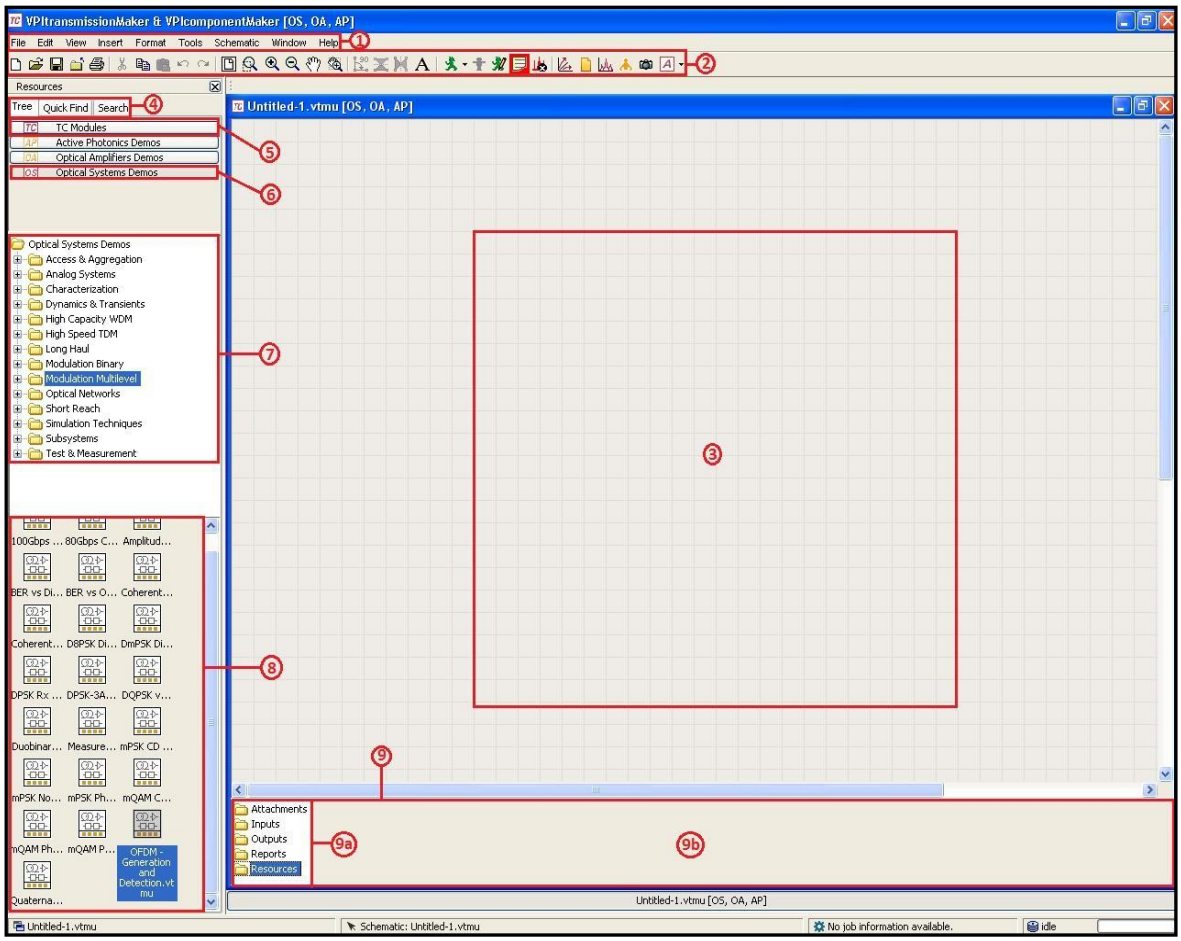

Fig. III.1 VPI Graphical User Interface [VPI]

The highlighted toolbar menu in (1) has the same function as in the most part of software programs menu, as any available action offered by VPI can be executed from here: creating and editing a simulation scenario, preferences configuration, visualization of parameters, etc.

In (2), the most typically used options from the toolbar menu are available as shortcuts, with functions such as creating a new scenario, saving, zooming, executing or stopping the simulation, etc.

When a new file is created (by clicking *File→New* in the toolbar menu or using the corresponding shortcut), an empty schematic as the one in (3) appears. In order to add already existing modules, the *Quick Find* or *Search* tabs in (4) can be selected to look for them.

If the name of the desired module is not known, the *Tree* tab in (4) should be selected, and by pressing the *TC Modules* button in (5), all the available modules can be accessed by categories.

Another interesting option is offered by the *Optical Systems Demos* button (6), which displays the category panel (7) containing all the demonstration simulations offered by VPI. By selecting a category, another panel containing

the corresponding demos appears. In Figure III.1, this is indicated by (8), where the OFDM Generation and Detection demo is selected (highlighted in blue).
Finally, the schematic's *Package Explorer* is highlighted in (9), consisting of a folder browse panel (9a) and a contents panel (9b). The folder panel is used to attach and store any data to be used by the schematic. The contents panel shows the files and documents contained in the currently selected folder in the folder panel.

III.1.2. Simulation hierarchies

VPI is hierarchically organised. This allows an easier management of the modules taking part in a simulation, as they can be treated independently or as a group when necessary.

Figure III.2 shows the three levels in which modules can be classified: those are the universe, galaxy and star. As it can be deduced by their names, the star represents the lowest level of the simulation interface, the galaxy belongs to the second level and the universe is the third and highest level.

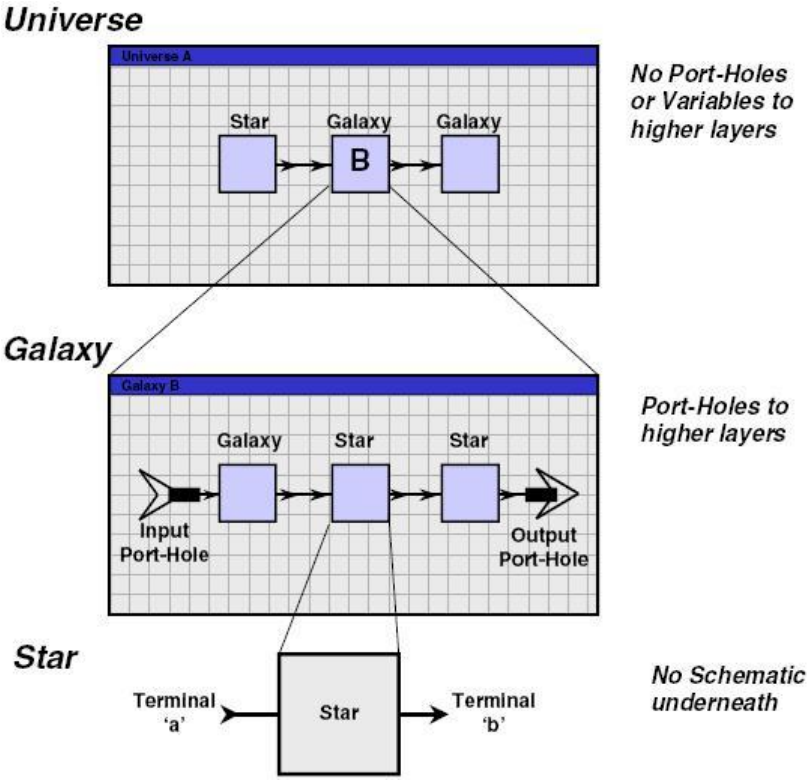

Fig.III.2 VPI hierarchy [VPI manual]

A star represents a unique module with a specific function which can't be subdivided into other modules. Thus, a galaxy can be described as a second level module formed by a set of interconnected stars (or even other galaxies). In order to be implemented on a universe, a galaxy must contain at least one input or output port (see Figure III.2).

The universe is the only module that can be executed by the user. It represents the whole simulation scenario, and it can consist of a combination of interconnected stars and galaxies. From a universe point of view, a galaxy acts as another unique module and the stars inside this galaxy can't be seen from the main schematic. However, the galaxy schematic can be displayed by right-clicking on it from the universe schematic and selecting the *Look inside* option.

III.1.3. Simulation parameters

When executing a simulation, any star, galaxy or universe belonging to it will operate according to certain parameters. The value for these parameters can be changed from the corresponding *Parameter editor window* (PEW). Figure III.3 is an example of a PEW corresponding to a laser module:

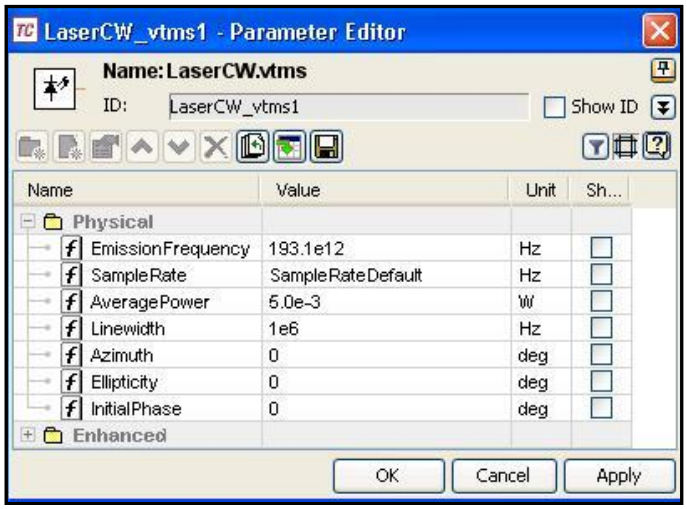

Fig. III.3 Parameter editor window (PEW) of a VPI laser module [VPI]

The Parameter editor of a module can be accessed by right-clicking on it and selecting the *Edit Parameters* option, or just by double-clicking on the module. In the case of a universe or when being inside a galaxy, the same operations can be done by clicking on the background.

Because of the hierarchical organization, any parameter which is shared by more than one module, even if it is used in different levels, will take the value of the highest level in which it is used.

For instance, consider a transmission system where the scenario itself is a universe containing various galaxies (say one coder and one decoder), and these galaxies contain at the same time other modules (stars) to implement its respective functions. If, for example, the roll-off parameter of a pulse shaping filter acting as a star inside both the coder and decoder modules is defined in the universe PEW, any change in its value from this level will be applied to both modules belonging to the galaxies.

On the other hand, if the value of this parameter is changed directly from the pulse shaping star inside the coder, it will only affect this module, leaving the one inside the decoder untouched.

This feature will be used in the customized simulations presented in the next chapter when a simultaneous change is desired for any parameter of both the OFDM coder and decoder modules.

Thus, two types of parameters can be defined: global parameters, which affect to all the modules within a simulation (lower levels included), and the specific ones, belonging to a single module.

III.1.3.1. VPI global parameters

Besides the parameters that can be defined by the user to be used by all the modules in a simulation, VPI provides a set of already defined global parameters, which are very important for the correct and efficient operation of the simulator. The most relevant for this work's purpose are:

- *TimeWindow*: this parameter sets the period in which a block of data is represented. This time will inevitably fix the spectral resolution of the simulated signals setting, i.e., the resolution of spectral displays.
- *LogicalInformation*: This is a tool used by VPI to send information between modules within the same simulation. It removes the need for sneak wires between the transmitters and some modules such as BER Estimators, Clock Recovery modules and the Channel Analyzer.
- *SampleRateDefault*: it specifies the sampling frequency when working in Block Mode. It is defined as the number of samples taken by second and determines the maximum frequency that can be simulated.
- *BitRateDefault*: it defines the transmission bit rate by setting the BitRate parameter of emitters, bit generators, etc. to BitRateDefault.

III.1.3.2. Restrictions on Global Parameters

As VPI works with the FFT algorithm, when working with periodic signals a series of restrictions have to be considered. First, the number of samples by Time Window has to be a power of two. This condition sets a limitation when selecting the Time Window and the Sample Rate, as expressed in (III.1):

$$\#samples = Time\ Window \cdot Sample\ Rate = 2^n \qquad \textbf{(III.1)}$$

Additionally, the time resolution has to be considered, given by (III.2). This will determine the maximum allowed simulation frequency given by (III.3).

$$dt = \frac{1}{SampleRateDefault} \qquad \textbf{(III.2)}$$

$$f_{max} < \frac{1}{2dt} = \frac{SampleRateDefault}{2} \quad \textbf{(III.3)}$$

Finally, the frequency resolution will be given by Expression (III.4). A proper selection of the Time Window is required in order to obtain a correct signal frequency spectrum. At the same time, the Time Window determines the minimum allowed simulation frequency given by (III.5), since the period of the simulated signal T always has to be smaller than the Time Window.

$$df = \frac{1}{TimeWindow} \quad \textbf{(III.4)}$$

$$f_{min} > \frac{1}{TimeWindow} \quad \textbf{(III.5)}$$

III.1.4. Custom modules

III.1.4.1. Creating and adding galaxies

To create a new galaxy, the user has to click on the *File - New* option in the toolbar menu, and a new schematic will appear. At first it will be considered as a universe, though it will automatically saved as a galaxy when input and output ports are used in the schematic. These ports can be found in the *Tree* tab of the GUI, pressing the *TC Modules* button and selecting the *Wiring Tools* category.

To add a customized galaxy module, the option *Insert – Add module* in the tool bar allows loading it into a universe or galaxy schematic by just selecting them from the corresponding location (if known). VPI modules can also be loaded in this way.

When adding an already existing galaxy to a schematic, the user can choose between inserting a copy or a link of the mentioned galaxy. Figure III.4 shows the VPI message appearing in this case for a galaxy named *RF_Upconversion*:

Fig. III.4 Copy or link to an already existing galaxy [VPI]

If the *Copy* option is selected, VPI will copy the entire galaxy to the *Resources* folder in the schematic's *Package Explorer*, and any change on the galaxy will not be applied to the original one. On the other hand, selecting the *Link* option will cause that the galaxy is executed from the original location, so any modification will be saved, affecting it even when it is added to other scenarios.

III.1.4.2. Creating and linking parameters

Although any value of a star module parameter can be changed when running a simulation, the parameter properties cannot be edited. Thus, new parameters can only be created for either galaxies or universes. This can be done by accessing the PEW and clicking the *Create parameter* button, as shown in Figure III.5:

Fig. III.5 Create parameter button [VPI]

After clicking the button, a menu in which the parameter settings can be configured will appear, as shown in Figure III.6:

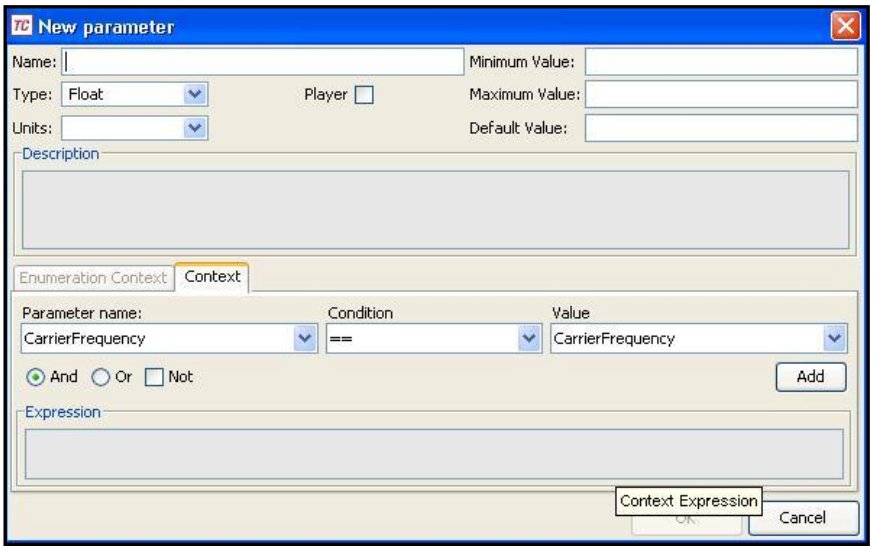

Fig. III.6 New parameter settings [VPI]

In this case, a new parameter is going to be created in a category called *RF galaxies*. New categories can be created for a better organization of the parameters, appearing as expandable folders as in Figure III.5. The *Create category* button in the same figure (a yellow folder icon to the left of the *Create parameter* button) allows to create a new category. To insert a parameter into a category, it just has to be dragged into the corresponding folder.

Any parameter can be shared by modules belonging to different simulation levels as long as it has the same name for every module containing it.

When creating a new simulation scenario where modules of different levels will share some parameters, the usual (and easier) procedure is to create parameters in the lower level and then expand them to the upper levels.

This expansion of a parameter is done by right clicking on the created parameter and selecting the *Create Schematic Parameter* option, as shown in Figure III.7. This way, the parameter and its corresponding category will be automatically created in the upper level with the same settings.

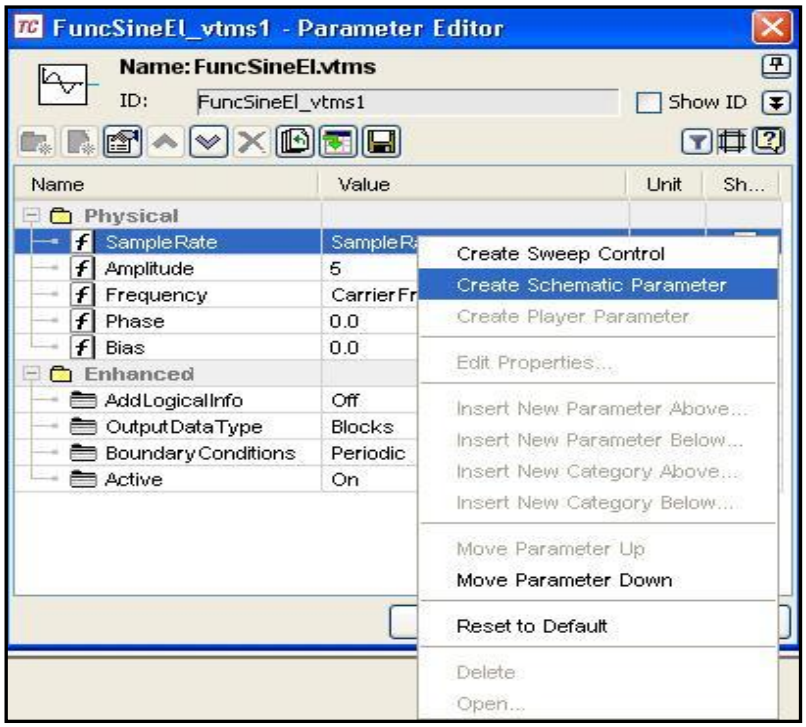

Fig. III.7 Create Schematic Parameter option [VPI]

In order to make the parameters management easier, the highest level parameter should be the only one indicating the value used for the simulation, while the lower level ones should just indicate its name in the *Value* field. However, this field can be given another value if a module belonging to a lower level has to work with other characteristics than those of the higher level ones.

III.1.4.3. Cosimulation

Cosimulation is a technique in which some part of the simulation is handled by an application other than the *VPI Transmission Maker* simulator. It allows three different programming languages to interact with VPI: Matlab, Phyton and C/C++. This technique has played a very prominent role in this Master Thesis, as it has been used to build a complete optical OFDM simulation tool by the combination of the Matlab programming for the OFDM coding and decoding and VPI modules for the simulation of the RF and optical paths.

The main module to carry out the cosimulation is called the *CosimInterface* module, and it is represented in Figure III.8:

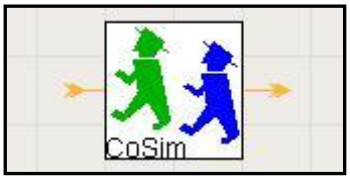

Fig. III.8 *CosimInterface* module [VPI]

To execute a programming code, the code file must be attached to the *Input* folder of the schematic containing the *CosimInterface* module, and its main function (which name must be the same as the code file name) has to be indicated in the *RunCommand* parameter value of the module's Parameter editor. This process is shown in Figure III.9 for the case of a Matlab code.

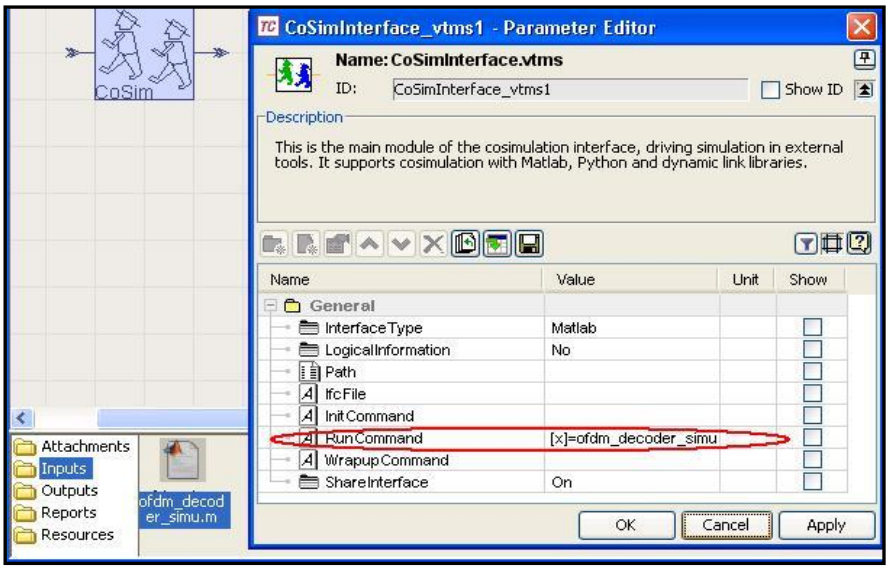

Fig. III.9 Main code function indicated in the *RunCommand* parameter [VPI]

In this case, the variable *x* will take the output value of the function *ofdm_decoder_simu*. Note that this name is the same for the Matlab file attached to the *Input* folder of the schematic.

VPI provides other cosimulation modules which act as inputs and outputs of the *CosimInterface* module. Those are used to indicate the type of data that is going to be inserted and extracted from the cosimulation, allowing the use of electrical or optical signals, floating numbers, complex numbers, etc. As an example, Figure III.10 shows an interconnection of a *CosimInterface* module with one optical input (*CosimInputOpt*) and one optical output (*CosimOutputOpt*).

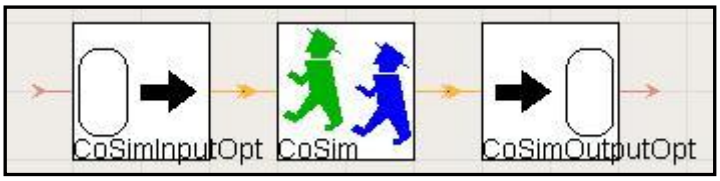

Fig. III.10 *CosimInterface* interconnection for optical signal processing [VPI]

This way, an optical signal generated with VPI modules could be processed by one of the mentioned programming software, which allows the user to modify the signal parameters and extract them in a customized way.

The *CosimInterface* module will be the key to the performed simulations in the next chapter, acting as an interface for VPI to access the Matlab codes programmed for this work, which contain the OFDM coder and decoder functions.

III.2. OFDM Generation and Detection Demo

III.2.1. General schematic

The next figure shows the universe schematic view for the OFDM Generation and Detection demo provided by VPI in *Optical Systems Demos/Modulation Multilevel* in the left panel labels.

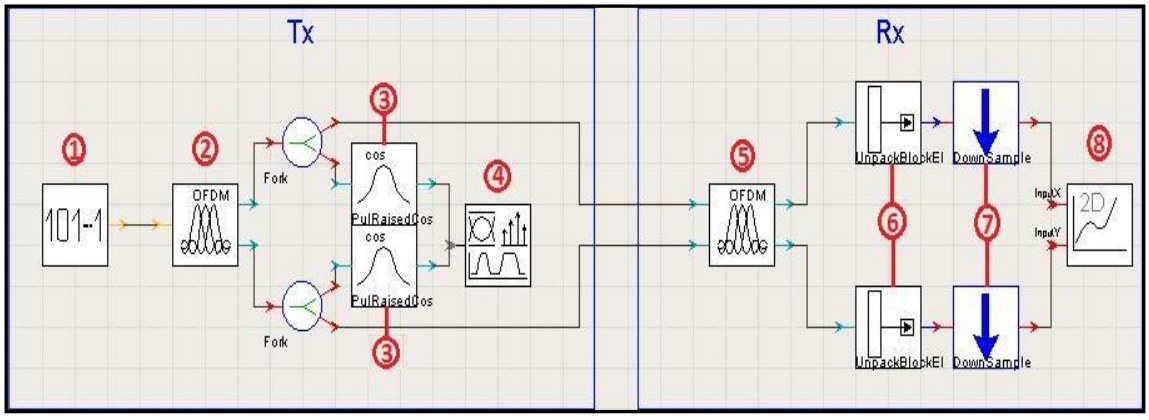

Fig. III.11 OFDM Generation and Detection [VPI]

The goal of this section (as well as the following one) is to learn from each demo towards a new definition of a simulation setup for optical OFDM systems.

In this case, a complex-baseband OFDM signal is generated in an OFDM coder (1) connected to the OFDM decoder (5) by means of VPI wires, so the received signal is directly detected without any transmission channel between transceiver and receiver. This means an ideal channel transmission.

Also, two visualizer modules (4,8) can be seen, which function is to extract the relevant results from the simulation. Before the first visualizer (on the left in the figure) two pulse shaping modules (3) will generate a Nyquist response from an incoming electrical impulse.

The transmission is initiated in a PRBS or pseudo random bit sequence generator (1). According to the module's definition in the Reference Manual (right-click on the module and select the *Help* option) the output of this module is a sequence of random integer numbers, forming a vector of size *TimeWindow*Bitrate* that will be fed to the coder. See the Reference Manual in [W6] for more details about the characteristics of this random sequence and the available types of sequence to select from the PRBS Parameter editor window.

Despite not being able to see the internal structure of the OFDM coder galaxy, its operation principles can be guessed based on the acquired concepts during the investigation prior to the realization of this chapter.

For an M-QAM modulation, an OFDM coder in its simpler form (omitting zero padding and cyclic prefix overheads) would first pack the bit sequence coming from the PRBS into $\log_2 M$ sets, assigning one QAM symbol to each set. Thus, the parameter BitsPerSymbolQAM from the schematic's PEW allows changing the M factor for the QAM modulation, as shown in Figure III.12:

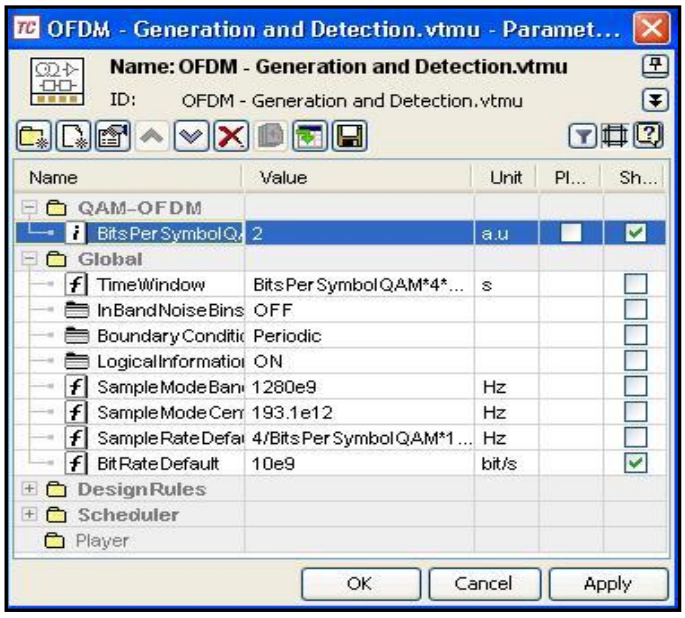

Fig. III.12 Configurable parameters from the universe schematic [VPI]

Once the bits have been converted to QAM symbols, the coder will perform an IFFT operation for each N symbols forming an OFDM symbol, resulting in a sequence of floating numbers of size *TimeWindow*BitRate/BitsPerSymbolQAM*, meaning a reduction of a factor $\log_2 M$ for the sequence length.

By checking the Reference Manual for the coder module, it can be seen that its two outputs represent electrical samples of the real and imaginary components of the complex OFDM symbols. After several tests and careful readings of the available documentation on the subject, it has been deduced that an upsampling operation is carried on the sequence at the output of the IFFT stage in order to be converted into electrical samples.

Another key to the above conclusion lies on the *UnPackBlockEl* (6) and *Downsample* (7) modules used to convert the electrical samples at the output of the decoder into numerical samples, as it will be seen later.

Thus, the original sequence length (*TimeWindow*BitRate*) is recovered to match the sampling rate required by VPI, obtaining at the output the electrical samples that represent the analogue OFDM signal.

Note that the OFDM coder has two outputs which are not only connected to the decoder, but also processed by the *PulseRaisedCosQAM* modules (3) serving as pulse shaping filters. As it was explained in Chapter I, the most suitable impulse response for an OFDM signal is the square-root raised cosine approach, so the *squareRootRaisedCosine* option should be selected as the Nyquist response parameter for these blocks.

Once this type of filtering is applied, both parts of the signal are ready to be represented, so the *SignalAnalyzer* module (4) is used as an interface to the *VPI Photonics Analyzer* tool, where the signal will be displayed. The results of this representation will be described in Section III.2.4.

At the receiver side, the decoder module performs the opposite operations carried on in the coder module, providing the electrical samples representing the real and imaginary parts of the decoded complex information symbols. These parts are going to be fed to another kind of analyzer (8), which will plot the received constellation based on the received information symbols.

But before that, as both inputs and outputs of the decoder belong to the electrical type, the electrical samples of each branch have to be transformed into floating-type values that will represent samples of the electrical OFDM signal. This function is carried on by the *UnpackBlockEl* modules, as it can be seen in (6) from Figure III.11.

Once the electrical signal is sampled, the number of samples needs to be reduced so just the correct amount of information symbols is represented on the constellation diagram.

As it was explained in the coder case, this is because VPI needs the number of samples of the original bit sequence to be at least equal to the number of samples to be represented as an electrical signal. As the coder internal sequence is organized in symbols (not in bits), it is supposed that this sequence is internally upsampled so it can be correctly processed by the software.

Thus, two *DownSample* blocks (7) are used to provide the exact amount of information symbols to be represented by the next module. The downsampling factor indicated in the Parameter editor of these blocks is set to:

$$factor = SampleRateDefault/(BitRateDefault/BitsPerSymbolQAM) \quad \textbf{(III.6)}$$

As the *SampleRateDefault* parameter is set to $4/BitsPerSymbolQAM \cdot BitRateDefault$ for this demo (in order to have a frequency simulation window that is 4 times larger than the required optical bandwidth of the optical OFDM signal), the downsampling factor (and also the internal upsampling factor of the coder) will be 4 for any type of subcarrier modulation and bitrate.

The constellation diagram is plotted by the *NumericalAnalyzer2D* module (8), which also acts as an interface to the VPI Photonics Analyzer tool.

III.2.2. Coder and decoder parameters

Figure III.13 shows the OFDM coder parameters that can be changed from its PEW. The same parameters are shared by the decoder module, which performs the same functions as the coder in the reverse order.

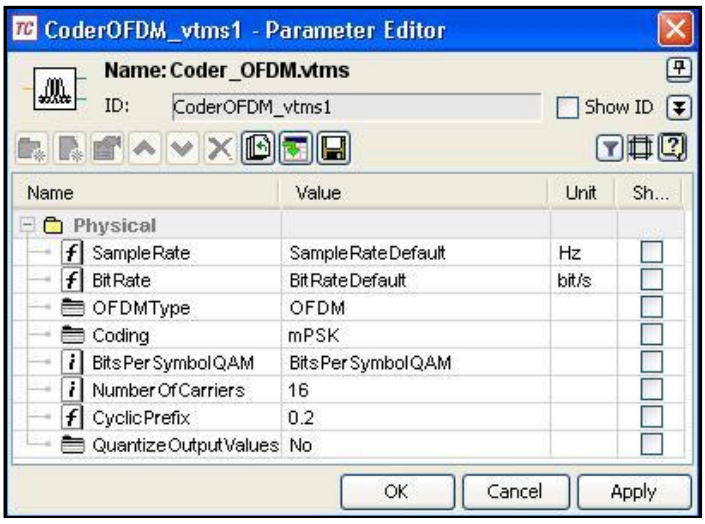

Fig. III.13 Coder (decoder) parameters [VPI]

Three of the parameters are shared with those of the universe schematic: *SampleRate*, *BitRate* and *BitsPerSymbolQAM*. Thus, any change in their values will not have any effect on the simulation unless it is done in the upper level.
The rest of the parameters (all of them belonging to the *Physical* category) are:

- *OFDMType*: This parameter allows to choose between three different modulation types: OFDM, where no zero padding is used; DMT (Discrete Multi Tone), where half of the inputs of the IFFT are the complex conjugate of the other half so a real OFDM signal is created at the transmitter output, as explained in Annex 1; and Zero Padding. The latter technique is used to create a gap between the OFDM signal and the DC component, as described in Chapter I.
- *Coding*: Select either mQAM or mPSK coding to modulate subcarriers.
- *NumberOfCarriers*: Number of subcarriers taking part on the modulation. If the Zero Padding technique is used, only half of the subcarriers will be used to encode the signal, meaning a loss of 50% of the effective data rate. The same will happen with the DMT modulation type.
- *CyclicPrefix*: The length of the cyclic prefix relative to the symbol length, ranging from 0.0 to 1.
- *QuantizeOutputValues*: If this parameter is set to *Yes*, the output values of the coder are quantized. The number of quantization levels and the higher quantization level should be indicated afterwards. This technique is useful to simulate the effect of a DAC and also to clip the signal when it exceeds a determined level.

If any of these parameter values needs to be changed, it should be done in both coder and decoder. Thus, one way to achieve an easier configuration of the schematic would be to create schematic parameters as explained in the last section, so just a single parameter change is required to affect both modules.

However, the main disadvantage of the coder and decoder modules is that all the performed operations are internal, meaning that they don't allow looking inside them for a detailed analysis of the working procedures. Despite some basic concepts are explained in the Reference Manual, it can be said that those modules are quite rigid in terms of showing the structure and organization of the internal operations carried on inside them.

The problems indicated in the last paragraphs have been the cause of a need for new coding and decoding tools where every operation can be checked and even modified. Hence, custom coder and decoder modules have been developed to implement the same operations as those of VPI, as it will be seen in Chapter IV.

III.2.3. Simulation results

When running the simulation, two graphs are going to be shown in the Analyzer tool: the electrical signal spectrum and the received constellation diagram. As the signal transmission is done over an ideal channel, no dispersion will appear on the constellation diagram, so for case of 4-QAM modulation (mQAM coding with *BitsPerSymbolQAM* parameter set to 2) it will be displayed as 4 points forming a square, each of them representing one information symbol.

This case is represented in Figure III.14 for the OFDM type of coding. The parameters for this simulation are:

- *BitRateDefault* = 10 Gbps
- *BitsPerSymbolQAM* = 2
- *SampleRateDefault* = 4/BitsPerSymbolQAM*10e9 = 2*BitRateDefault
- *TimeWindow* = BitsPerSymbolQAM*4*1024/10e9 = 8192/BitRateDefault
- *NumberOfCarriers* = 16
- *CyclicPrefix* = 0.2

Moreover, the pulse shaping filter has been set with the following parameters:

- *RollOff* = 0.18
- *SymbolRate* = BitRateDefault/BitsPerSymbolQAM

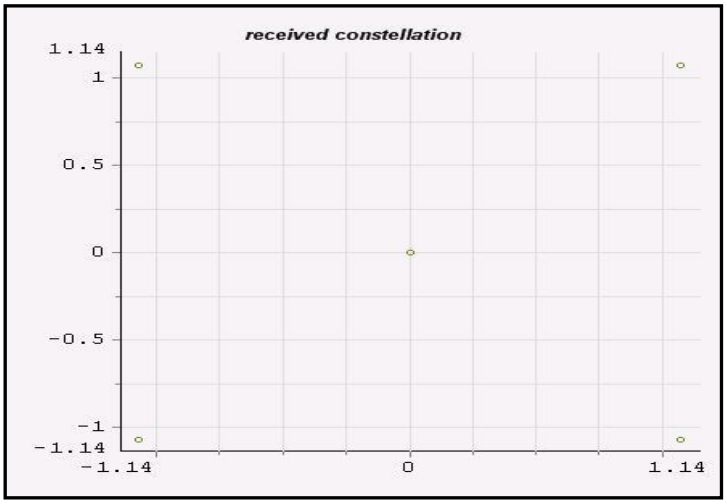

Fig. III.14 4-QAM received constellation diagram [VPI]

Apart from the 4 possible information symbols, at least one symbol is also represented in the centre of the diagram (circle in [0,0]). This is because VPI organizes the sequence to be transmitted by first calculating the required information symbols according to the bits per symbol and cyclic prefix parameters, discarding a number of bits from the original sequence which will be occupied by the bits representing the required cyclic prefix quantity.

If the resulting number of OFDM symbols does not cover the whole sequence, VPI fills it with zeros to compensate for any differences between the effective and transmitted data rates, and symbols in [0,0] are represented as long as those padded zeros are not previously extracted. This is another point to be improved by the upcoming custom simulations.

The transmitted signal spectrum will be represented by means of a signal analyzer for both the real and imaginary components of the OFDM signal. As negative frequencies do not exist for a real system, a complex-baseband OFDM signal like the one which is being generated will be represented as in Figure

III.15, where the real and imaginary parts (in green and blue, respectively) are superimposed:

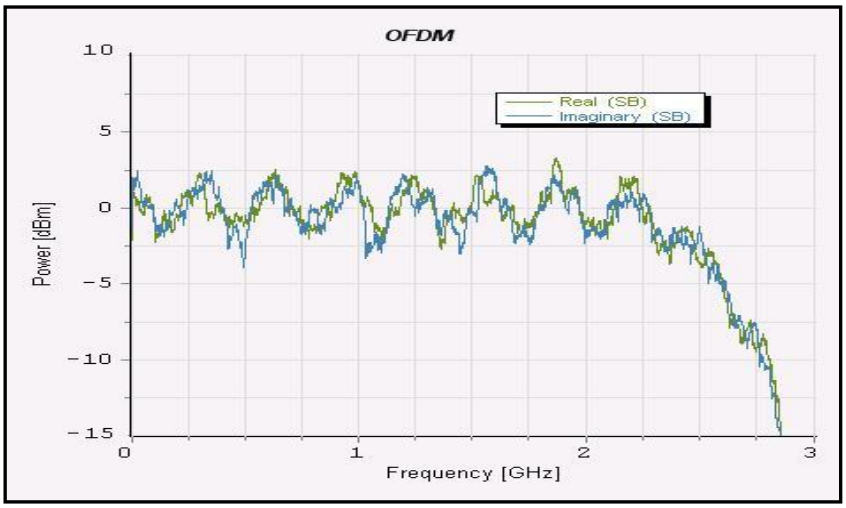

Fig. III.15 Superimposed OFDM signal spectrum [VPI]

Because of this superimposition of the signal, just half of the OFDM bandwidth will be represented. The OFDM signal bandwidth is calculated as the transmission bitrate divided by the number of bits per symbol, so the expected electrical bandwidth for this case should be 2.5 GHz, as just half of the spectrum is depicted.

The exceeding bandwidth of nearly 300 MHz that can be identified in Figure III.15 is due to the roll-off factor of the filter applied in the pulse shaping module.

Two more simulation results are shown in Figures III.16 and III.17, representing the transmitted electrical spectrum and received constellation diagram for the other two possible modulation types: Zero Padding and DMT. The parameters used for these simulations are the same as before.

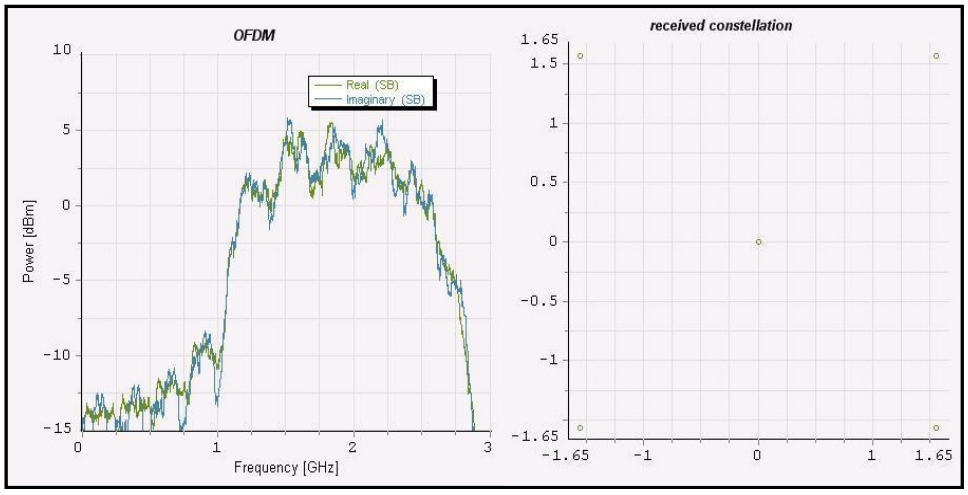

Fig. III.16 Zero Padding modulation [VPI]

For the Zero Padding simulation, zeros have been added at both edges of the IFFT input sequence, as said before. The resulting gap represents nearly half of the ideal signal bandwidth (that is, 2.5 GHz), as it can be seen in Figure III.16.

Again, the received constellation is ideal, though just half of the received information symbols are being represented due to the use of zero padding for half of the IFFT input sequence. This could be appreciated in a non-ideal channel transmission where dispersion would separate the received symbols in the constellation diagram. The zero padding observed could be used in accordance with the following section as a technique to avoid the RF upconversion stage and yet provide the required guard band for the use of conventional IM/DD optical transmission systems.

The spectrum of the transmitted signal for a DMT modulation can be seen in Figure III.17, where only the real part of the signal is represented, while the imaginary component is zero. It can be seen how the use of the complex conjugate in half of the input IFFT sequence allows the elimination of the negative band at a cost of reduced bitrate efficiency (see Annex A).

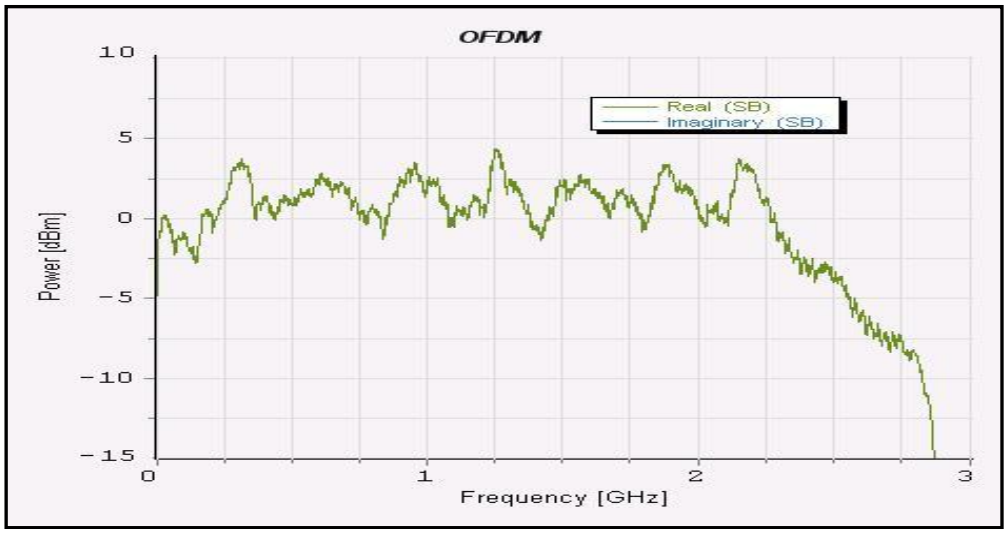

Fig. III.17 DMT modulation [VPI]

Other parameters such as cyclic prefix or bits per symbol will be changed in the simulations performed with custom modules in Chapter IV, so it can be seen the effect on both the signal spectrum and the received constellation.

III.3. OFDM for Long-Haul Transmission Demo

III.3.1. General schematic

In this simulation scenario, the OFDM signal is generated and detected as in the last demo, though two major changes are applied: those are RF frequency up/downconversion and optical signal modulation and demodulation. Also, the transmission is done over a 1000 km optical fibre link. Figure III.18 shows the universe schematic for the simulation, which can be found in the left panel labels of VPI-TM in: Optical Systems Demos/Long Haul/.

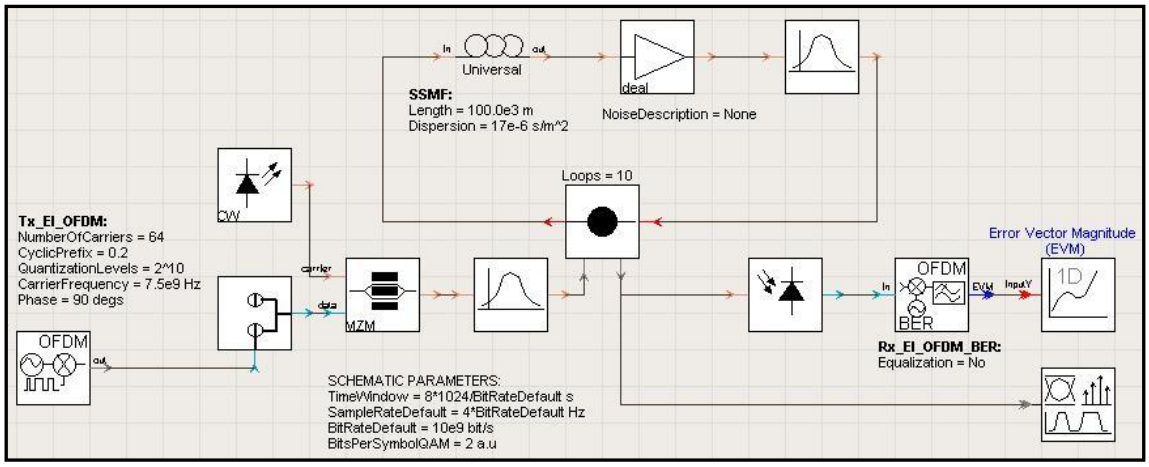

Fig. III.18 Universe of the *OFDM for Long-Haul Transmission* demo [VPI]

The OFDM coder module is now placed inside an OFDM transmitter galaxy (left bottom in the figure), where a frequency upconversion is applied to the signal after being generated, as it will be seen later by looking inside the galaxy. This technique was described in section I.3.1, and is used to create a gap between the OFDM signal spectrum and the electrical DC component, so the unwanted mixing products appearing due to the IM modulation and direct detection (DD) method used fall outside the OFDM bandwidth.

For a 10 Gbps bitrate with 4-QAM modulation, an OFDM bandwidth of 5 GHz is required and thus an RF carrier of 7.5 GHz is used to generate a 5 GHz gap. This will be seen at the simulation results section at the end of the chapter.

Once the signal is upconverted to an RF frequency, it is optically modulated by a Mach-Zehnder modulator (MZM), giving rise to the *RF upconversion based on Intensity Modulation* configuration described in section II.5.1.1 (Figure II.15).

Then, the optical signal is filtered to suppress the lower sideband (see section II.3 to see why optical single sideband is needed), and transmitted through a fibre link consisting of a loop circuit where the signal covers 100 km with amplification and filtering stages for each loop.

At the receiver side, a single photodiode is used in DD configuration, and the resulting photocurrent is fed to the OFDM receiver galaxy, which holds the

OFDM decoder module inside. The frequency downconversion is also applied within this module to recover the original baseband OFDM signal, just before the decoding functions.

Three kinds of output results are provided by this demo by using the corresponding visualizer modules:

- Received constellation: the required numerical analyzer is located inside the receiver galaxy
- Spectrum at the receiver input (right bottom visualizer in Figure III.18)
- The error vector magnitude (EVM) at the receiver output. This value can be considered as an indicator of how far the received constellation points are from their ideal location.

The *1D* numerical analyzer in charge of calculating the EVM will obtain information about the emitted sequence by means of the virtual optical channel feature of VPI. This means that the correct *ChannelLabel* value should be assigned to the module providing this information, which is placed inside the receiver galaxy (see section III.3.3).

The schematic parameters of this demo are the same as those of the OFDM Generation and Detection demo's universe parameters in Figure III.12, allowing the change of global parameters and the number of bits used to represent one QAM symbol.

However, the galaxies that represent the OFDM modulator and demodulator have a much more complicated structure, as described in the following sections:

III.3.2. Inside the OFDM transmitter module

As it can be seen from Figure III.19, the structure of the OFDM coding and pulse shaping functions is identical to the one used in the OFDM Generation and Detection demo (see Figure III.11).

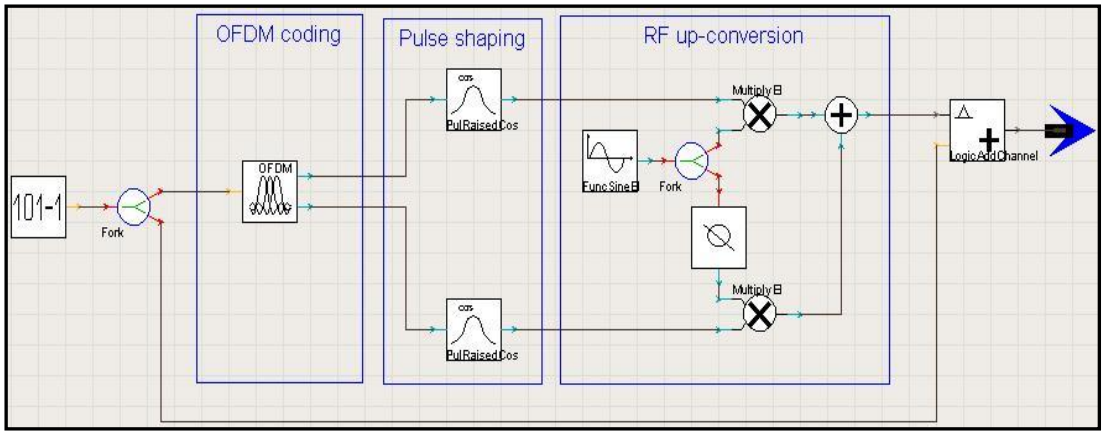

Fig. III.19 Schematic of the OFDM transmitter module [VPI]

However, this time an RF upconversion stage is added to convert the baseband OFDM signal into a passband centred at an RF frequency, in this case 7.5 GHz. This is simply done by multiplying both the real and imaginary components of the OFDM signal (that is, inphase and quadrature) by an electrical sine waveform provided by the *FuncSineEl* module. A 90º constant phase shift will be applied to the quadrature component, and both parts are added to form the upconverted electrical OFDM signal described in expression (I.6). This operation is performed by the *PhaseShiftEl* module, which connects the sine function generator to the lower branch of the schematic.

Once the final electrical OFDM signal is obtained, it is added to the *LogicAddChannel* module along with the original PRBS sequence. As it was said for the definition of the *LogicalInformation* global parameter, this module is used to send information between modules within the same simulation. For instance, the EVM will be calculated at the receiver without the need of any wires between it and the OFDM transmitter galaxy.

The available parameters of the transmitter module are shown in Figure III.20, where some new categories have been defined in order to achieve a better organization. Two of them are important to understand the simulation, so they are described below.

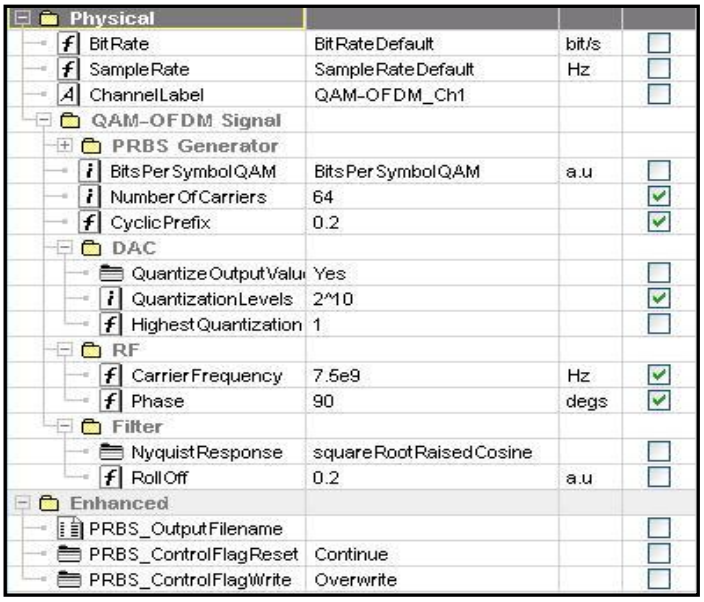

Fig. III.20 OFDM transmitter parameters [VPI]

- *ChannelLabel*: indicates the name of the logical channel. It must be the same for all of the modules using the original sequence that was added to the *LogicAddChannel* module.

- *CarrierFrequency*: Indicates the RF frequency at which the baseband OFDM signal will be upconverted. This value is set from the schematic parameter, so it will also affect the RF downconversion stage of the OFDM receiver galaxy.

The main category in this PEW is the *Physical* category, which contains the *QAM-OFDM Signal* subcategory. At the same time, *QAM-OFDM Signal* is divided into other subcategories, such as the PRBS generator, DAC, RF and Filter. As these smaller categories are declared as galaxy parameters, they can be edited from the main schematic by double-clicking on the module, without the need to look inside and change them on the corresponding module. The same can be applied to the OFDM receiver galaxy.

III.3.3. Inside the OFDM receiver module

Once again, the OFDM receiver module will perform the same operations as the transmitter in a reversed order. First of all the signal is downconverted by multiplying it by the same RF frequency as before and applying a 90º phase shift to the quadrature component, as shown in Figure III.21:

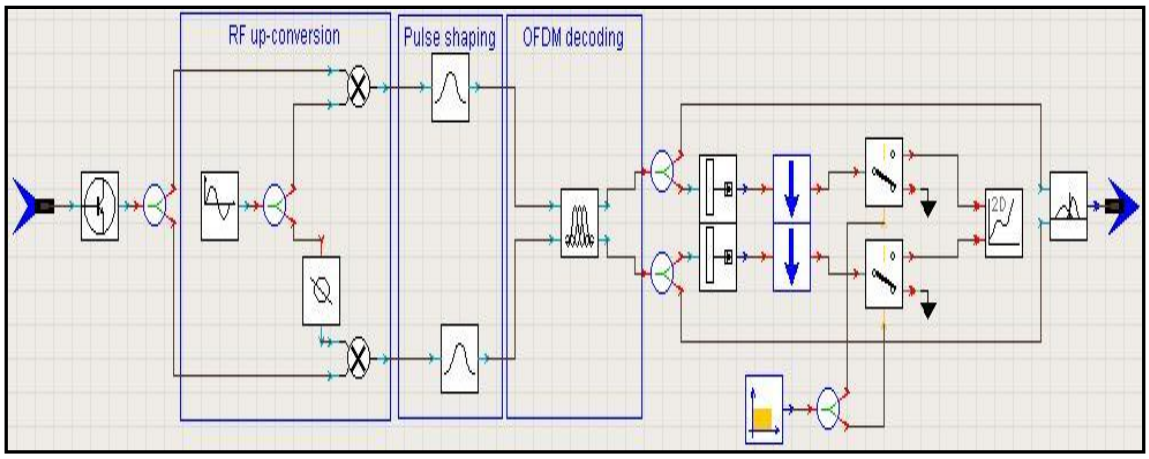

Fig. III.21 Schematic of the OFDM receiver module [VPI]

After that, both components pass through a pulse shaping filter and the resulting electrical signal is fed to the OFDM decoder module, which provides the decoded versions of the inphase and quadrature components.

The constellation diagram representation is done in a similar way as in the OFDM Generation and Detection demo, though this time another function is used between the decoder and the signal analyzer: two switches are connected to a rectangular pulse generator (lower module in the figure).

This modification is used to extract the redundant information inside the sequence, which was mentioned before. The rectangular pulse indicates the period of time in which the switches allow the signal to flow as an input to the signal analyzer module. The rest of time, any sequence coming from the decoder is going to be discarded. This way, only the received information symbols are going to be represented in the constellation diagram, omitting the padded zeros used to compensate for any differences between the effective and transmitted data rates.

The decoded OFDM sequence is also connected to another module (on the right edge of the image). This module is called *BER_El-mQAM*, and its function is to estimate the Symbol Error Rate (SER) and/or the EVM of an electrical mQAM signal, taking I and Q electrical signals as inputs. The module automatically performs clock recovery, amplitude and phase correction of the received constellation. Thus, it will be able to perform these calculations as long as its *ChannelLabel* parameter indicates the right logical channel name.

The following figure shows those parameters of the OFDM receiver module which have not appeared until now:

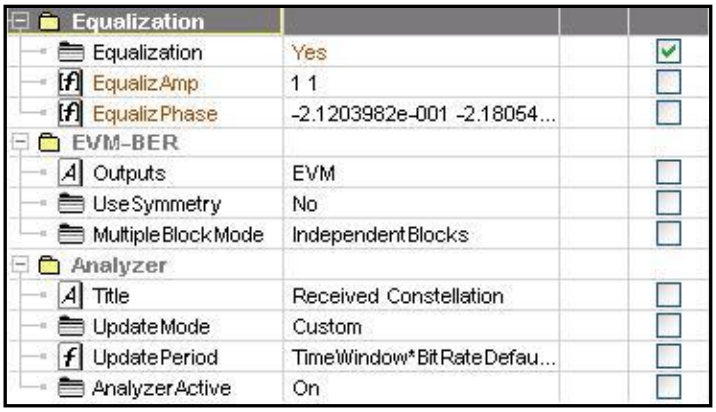

Fig. III.22 OFDM receiver parameters [VPI]

The *EVM-BER* and *Analyzer* categories deal with the representation settings for the EVM/SER and the received constellation, respectively. Thus, the parameters indicated in these categories are going to be applied on the *BER_El-mQAM* and signal analyzer modules.

The *Equalization* category (if the *Equalization* parameter is set to *Yes*) allows the compensation of the chromatic dispersion suffered by the OFDM signal during the optical channel transmission. The amplitude and phase coefficients to be used have to be written as values in the corresponding parameters in order to obtain the desired results. This should improve the EVM measure, as well as achieving a proper constellation representation with less dispersion between points (as shown in section III.3.5).

The equalizer coefficients for this demo are shown in Figure III.23, where Matlab has been used to represent the applied phase equalization array (in radians) for the 64 modulated subcarriers:

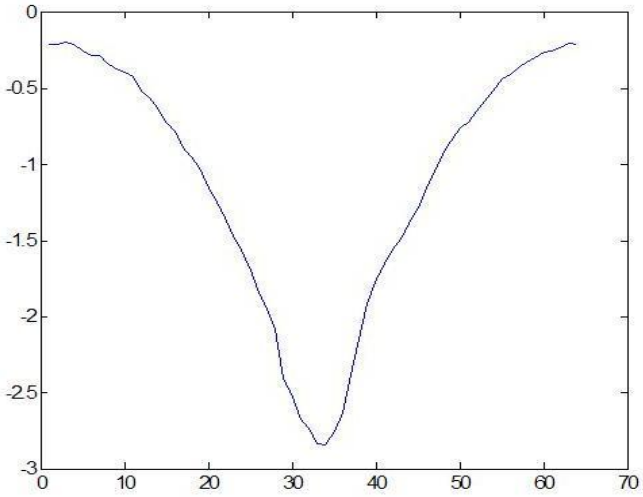

Fig. III.23 Phase equalization curve [VPI]

It is thought that these coefficients have been experimentally extracted from a training sequence after identifying the optical channel properties and are only valid for the specific settings in the demo. If, for instance, the length of fibre, the bit rate or the QAM levels are changed, a different sequence for the equalizer must be used, which is not provided by the demo.

It will be seen that the custom simulations use a very similar equalizer shape that comes from the simplified fibre model in which chromatic dispersion is considered as the only relevant effect.

III.3.4. Optical channel path

The optical channel path is composed by an optical modulation stage, the fibre link and a photodiode in direct detection configuration at the receiver.

Figure III.24 shows the optical modulation stage, where the two inputs of the MZM correspond to its driver (connected to OFDM coder output) and a laser at continuous wave (CW) mode.

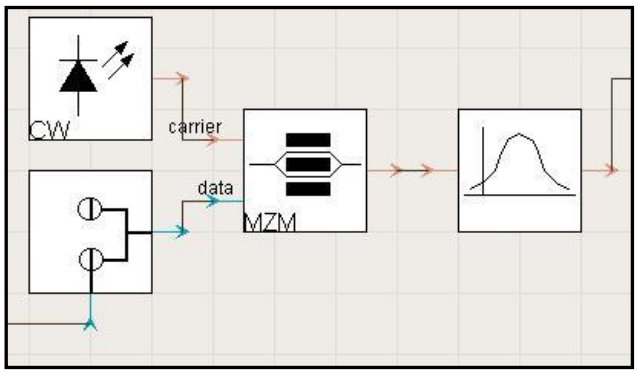

Fig. III.24 Optical modulation stage [VPI]

The driver basically sets the optical modulation index relative to the half-wave voltage of the MZM. Since the used MZM module is set by default at the quadrature point (QP), the bias is set to 0.

The laser operating at CW provides the optical carrier to be modulated, and its most relevant parameters are:

- Emission frequency: 193.12 THz.
- Average power: 5 mW
- Linewidth: 1 MHz

Meaning that the laser operates at 3rd window, and thus the dispersion coefficient of the optical fibre has to be set accordingly. A random noise is generated in the laser, where the maximum allowed spectral density variation within the noise bandwidth is set to 3 dB.

An optical filter is then used to suppress the lower sideband resulting from the optical modulation. The used filter is of Gaussian type, centred at $f = f_o + f_{RF}$, where f_o is the optical carrier frequency (193.12 THz) and $f_{RF}$is the electrical carrier frequency at which the electrical OFDM band was upconverted (7.5 GHz). The filter bandwidth is set to 18 GHz.

As it can be seen from Figure III.18, the fibre link is composed of a loop where a universal fibre module simulates the wideband nonlinear signal transmission over optical fibre. After the fibre span, the signal goes through amplifying and filtering stages to compensate for attenuation. The number of loops of the link is set to 10, so for a fibre length of 100 km (default) the transmission distance will be 1000 km.

The most important parameters of the fibre for this simulation are the ones belonging to the *Physical* category, as represented in Figure III.25:

Physical			
Number Of Fiber Spans	1		☐
Length	100.0e3	m	☑
Attenuation Description	Attenuation Parameter		☐
Attenuation	0.2e-3	dB/m	☐
Reference Frequency	(193.1e12+7.5e9)	Hz	☐
Dispersion Description	Dispersion Parameters		☐
Dispersion	17e-6	s/m^2	☑
Dispersion Slope	0.08e3	s/m^3	☐
PMD Coefficient	0.1e-12/31.62	s/(m...	☐

Fig. III.25 Optical fibre physical parameters [VPI]

The used attenuation and chromatic dispersion coefficient ($17 \cdot 10^{-6} s/m^2$) are typical values for a transmission in 3rd window. The rest of values are set to default.

Another important parameter to take into account is the *ReferenceFrequency*. This frequency is where the dispersion characteristic of the fibre is centred. It means that the optical group delay is considered zero at the specific frequency, and therefore the waveforms in that subcarrier frequency are the ones at the beginning of the time sequence at the receiver end.

Since the dispersion coefficient D (derivative of the group delay against wavelength) in 3rd window is positive, the lower frequencies will arrive later (after the reception window time has started) and higher frequencies will arrive sooner (before the reception window time has started). This will be an important concept to bear in mind for the correct choice of this reference frequency in the simulations.

It is interesting to see that this reference frequency is set in the demos equal to the sum of the optical carrier and the RF carrier, just at the optical frequency where the OFDM spectrum is centred. The analysis about how and why to choose the reference frequency precisely equal to that value and the derived implications is carried out in section IV.3.4.

At the receiver, after DD and decoding, chromatic dispersion is compensated by correcting the phase of each sub-carrier separately. The equalized phase offsets correspond to the relative accumulated dispersion values experienced by each sub-carrier during its transmission through optical fibre.

III.3.5. Simulation results

A list of the parameters used for this demo can be found below. These will be the basis from where the simulations in the following chapter have been done. If different values for any of these parameters are used, it will be explicitly stated.

- *BitRateDefault* = 10e9 bps
- *TimeWindow* = 8*1024/BitRateDefault seconds
- *SampleRateDefault* = 4*BitRateDefault samples/second
- *BitsPerSymbolQAM* = 2
- *NumberOfCarriers* = 64
- *CyclicPrefix* = 0.2
- *CarrierFrequency* = 7.5 GHz
- *Reference frequency* = 193.1 THz + CarrierFrequency

As the equalization coefficients represented in Figure III.23 are only calculated for the dispersion parameters shown in Figure III.24 in a 1000 km transmission distance (10 loops), any change in the fibre Physical parameters will distort the form of the received constellation.

With this, once the simulation is executed, the VPI Photonics Analyzer tool will display the received optical spectrum, the received constellation diagram and its corresponding EVM.

The received optical spectrum is plotted just after the fibre link, before the signal is detected by the photodiode. The result is shown in Figure III.26:

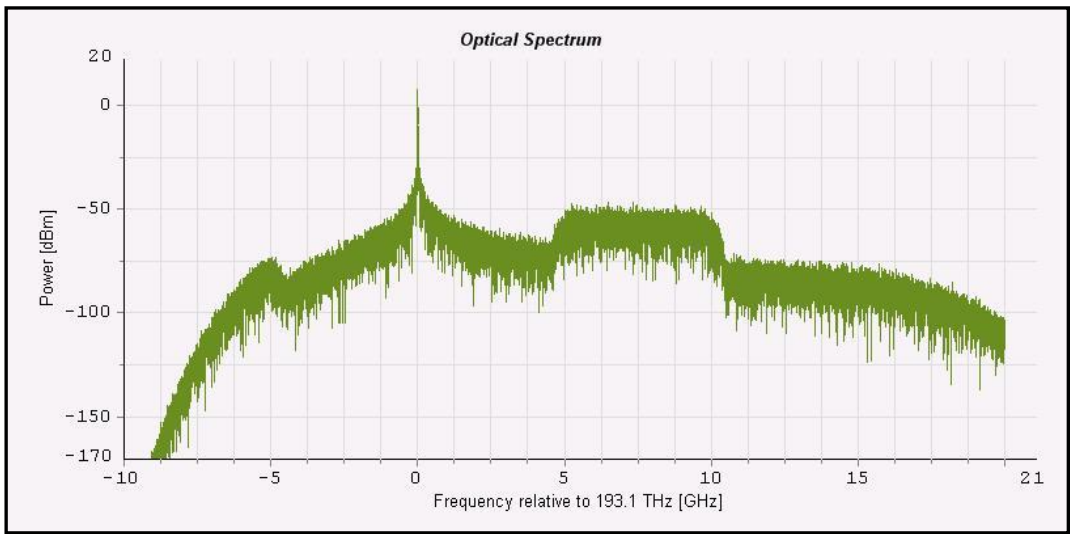

Fig. III.26 Optical signal before photodetection [VPI]

The frequency values (in GHz) in the *x* axis are relative to 193.1 THz, so this is the real frequency for the 0 Hz value in the graph. This will also be the frequency for the optical carrier signal, which is separated by a 5 GHz gap from both the suppressed lower sideband (left in the graph) and the optical OFDM signal centred at 7.5 GHz from the optical carrier. This gap is the one in which the mixing products appearing due to direct detection will fall off.

This is the only graph showing the OFDM signal in the schematic, so other analyzer modules will be used in the next chapter's simulations in order to evaluate the signal spectrum at each stage.

At the receiver, if the *Equalization* parameter is set to *No*, there is no phase correction and the received constellation continuously rotates as explained in section II.2. This is shown in Figure III.27, which results in an EVM of 1.007.

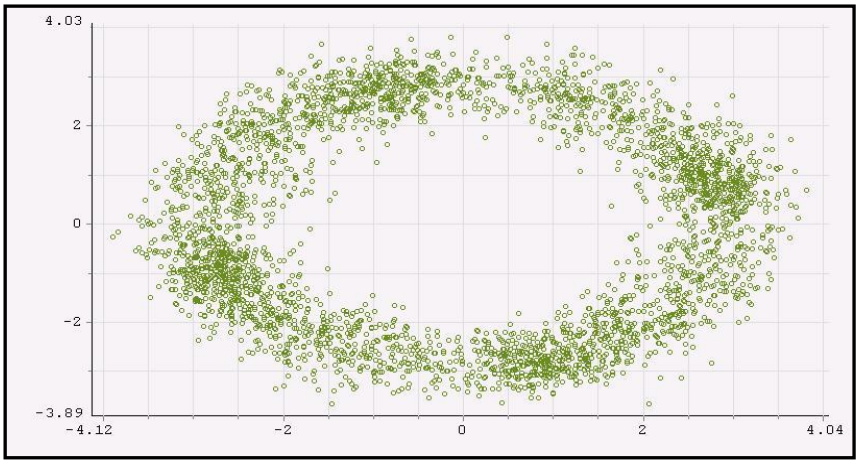

Fig. III.27 Received constellation without equalization [VPI]

Figure III.28 shows the received constellation when the Equalization parameter is set to *Yes*, and the before mentioned equalization coefficients are properly indicated in the PEW. The situation of the constellation points results in an EVM of 0.177, obtaining an obvious improvement with respect to the previous results.

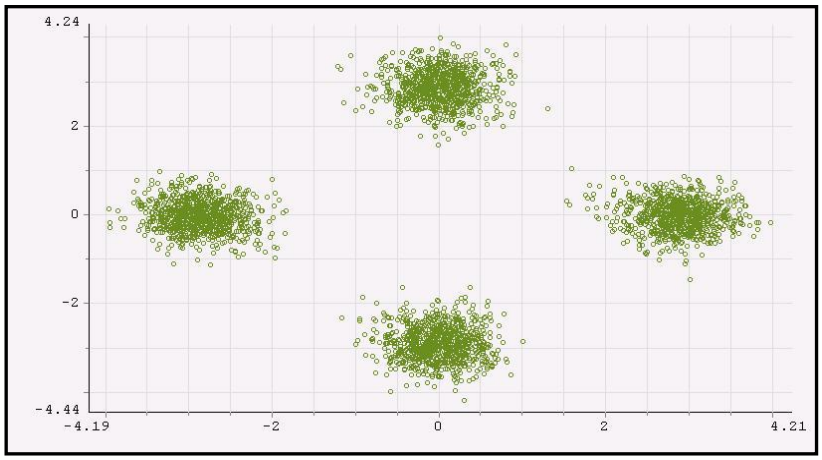

Fig. III.28 Equalized received constellation [VPI]

It is worth mentioning that the expected constellation should have the form of a typical 4-QAM. Instead, a 45º rotation is found. This point will be studied in more detail when describing the results for the customized simulations.

As it has been said before, the equalization coefficients used in this demo can only be used for a 1000 km transmission distance. This will not happen in the simulations performed in the next chapter, where an ideal equalization only based on the effect of chromatic dispersion is used for any distance, obtaining the corresponding equalized constellation diagram. What this result also shows is that for the default fibre and laser parameters considered, indeed, chromatic dispersion is the main effect to equalize.

Also, no significant effect can be seen when applying cyclic prefix to the sequence, meaning that the received constellation diagram in Figure III.28 will have the same appearance for any CP value, apart from the fact that less information symbols are going to be represented as more cyclic prefix is added. A possible explanation for this issue would be an incorrect procedure of the cyclic prefix extraction at the receiver, as explained in section IV.3.4.

The lack of transparency in the coder and decoder operations can also be pointed again as an aspect to improve for this demo.

Moreover, the use of zero padding for the OFDM coder and decoder is configured to create a gap between the OFDM signal and the optical carrier, though in this demo this gap is created by means of frequency upconversion. Thus, the use of zero padding is useless in this scenario as long as the up/downconversion stages are not removed. Another possibility that will be taken into account in the next chapter's simulations is the use of zero padding as an oversampling technique.

CHAPTER IV - CUSTOMIZED SIMULATIONS

This chapter deals with the customized simulations performed in VPI. These simulations were built to perform the same functions as the last chapter's demos, though they present a transparent operational system which can be modified even from the lowest level (that is, from the code sentences).

Before describing the simulations, the customized modules built in VPI and its related parameters are described, so the different system operations can be understood when having a look at the simulation scenarios.

In order to understand each step for the creation of these modules, it is necessary to comprehend the Matlab code that will be executed when running the simulations. Hence, brief extracts of the code are introduced while describing the modules. All the coding functions can be found in Annex D.

IV.1. Custom modules and Matlab code implementation

IV.1.1. Parameter settings

Before getting into the operation of the customized modules, it is important to understand the parameters that will be used by them. Some of these parameters have already been defined in the last chapter, so this section will focus on the reasons why determined values are assigned to the parameters.

IV.1.1.1. Fulfilling VPI restrictions

Expression (III.1) in the previous chapter indicates that the product of the simulation time window and the used sampling rate must be a power of 2. Another simple rule to avoid problems when running a simulation in VPI is that the product of the time window and the bitrate is also set to a power of 2.

A good way to meet these rules is to first decide on a bitrate and then set the *SampleRateDefault parameter* so that the ratio *SampleRateDefault*/ *BitRateDefault* is a power of 2. Also, the *TimeWindow* parameter should be set to equal the number of bits in a simulated block dived by the bitrate. The number of bits has to be a power of 2. Following these tips, the parameter values for the customized simulations will be:

- *BitRateDefault* = 10e9 bps
- *SampleRateDefault* = 4**BitRateDefault* = 40e9 Hz
- *TimeWindow* = 8*1024/*BitRateDefault* = 819.2 nsec

Thus, the simulated sequence will consist of a block of 8*1024 = 8192 bits transmitted at 10 Gbps, resulting in a temporal window of 819.2 nanoseconds.

These parameters must be taken into account when processing the input bit sequence in the Matlab code, so they will be declared as cosimulation input parameters, as shown in the next section.

IV.1.1.2. Coding parameters

This schematic category contains the parameters affecting the coder and decoder modules, which are listed below:

- *BpS*: Number of bits used to represent each QAM symbol. The most typical values are 2 and 4, giving rise to a 4-QAM and a 16-QAM modulation, respectively.
- *Nc*: Number of information subcarriers entering the IFFT operation (also exiting the FFT). The symbols representing each subcarrier will be modulated in an X-QAM, where X depends on the *BpS* parameter.
- *N_FFT*: Total number of inputs of the IFFT stage (also FFT). This parameter determines the quantity of oversampling by means of zero padding added to the transmission. For instance, a 32 input IFFT with *Nc* set to 16 means that half of the IFFT (the 16 central positions) is padded with zeros.[1]
- *CP*: Cyclic prefix relative to the OFDM symbol length, ranging from 0 to 1. Typical values of CP in a real OFDM transmission range from 10 to 20%, so this parameter should be given a value between 0.1 and 0.2.

IV.1.1.3. RF galaxies' parameters

As the OFDM signal will be up/downconverted in the optical OFDM simulations, the *RF galaxies* category will be created to hold the parameters concerning the electrical up/downconversion. Those are:

- *CarrierFrequency*: As in VPI's demos, this parameter indicates the RF frequency at which the baseband OFDM signal will be upconverted at the transmitter, and then downconverted at the receiver.
- *Phase*: Value of the phase shift (in degrees) to be applied by the *PhaseShift* module, as explained in the last chapter.
- *RollOff*: The ratio of excess bandwidth above the filter's cut-off frequency.

[1] The Nc and N_FFT parameter values must be even, so the IFFT input sequence is properly allocated

Any change in these parameter values from the universe's PEW will affect both the upconverter and downconverter modules, so just one change is required for it to be effective in the modulator and demodulator.

This is an added feature with respect to the VPI demos, where the change of the value on any of the above parameters needs to be made in both the modulator and demodulators' PEWs.

IV.1.2. Code structure

In this section, the basic structure of the Matlab code is explained, describing the order in which the operations are carried out inside the coder and decoder modules. The specific code sentences used to process data will be inserted during the following subsections in order to provide an easier understanding for the use of each new module and code sentence.

The Matlab code for the OFDM coder module will need to process 6 parameters: those are the *TimeWindow* and *BitRate* global parameters and the four parameters belonging to the *Coding parameters* category. Apart from that, the bit sequence coming from the PRBS generator should also be declared (a detailed description of this process can be found in the next subsection). Thus, for an output data vector *y*, if *prbs* represents the incoming bit sequence, the main function for the OFDM coder Matlab code will be:

```
function[y]=ofdm_coder(prbs,TimeWindow,BitRate,BpS,Nc,N_FFT,CP)
```
(IV.1)

In a similar way to the VPI coder module, the first thing that the ofdm_coder function does is to calculate the required number of bits to represent the OFDM signal according to the indicated parameters.

It starts by calculating the number of OFDM symbols that can be contained in the sequence, taking into account the CP and zero padding overheads. This is calculated as:

```
NTS_OFDM=floor(length(x1)/(BpS*ceil(N_FFT*(1+CP))));
```
(IV.2)

Where *x1* is a previously defined vector containing the whole input sequence as expressed below:

```
x1=prbs(1:TimeWindow*BitRate);
```
(IV.3)

Once the total number of OFDM symbols is calculated, since each OFDM symbol contains Nc information symbols, the number of QAM information symbols (*NTS_INFO*), as well as the total number of bits representing the OFDM signal (*NTB_INFO*) are obtained:

```
NTS_INFO=NTS_OFDM*Nc;

NTB_INFO=NTS_INFO*BpS;
```
(IV.4)

Because the number of OFDM symbols may not exhaust the whole input sequence, a determined number of bits may be left aside, since they are not enough to form another complete OFDM symbol.

For instance, for a 200 bit input sequence, if the OFDM coder uses 8 subcarriers to modulate the information symbols with a 4-QAM and 2xoversampling configuration (N_FFT = 16), the total number of bits when a cyclic prefix of 10% is being used would be allocated into:

$$NTS\_OFDM = floor\left[\frac{200}{(2*ceil(16*1,1))}\right] = 5\ OFDM\ symbols \qquad \textbf{(IV.5)}$$

From these 5 OFDM symbols, 40 information symbols would contain the 80 bits of the sequence used to represent the OFDM signal. An OFDM symbol would have a total length of 36 bits, from which only 16 would contain information and 20 would be overheads, 16 for zero padding and 4 for cyclic prefix.

Therefore in the 200 bits sequence 5 OFDM symbols can be allocated, yielding a total of 80 (40) information bits (QAM symbols) + 80 (40) zero padding bits (QAM symbols) +20 (10) CP bits (QAM symbols) = 180 (90) bits (QAM symbols). The residual 20 (10) bits (QAM symbols) are the left aside, since they are too few to form another complete OFDM symbol. For this, 36 bits (18 QAM symbols) would be required. These left aside bits would have also to be taken into account for an errorless simulation to be carried out. Note that these means a bitrate efficiency of 80/200 = 40% of the original bitrate.

Instead of transmitting just 90 of the 100 possible symbols (the simulator would not allow it anyway), the remaining 10 symbols will be padded with zeros before transmitting the sequence, and then extracted at the receiver side as soon as the input sequence is detected.

As in the VPI demos cases, the reason to do that is the need to compensate for the difference between the original and the effective bitrates (or symbol rates in this case), so the signal can be properly processed in VPI.

Following with the last example, once the required values to allocate the bit sequence are calculated, the amount of bits corresponding to the signal representation (80) is modulated in 4-QAM according to the *BpS* parameter, obtaining a set of 40 complex symbols.

These symbols are reorganized into a matrix of Nc rows and NTS_OFDM files, resulting in an 8x5 matrix containing the OFDM symbols used to represent the OFDM signal. This matrix is shown in Figure IV.1, where the coder functions for the parameter values of the example have been executed in Matlab.

```
xx1_OFDM_INFO =

  -1.0000 + 1.0000i  -1.0000 - 1.0000i   1.0000 - 1.0000i  -1.0000 - 1.0000i   1.0000 + 1.0000i
  -1.0000 - 1.0000i   1.0000 + 1.0000i   1.0000 + 1.0000i  -1.0000 - 1.0000i   1.0000 + 1.0000i
   1.0000 - 1.0000i  -1.0000 - 1.0000i   1.0000 + 1.0000i  -1.0000 + 1.0000i   1.0000 + 1.0000i
  -1.0000 - 1.0000i  -1.0000 + 1.0000i  -1.0000 - 1.0000i   1.0000 + 1.0000i   1.0000 + 1.0000i
  -1.0000 + 1.0000i  -1.0000 + 1.0000i  -1.0000 + 1.0000i   1.0000 + 1.0000i  -1.0000 + 1.0000i
   1.0000 - 1.0000i   1.0000 + 1.0000i   1.0000 - 1.0000i  -1.0000 + 1.0000i   1.0000 + 1.0000i
   1.0000 + 1.0000i   1.0000 + 1.0000i   1.0000 + 1.0000i   1.0000 + 1.0000i   1.0000 - 1.0000i
   1.0000 - 1.0000i   1.0000 - 1.0000i  -1.0000 - 1.0000i  -1.0000 + 1.0000i   1.0000 + 1.0000i
```

Fig. IV.1 *Nc* x *NTS_OFDM* matrix containing the information symbols [Matlab]

After that, the indicated amount of zero padding is inserted as rows in the middle of the matrix, obtaining a *N_FFT* x *NTS_OFDM* matrix. This is shown in Figure IV.2:

```
xx1_OFDM_ZP =

  -1.0000 + 1.0000i  -1.0000 - 1.0000i   1.0000 - 1.0000i  -1.0000 - 1.0000i   1.0000 + 1.0000i
  -1.0000 - 1.0000i   1.0000 + 1.0000i   1.0000 + 1.0000i  -1.0000 - 1.0000i   1.0000 + 1.0000i
   1.0000 - 1.0000i  -1.0000 - 1.0000i   1.0000 + 1.0000i  -1.0000 + 1.0000i   1.0000 + 1.0000i
  -1.0000 - 1.0000i  -1.0000 + 1.0000i  -1.0000 - 1.0000i   1.0000 + 1.0000i   1.0000 + 1.0000i
         0                  0                  0                  0                  0
         0                  0                  0                  0                  0
         0                  0                  0                  0                  0
         0                  0                  0                  0                  0
         0                  0                  0                  0                  0
         0                  0                  0                  0                  0
         0                  0                  0                  0                  0
         0                  0                  0                  0                  0
  -1.0000 + 1.0000i  -1.0000 + 1.0000i  -1.0000 + 1.0000i   1.0000 + 1.0000i  -1.0000 + 1.0000i
   1.0000 - 1.0000i   1.0000 + 1.0000i   1.0000 - 1.0000i  -1.0000 + 1.0000i   1.0000 + 1.0000i
   1.0000 + 1.0000i   1.0000 + 1.0000i   1.0000 + 1.0000i   1.0000 + 1.0000i   1.0000 - 1.0000i
   1.0000 - 1.0000i   1.0000 - 1.0000i  -1.0000 - 1.0000i  -1.0000 + 1.0000i   1.0000 + 1.0000i
```

Fig. IV.2 *N_FFT* x *NTS_OFDM* matrix with zero padding [Matlab]

The 16 rows of this matrix form the input sequence of the IFFT. Thus, one inverse fast Fourier transform will be applied to each column, obtaining another 16 x 5 matrix of complex numbers, representing the symbol values for the temporal sequence of the OFDM signal.

After that, the corresponding CP quantity is added. In this case, it has been said that the CP requires the space for 10 QAM symbols, so the last 2 rows of the matrix (2 rows x 5 columns means 10 symbols) are copied to the beginning of a new matrix where the rest of it is left as before, resulting in an 18x5 matrix.

The last matrix will be serialized into a vector *y* which will be the sequence at the output of the coder, including the 10 zero-valued symbols at the end of it to compensate for the expected symbol rate.

The Matlab code corresponding to the decoder module will also need the same input parameters as in the coder except for the input sequence, which will not be the original one but the real and imaginary components of the OFDM signal (*y_real* and *y_imag*), as explained in Chapter III for the VPI demos.

Moreover, no less than 5 variables are going to be extracted from the code once it is processed. Those are the decoded bit sequence (*zz*) and two versions of the decoded real and imaginary components of the signal: one without symbol rate compensation (*I* and *Q*) and a compensated one (*I_EVM* and *Q_EVM*). As it can be deduced by their name, the latter components will be used for EVM calculation, while the first ones will be represented as constellation points by the signal analyzer. Thus, the main function of the decoder is expressed as:

```
function [I Q I_EVM Q_EVM zz] = ofdm_decoder_simu
  (y_real,y_imag,BitRate,TimeWindow,BpS,Nc,N_FFT,CP)
```
(IV.6)

Here, the same operations as in the coder are applied in the opposite order. First the zeros used to compensate for the bitrate difference are extracted, and then the sequence is parallelized (converted into a matrix) before extracting the rows corresponding to the cyclic prefix and performing the fast Fourier transform on a column-by-column basis. Next, the zero padded rows used for oversampling are removed from the FFT output matrix, so the matrix containing the original QAM information symbols should be recovered.

It will be seen that this is true for the simulations performed in the next section, where an ideal channel is used to transmit the electrical OFDM signal. However, when being transmitted on optical fibre the received signal will suffer from phase errors due to chromatic dispersion, so the corresponding equalization should be applied at this point.

For this reason, expression (IV.8) has been added to the Matlab code after performing the FFT operation, based on the ideal phase compensation expression (II.19) in Chapter II:

```
ephase=exp(-((lambda)^2/c*D*pi*((BW.*[0:1:(Nc/2)-1,
       -Nc/2:1:-1]./N_FFT)).^2)*L*i);
```
(IV.7)

Previously, the variables needed to perform this calculation should be defined according to the desired parameters (see Annex D).

However, it will be seen in section IV.3.4 that an additional equalization should be performed in order to compensate for a temporal delay which is different for each arriving subcarrier due to chromatic dispersion and the FFT window starting point, which is going to be changed with the CP extraction strategy explained in the same section.

Once equalized, the signal is serialized again and the inphase and quadrature components are ready to be extracted.

The final step is to demap the sequence, ideally obtaining the transmitted sequence of information bits, which is also going to be compensated (zero padded) for BER measuring.

IV.1.3. OFDM Coder

This module is responsible for coding a pseudo-random bit sequence (PRBS) into an OFDM signal. It has been seen that inside the coder the bit sequence will be transformed into a complex-valued matrix with each column representing an OFDM symbol ready to be transmitted according to the indicated coding parameters. The module's output (*y*) will be a serial sequence of this matrix.

Externally, this module consists of an input connected to a PRBS generator and an output carrying the coded OFDM signal, as shown in Figure IV.3:

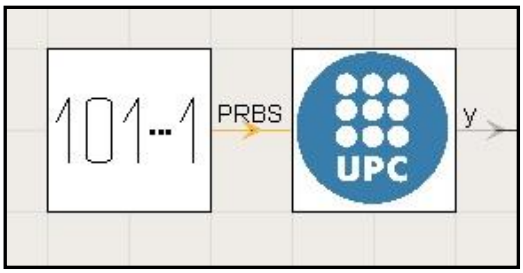

Fig. IV.3 PRBS generator connected to the OFDM coder [VPI]

The six parameters which will be accessed by the Matlab code must be created for this galaxy, all of them indicating the universal parameter name in the value field so they can be changed from the universe schematic, where they should also be defined.

Figure IV.4 shows the resulting Parameter editor for the OFDM coder galaxy, which will be the same for the OFDM decoder galaxy.

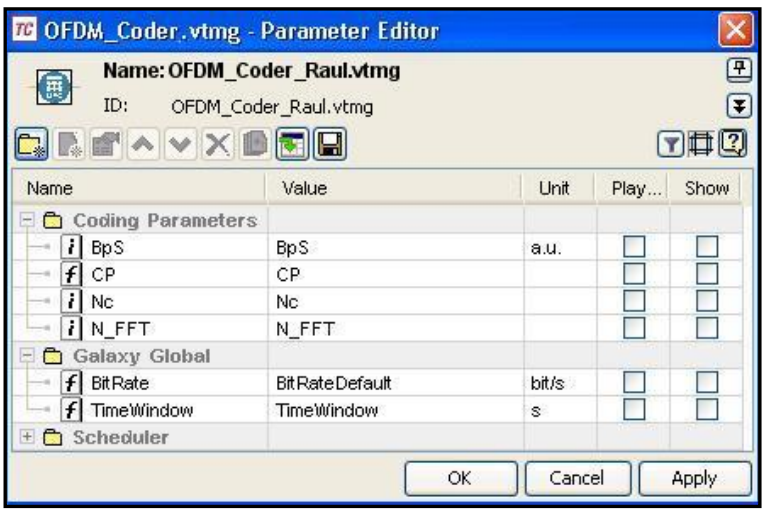

Fig. IV.4 OFDM coder (and decoder) Parameter editor [VPI]

By looking inside the module, it can be seen that the incoming bit sequence needs to be adapted in order to be used inside a Matlab code. Figure IV.5

shows the OFDM coder galaxy schematic, where the blue arrows represent the input (left) and output (right) ports.

The main block in this schematic is the CoSim module, which will act as an interface between VPI and Matlab. The rest of blocks are used to first declare the input bit sequence to the CoSim module, and then indicate the desired variable to extract from the code once it has been executed.

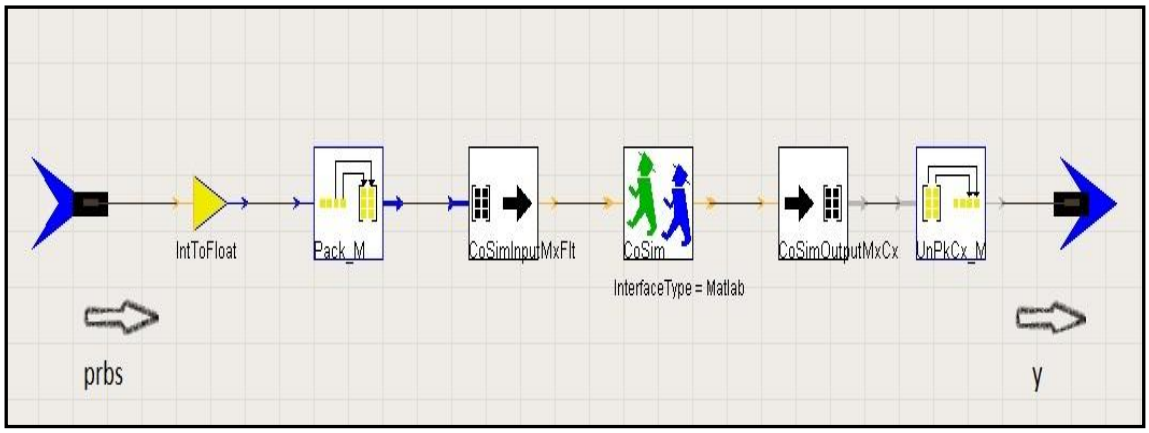

Fig. IV.5 Internal view of the OFDM coder [VPI]

For this, the PRBS coming from the input port is first converted from integer to floating values by means of the *IntToFloat* star. This is because the modules offered by VPI to declare or extract any variable from a Cosimulation operation do not work with integer numbers, but only with electrical or optical signal samples, complex numbers or floating point values.

Once converted, the *Pack_M* module produces an MxN matrix with the floating-point entries, filling the first row from left to right using the first N input values. In this case, the main interest is to create a vector to be processed by the Matlab code, so the parameters indicated to the module will be 1 row and $Bitrate \cdot TimeWindow$ columns, i.e. the whole input sequence of bits.

Next, the floating-point vector is processed by the *CoSimInputFlt* module, which declares a floating-point input variable to the CoSim block. It is important to remember that the name of this variable has to match with the one being used in the Matlab code, so the parameter name for this module must be *prbs*.

The CoSim module will then access the Matlab code, providing the values for the 6 input variables. As explained in Chapter III, this is simply done by indicating the code's main function name in the *RunCommand* parameter, not forgetting to attach the Matlab file to the *Input* folder of the galaxy schematic.

The CoSim module output is connected to another module which indicates the desired variable to extract from it once the cosimulation has been performed. Since the output signal of the OFDM coder is a complex vector where each value represents one symbol, so the *CoSimOutputMxCx* module has been chosen for this purpose, indicating the output vector *y* in the *Name* parameter.

The obtained vector size is then declared as an MxN matrix by means of the *UnPkCx_M* module. The size of this vector will depend on the number of bits used to represent each QAM symbol, so the matrix size to be indicated in this module will be 1 row x ($BitRate \cdot TimeWindow/BpS$) columns.

IV.1.4. OFDM Decoder

The description of the OFDM decoder Matlab code in section IV.1.2 indicated that 5 variables where extracted from it after the execution. Here, just two of them will be explained for simplicity. The 5-output configuration for the OFDM decoder will be seen in the simulations performed in section IV.3.

Thus, the OFDM decoder module will consist of two inputs and two outputs, as shown in Figure IV.6. This is because the real and imaginary parts are treated independently during the OFDM signal transmission, so the inphase and quadrature components can be created as described in Chapter I for a proper signal representation.

Fig. IV.6 OFDM decoder

The parameters to be created in this module are the same as those of the coder, shown in Figure IV.4. All of these parameters will be used by the Matlab code executing the decoder functions.

Internally, the decoder configuration is not so different from that of the coder, though four variables are processed. Figure IV.7 shows the decoder schematic with four ports, one for the input and output of each part of the signal.

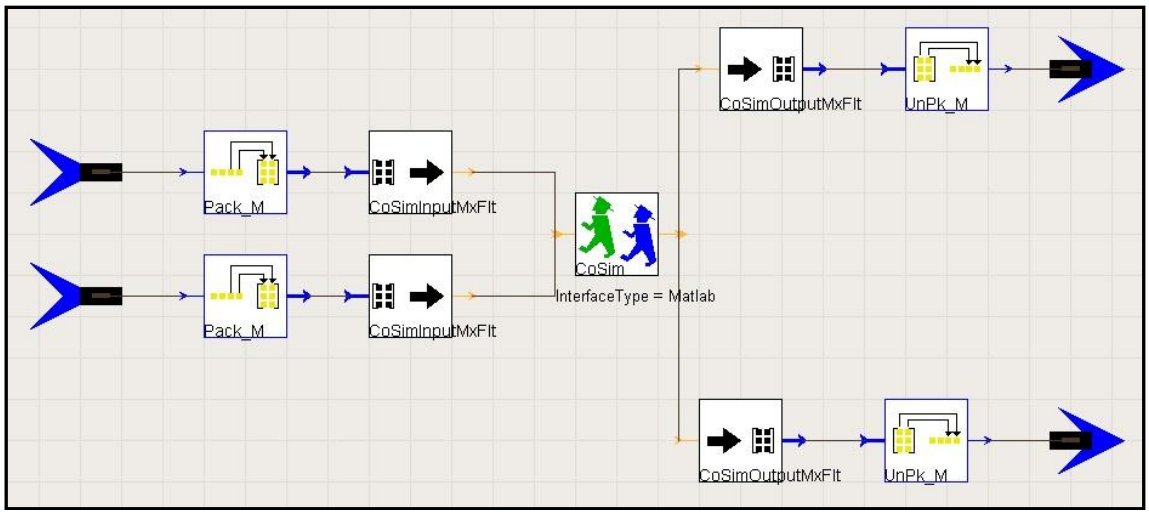

Fig. IV.7 Internal view of the OFDM decoder

For each signal component, the incoming values are inserted into a matrix with the same size as the one created at the coder output: 1 row x ($BitRate \cdot TimeWindow/BpS$) columns. Then the real and imaginary parts are named *y_real* and *y_imag* by the *CoSimInputMxFlt* modules and they are fed to the *CoSim* module, where both variables are going to be an input to the main code function along with the galaxy parameters.

As in the coder case, once the Matlab file is inserted into the *Input* folder of the scenario, the main function of the decoder code must be indicated in the *RunCommand* parameter of the *CoSim* module, so the desired output values are extracted from the code when its execution is finished.

It has been decided that the output of the CoSim module should be the received inphase and quadrature components of the signal, so after the proper resizing they can be represented in a numerical analyzer as the received constellation points. Thus, the extracted variables will be inserted into a 1xN matrix, where N has the following size:

$$N_c \cdot floor[TimeWindow \cdot BitRate/(BpS \cdot ceil[N\_FFT \cdot (1 + CP)])] \qquad \textbf{(IV.8)}$$

This size corresponds to the number of information symbols (or QAM symbols) within the OFDM transmission. The possible ideal values for these symbols with a 4-QAM subcarrier modulation are: (-1 - i), (-1 + i), (1 - i) and (1 + i).

Figure IV.8 is an example of this configuration for a 4-QAM modulation of the OFDM subcarriers, where a perfect constellation is received because of a transmission through an ideal channel.

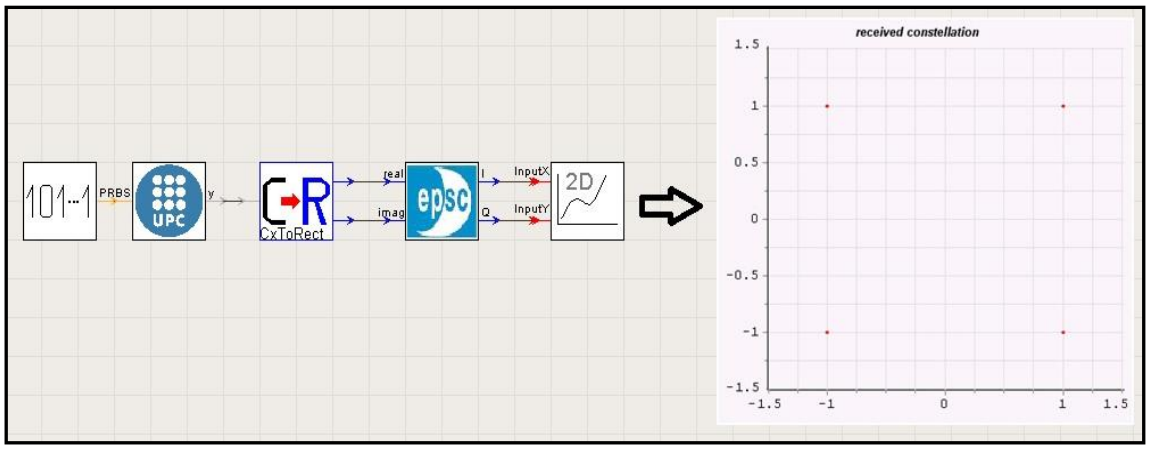

Fig. IV.8 OFDM transmission through an ideal channel

Note that a module has been inserted between the coder and decoder, which function is to separate the real and imaginary parts of an incoming set of complex numbers.

If the decoded stream of bits is wanted at the OFDM decoder output in order to compare it with the original PRBS sequence for a BER study, the *CoSimOutputMxFlt* module should be used, indicating the name of that variable in the decoder Matlab code (in this case, *zz*).

After that, the UnPack_M module should indicate the corresponding vector size so it can be available at the output of the module. Then, both the decoded and the original sequence can be compared through a BER estimator module provided by VPI, or by means of the customized sequence comparer presented in section IV.1.6.

IV.1.5. RF up/downconverters

These modules are in charge of performing the RF upconversion at the transmitter and the corresponding RF downconversion at the receiver. The external appearance of both of them is shown in Figure IV.9, where the RF upconversion module is connected to the OFDM coder and the RF downconverter outputs are fed to the decoder module as the received I and Q components of the baseband OFDM signal.

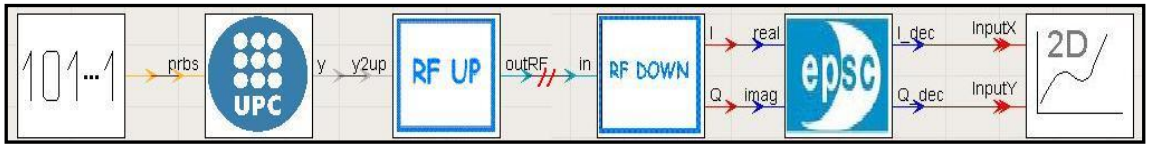

Fig. IV.9 RF up/downconverters connected to the OFDM coder and decoder

Their internal structure is very similar to those of the OFDM transmitter and receiver modules used in the Long-Haul Transmission demo.

However, it is important to notice a couple of differences between the RF upconversion stage in VPI's OFDM transmitter and the customized RF upconversion module, which internal schematic is shown below:

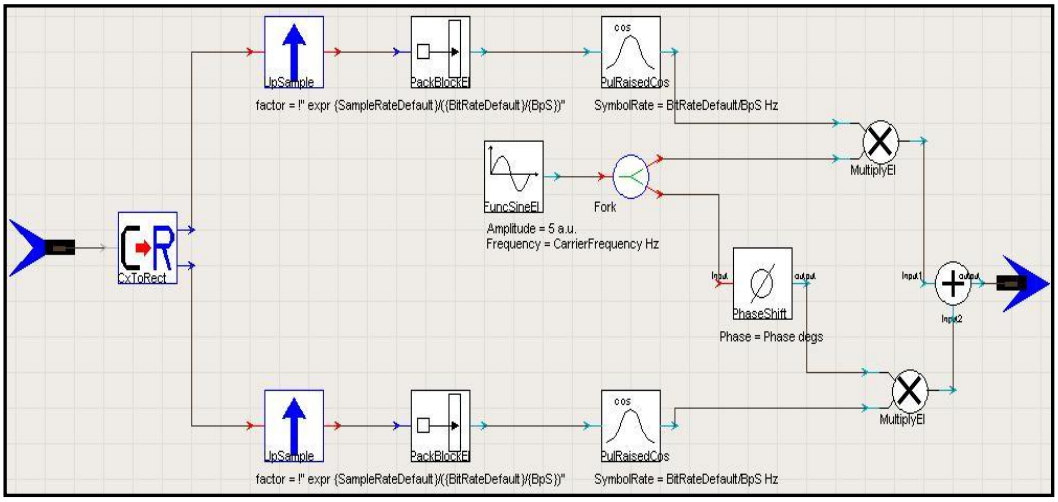

Fig. IV.10 RF upconverter schematic [VPI]

As it can be seen from Figure IV.10, the input sequence corresponding to the coded OFDM baseband signal is separated by the *ComplexToRect* module into the real values of the I and Q components of the signal. This operation is internal to VPI's OFDM coder, so this module is not used in the Long-Haul Transmission demo.

The other difference is the use of the upsampling modules for both parts of the signal. This operation inserts a given number of samples according to the *factor* parameter, in order to compensate for the difference between the number of samples of the original sequence and the number of samples of the coded OFDM sequence, which is going to be converted into electrical values in the next stage.

In this case, the I and Q sequences are represented by a vector of $BitRate \cdot TimeWindow/BpS$ values, while the original sequence is formed by $BitRate \cdot TimeWindow$ samples, so the upconverting factor should be set to no less than the value of *BpS*. This will produce new samples (usually zero-valued) that will be allocated between the original samples as indicated in the Parameter editor.

The downconverter schematic is depicted in Fig. IV.11, where each downsampling module is set with the same factor value as the upsamplers used in the RF upconversion. The downsamplers are used in order to recover the exact number of samples representing the received symbols, including the ones used for zero padding, cyclic prefix and (if any) the ones used for symbol rate compensation.

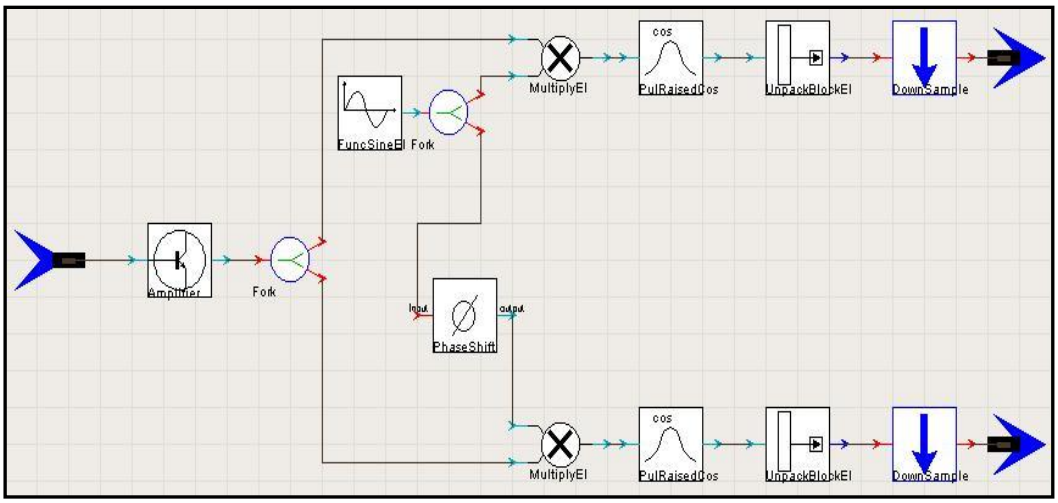

Fig. IV.11 RF downconverter schematic [VPI]

The parameters that have to be created for both the up and downconverter galaxies are those belonging to the *RF galaxies* category, that is: *CarrierFrequency*, *Phase* and *RollOff*. Any change in the main schematic of the next section's simulations will affect both modules.

IV.1.6. Sequence comparer

Another galaxy has been created to compare the original sequence coming from the PRBS generator and the decoded bit sequence extracted from the OFDM decoder module. This will lead through a simple operation to obtain the BER for the simulated transmission.

Figure IV.12 shows a possible interconnection scenario for the sequence comparer, where a new version of the OFDM decoder module has been designed to output the decoded sequence.

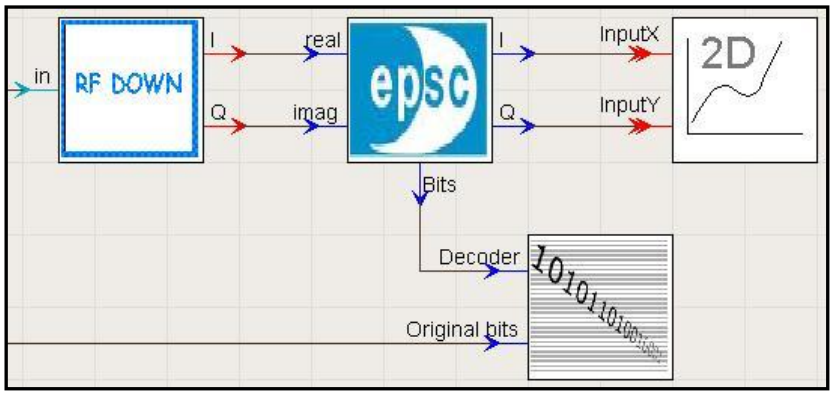

Fig. IV.12 Sequence comparer interconnection scenario [VPI]

Internally, this module declares both sequences to a *CoSim* module, which will access the corresponding Matlab code in which the sequences are compared. Figure IV.13 shows the schematic for this galaxy:

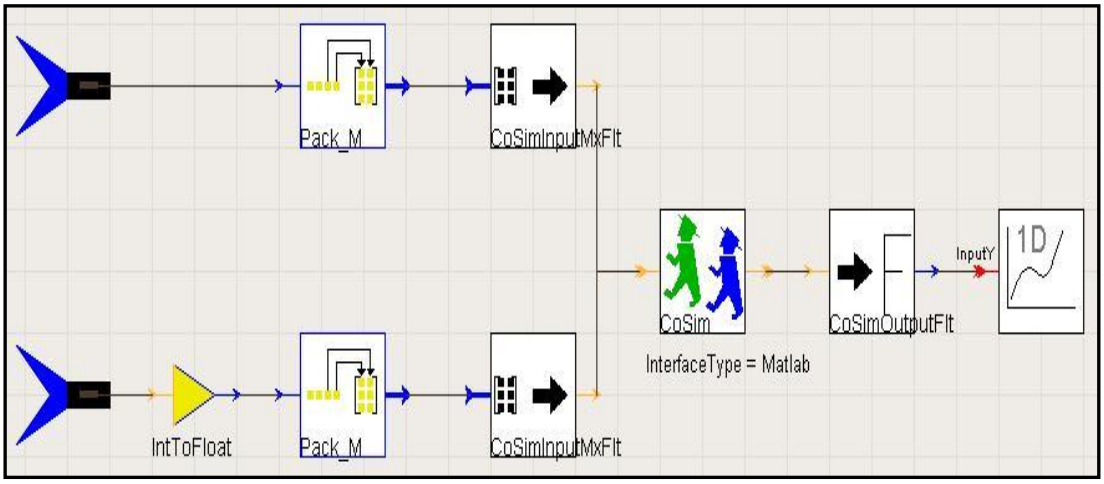

Fig. IV.13 Sequence comparer schematic [VPI]

The Matlab sentence used to perform the comparison for sequences *a* and *b* is:

```
dif=sum(ne(a,b));
```
(IV.9)

As a result, the *dif* variable will take the value of the total number of bits (or vector positions) which are not equal between both sequences. Thus, a simple operation relating the number of errors in the transmission (*dif*) and the total number of information bits will provide the value for the BER as:

```
BER=dif/NTB_INFO;
```
(IV.10)

This value will be extracted from the Matlab code by means of the *CoSimOutputFlt* module connected to the *CoSim* output, and then displayed by the VPI Photonics Analyzer through a numerical analyzer module.

More numerical analyzer modules can be placed at the sequence comparer inputs to display the whole transmitted and received sequences, though this should just be done when working with short sequences.

IV.2. Electrical OFDM Generation and Detection

IV.2.1. Universe schematic

The customized coder and decoder modules have been used to create this simulation, which functions are similar to those presented in the OFDM Generation and Detection demo in Chapter III. Figure IV.14 shows the Electrical

OFM Generation and Detection schematic, where some modifications have been done with respect to the demo in order to adapt the customized modules.

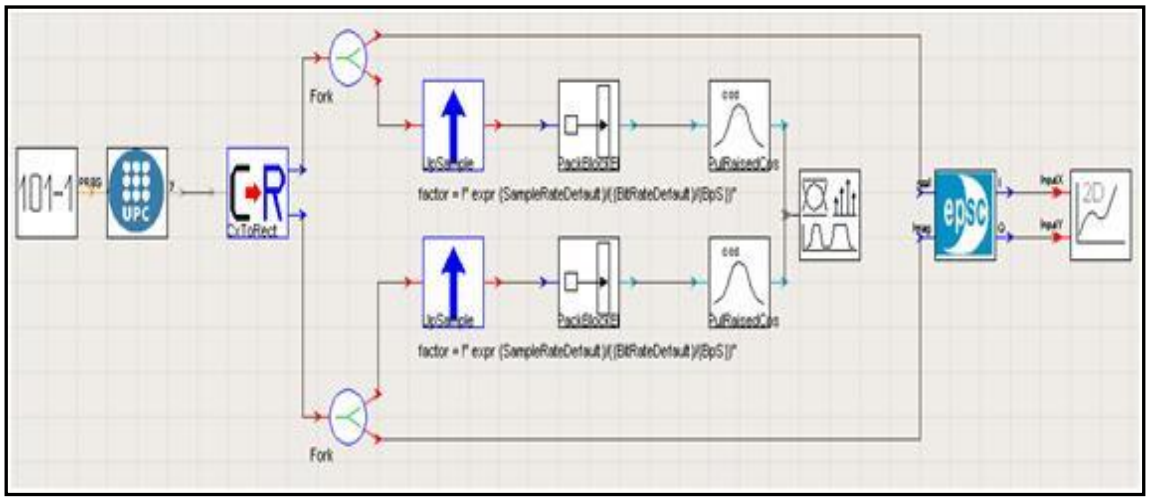

Fig. IV.14 Generation and detection of an OFDM signal [VPI]

These modifications are the same as in the first part of the RF upconverter galaxy, that is, the complex sequence coming from the coder is split into its real and imaginary components, and then upsampled to compensate for the number of samples to process in the following modules before the signal representation.

As in VPI's demo, the coder and decoder are connected through VPI wires, so there are no distortions caused by the transmission path. The Parameter editor of the schematic is shown in Figure IV.15, where the names of each parameter and category correspond to those of the coder and decoder, so they can be changed from there instead of having to do it once for each module.

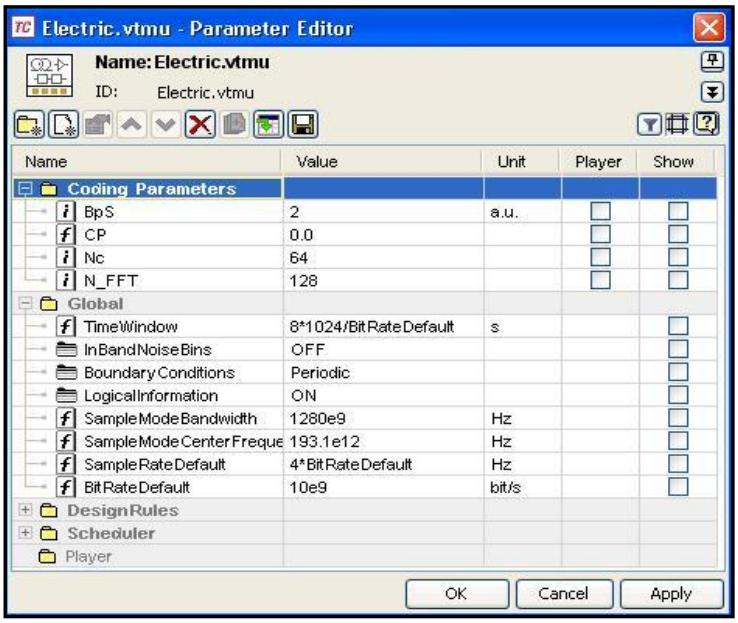

Fig. IV.15 Parameter editor of the universe schematic [VPI]

In order to see the theoretical concepts described in Chapters I and II applied in a simulation scenario, the next subsections show different tests which have been performed in this scenario, so the effects of changing any of the parameters in an OFDM transmission can be observed.

The signal analyzer connected after the pulse shaping modules will be used to display the spectrum of the electrical OFDM signal in every performed test. After that, the ideally received constellations for a 4-QAM and a 16-QAM types of OFDM coding are shown, where the zero-valued symbol problem appearing in VPI's OFDM Generation and Detection demo has been solved.

IV.2.2. Raw transmission

The first simulated transmission doesn't include zero padding nor cyclic prefix, and the PRBS generator has been established to transmit only ones at a rate of 10 Gbps, so that every single subcarrier can be identified after plotting the generated OFDM signal. This is why it can be called a "raw" transmission.

Figure IV.16 shows the comparison between this first simulation and the same one with the PRBS generator's *Type* parameter set to PRBS mode, where 32 modulated subcarriers are carrying information in a 4-QAM modulation.

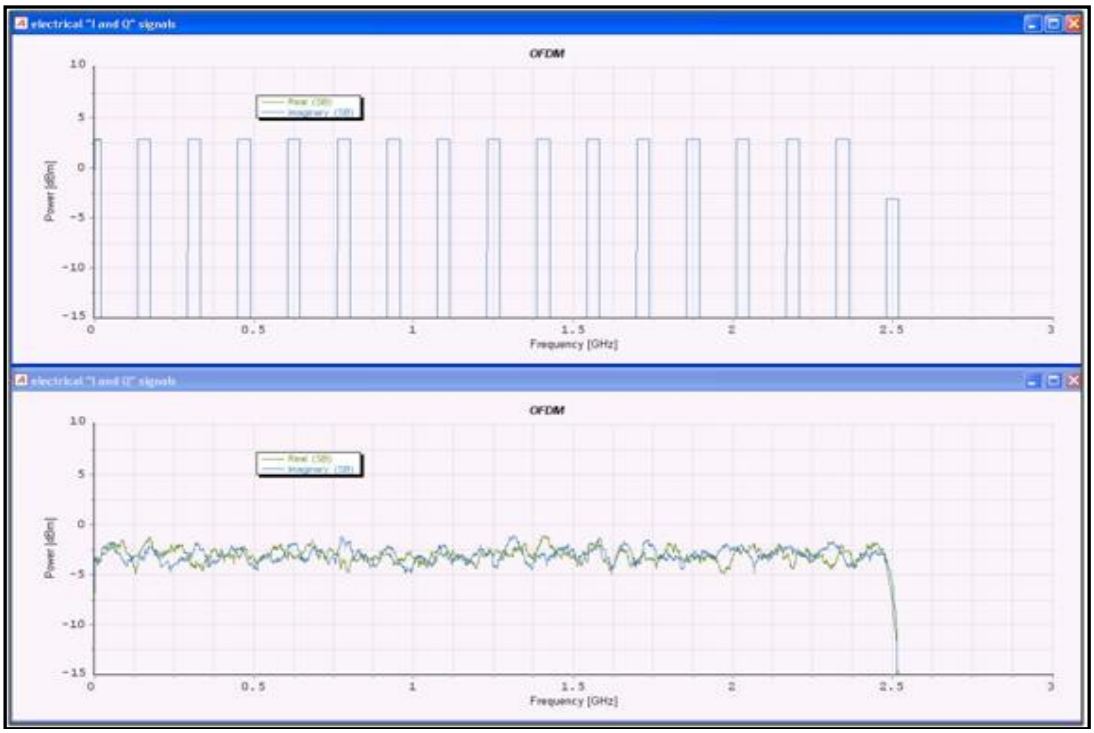

Fig. IV.16 Raw OFDM transmission: Ones vs. PRBS [VPI]

As in VPI's demos, both the real and imaginary parts are superimposed in the graphs, only representing half of the OFDM band. Thus, the 16 subcarriers corresponding to each side of the spectrum can be identified, the last one of them being centred at 2.5 GHz.

Note that there is no bandwidth excess, meaning that the spectrum falls off very abruptly. This will not happen in a practical filter, so a roll-off factor needs to be applied in order to simulate a more realistic scenario. Thus, the resulting effect of a change in this parameter will be the next test to conduct.

IV.2.3. Roll-off factor

The pulse shaping modules in charge of retaining the I and Q components of the OFDM signal are ideally rectangular. However, this is not realizable in practice, so a raised cosine characteristic is fitted to the ideal low-pass filter as a practical solution. Thus, a roll-off factor will be defined as the ratio of excess bandwidth above the maximum frequency of the signal to be represented.

Figure IV.17 represents the real and imaginary components of a baseband OFDM signal transmitted at 10 Gbps, where a square root raised cosine Nyquist response with different roll-off factors has been applied for its representation. The upper figure represents the I and Q components after passing through an ideal filter (α = 0), and in the lower case a roll-off factor of 0.2 has been applied. Note that the excess bandwidth is approximately 360 MHz for this case.

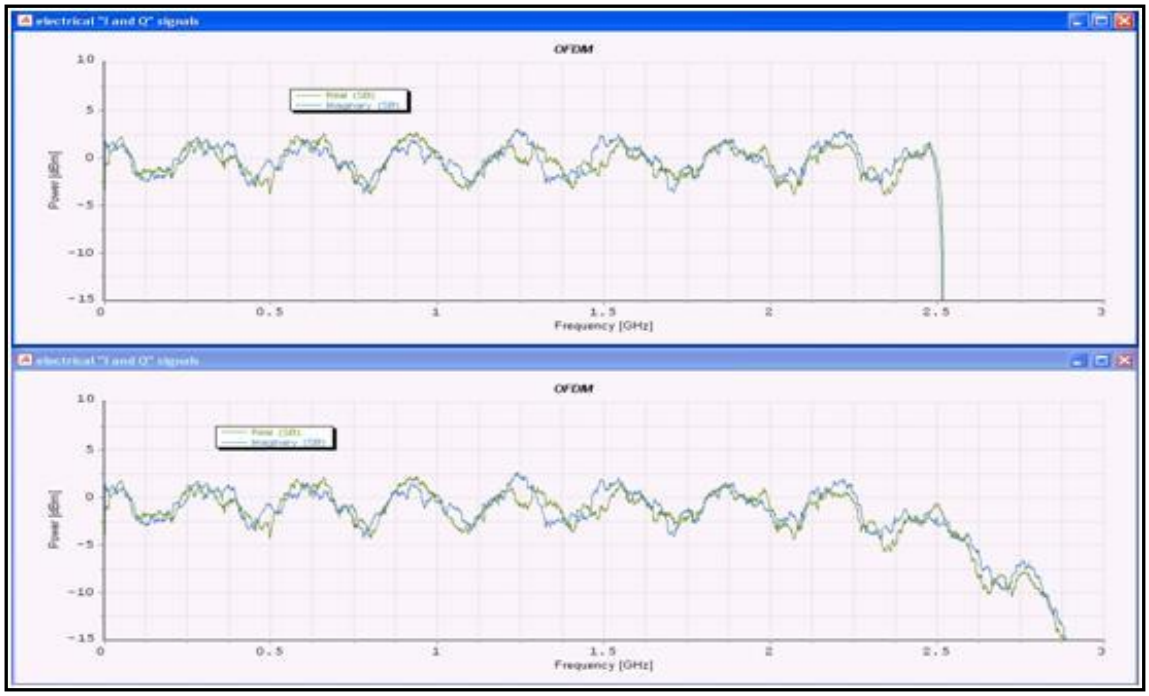

Fig. IV.17 Filtered OFDM signal with roll-off factors of 0 and 0.2 [VPI]

The roll-off factor in the lower case will be applied in every of the following simulations, serving as an approach to a real OFDM system.

IV.2.4. Zero Padding

In Chapter I, it was seen that there are two ways of using zero padding at the input sequence of the IFFT: zeros can either be inserted at the middle of the sequence (oversampling), or at the edges, creating a frequency gap with respect to the optical carrier.

The results of applying zero padding to half of the IFFT inputs (at the edges) in the generation of an OFDM signal can be seen in the lower graph of the next figure, where 4-QAM has been used for each subcarrier modulation with a 10 Gbps data rate. The upper graph represents an OFDM signal generated with the same characteristics except for zero padding, which has not been applied.

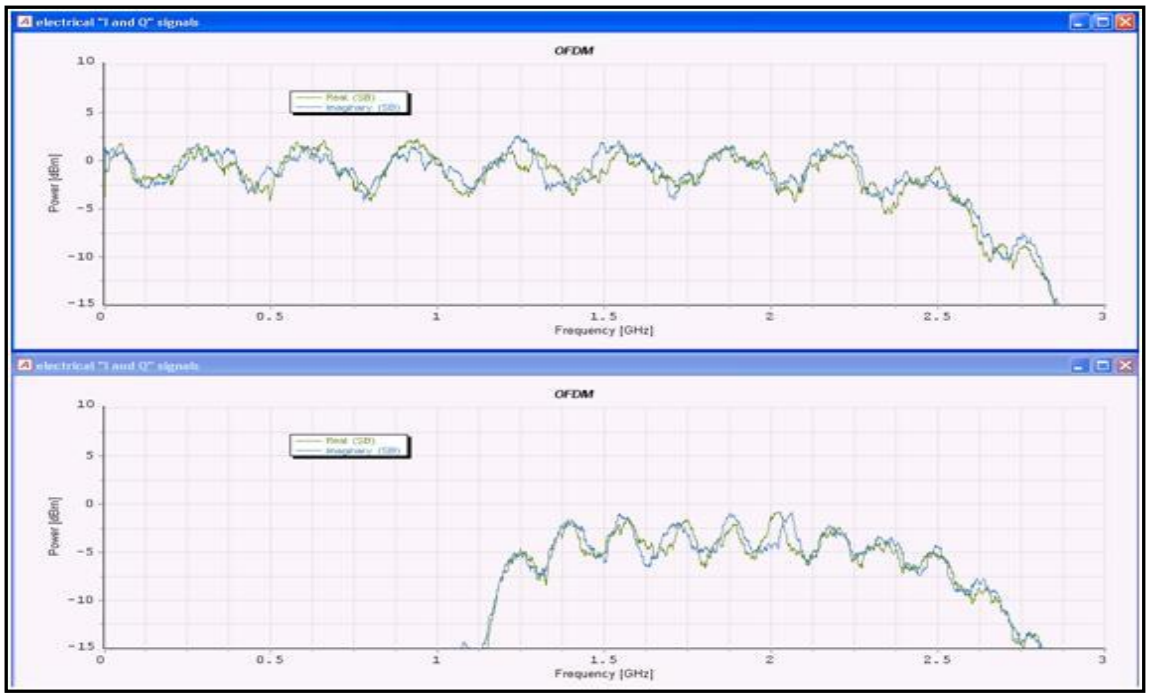

Fig. IV.18 Gap generation by means of zero padding [VPI]

It can be seen that the frequency gap due to zero padding has occupied half of the spectrum to transmit. This will be the main drawback when using this technique, though it is an alternative to the use of analogue components such as RF mixers performing the up/downconversion functions.

If zero padding is applied on the central half of the input sequence of the IFFT, the spectrum is compressed as explained in Chapter I, allowing the use of simpler filters to erase the aliases resulting from the sampling stage. The resulting spectrum after this process is shown in Figure IV.19.

Again, only half of the IFFT inputs are going to be used by information symbols, meaning a loss in bitrate efficiency. On the other hand, off-the-shelf DACs will be able to be used to obtain the analogue OFDM signal after the IFFT stage.

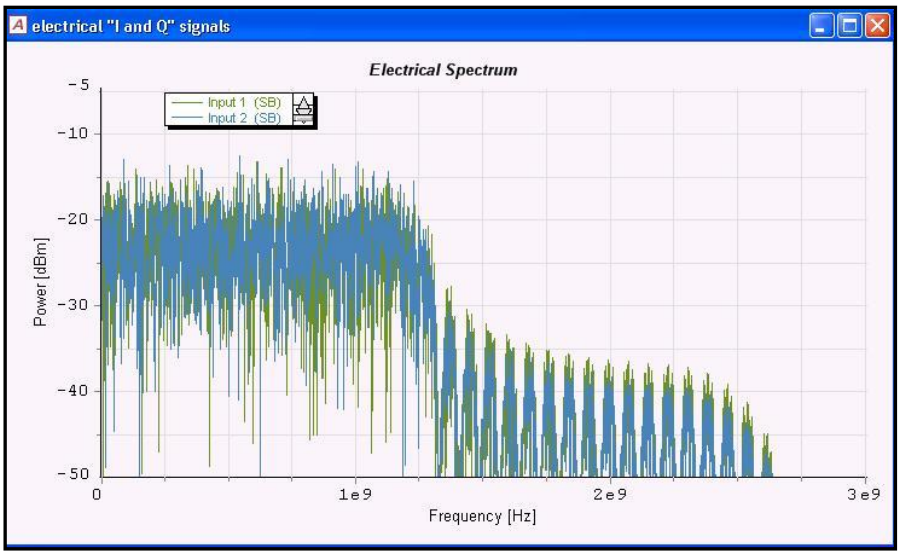

Fig. IV.19 Oversampling by means of zero padding [VPI]

Any kind of zero padding will be extracted at the receiver after the FFT operations in the same way as it was inserted, recovering the original spectrum.

IV.2.5. Cyclic Prefix

The effect of a change in the OFDM spectrum due to an increase of the cyclic prefix proportion can be seen in Figure IV.20, where in the upper figure a CP corresponding to 25% of the OFDM symbol length has been applied, while in the lower one no CP is used. For a better appreciation of the spectrums, only one component of the signal has been represented (the real one).

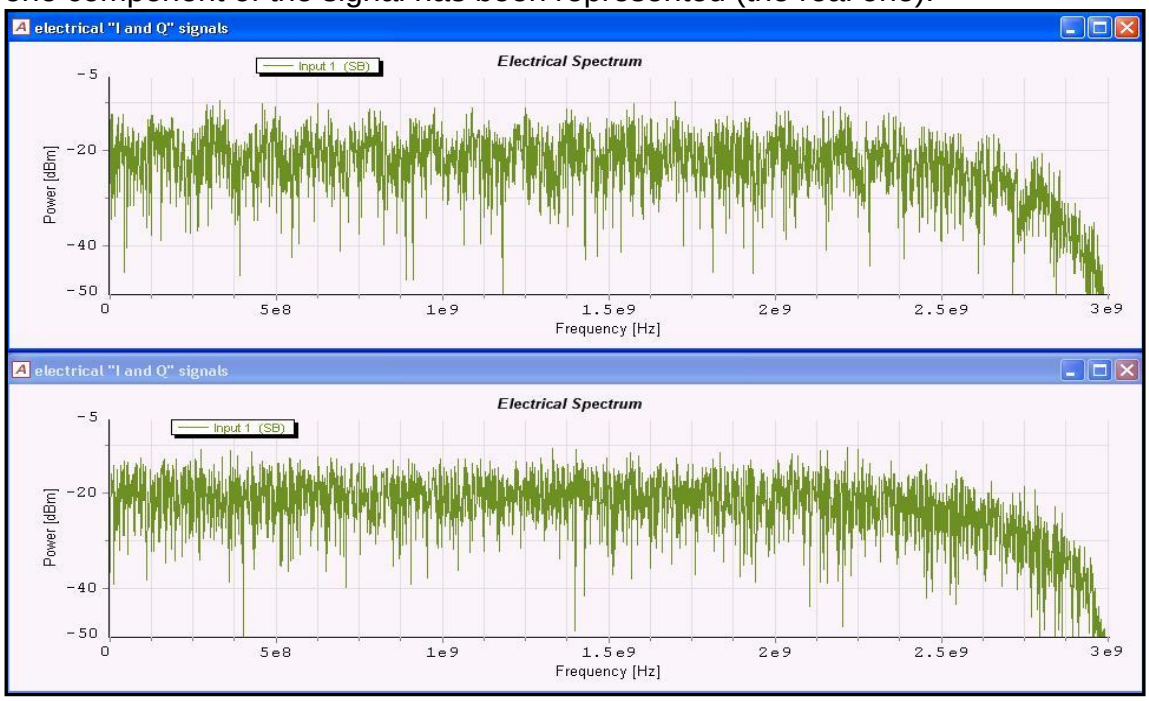

Fig. IV.20 No CP vs. CP = 25% of the OFDM symbol length [VPI]

By inserting CP into the OFDM sequence, a ripple can be appreciated in the OFDM signal spectrum. This is because the sincs representing the subcarriers are narrower in frequency than before, so their maximums don't match up exactly with their neighbours' nulls. This effect was referred in Chapter I, and a more detailed description of it can be found in Annex B.

IV.2.6. Received Constellation

In an ideal channel condition, X points will be represented in the received constellation diagram for an X-QAM modulated OFDM signal. This is because there is no distortion causing any phase or amplitude error in the reception of symbols, so all of them are represented exactly in their theoretical location.

In this case, a 4-QAM and 16-QAM modulation transmissions are performed in the Electrical OFDM Generation and Detection scenario, giving rise to the constellations depicted in the next figure:

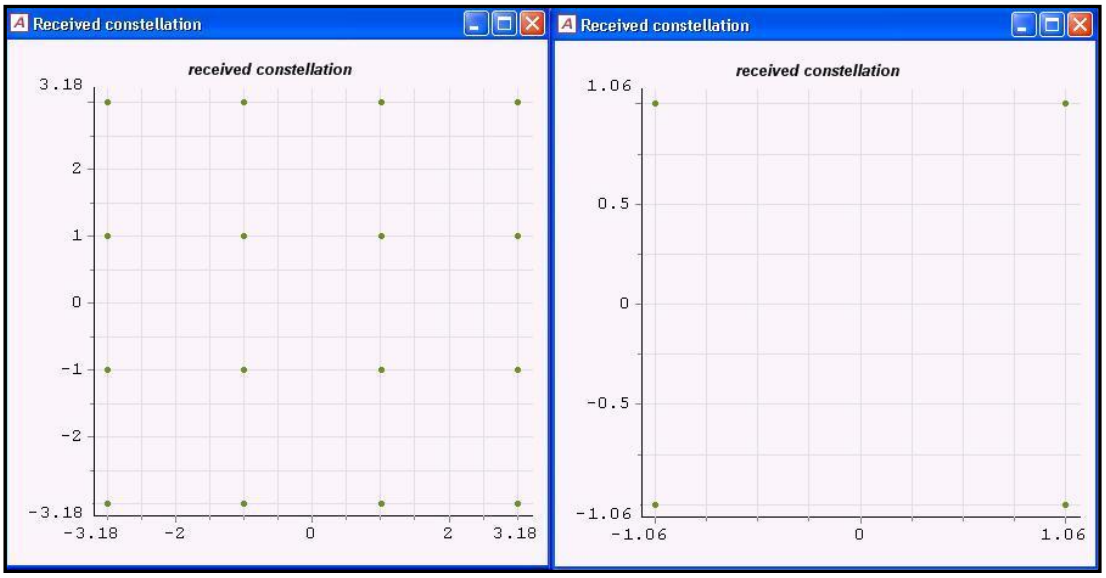

Fig. IV.21 Received constellations for a 4-QAM and a 16-QAM modulation [VPI]

Note that, contrary to VPI demos, no points are plotted in the [0,0] position of the constellation. This is because the customized OFDM decoder module extracts the precise number of information symbols to plot the constellation diagram. The variables used for this purpose are the uncompensated I and Q received components of the signal, as explained in section IV.1.2.

IV.3. Optical OFDM

IV.3.1. Universe schematic

An optical OFDM testing scenario has been created based on the *OFDM for Long-Haul Transmission* demo described in Chapter III. The universe schematic is shown in Figure IV.22, where the OFDM coder and decoder galaxies with their corresponding RF up/downconversion stages appear again as the OFDM signal transmitter and receiver, respectively.

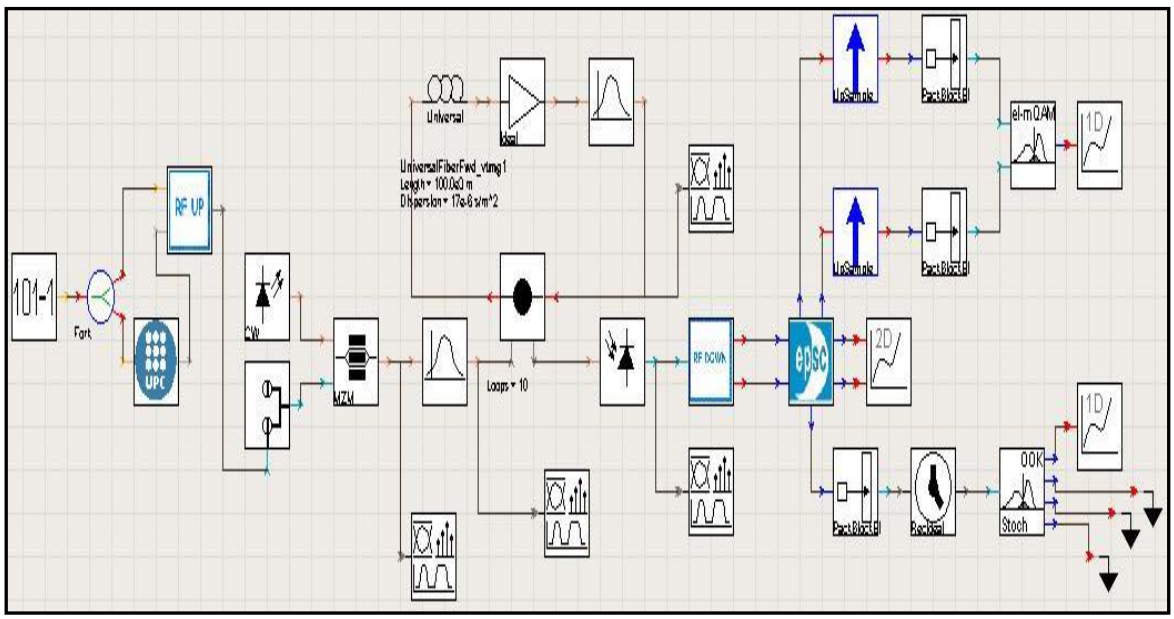

Fig. IV.22 Optical OFDM system scenario [VPI]

This scheme corresponds to the *RF upconversion based on Intensity Modulation* configuration described in section II.5.1.1, which is the same as in VPI's demo, though this time oversampling is applied to the OFDM coder by means of zero padding the input sequence of the IFFT.

Also, the same optical transmission channel as in the demo has been applied. This means that a 100 km optical fibre with the same physical parameters as before is going to be used as a component of an N-loop transmission circuit along with the corresponding amplification and filtering stages.

In this customized scenario, equalization is based on the fibre model described in Chapter II, meaning that it will just compensate for chromatic dispersion.

Also, 4 signal analyzers are used so that (apart from the constellation diagram) the spectrum of the signal can be seen at specific points of the system.

At the receiver end, the decoder galaxy has been modified over the previous version in the Electrical OFDM Generation and Detection schematic. This is because the EVM of the received constellation and the BER of the received bit sequence are going to be measured, so the corresponding variables of the

Matlab code have to be extracted from the cosimulation process as explained in section IV.1.2. The new modules inserted to measure the EVM and BER values are also explained in this chapter.

The schematic parameters for this simulation can be seen in Figure IV.23, where no new categories are used. Note that, as in the VPI simulations, 64 4-QAM information subcarriers are going to represent the OFDM signal, though 128 IFFT/FFT inputs will be necessary in order to apply oversampling by means of zero padding. The input bit sequence will be formed by a block of 8*1024 = 8192 bits.

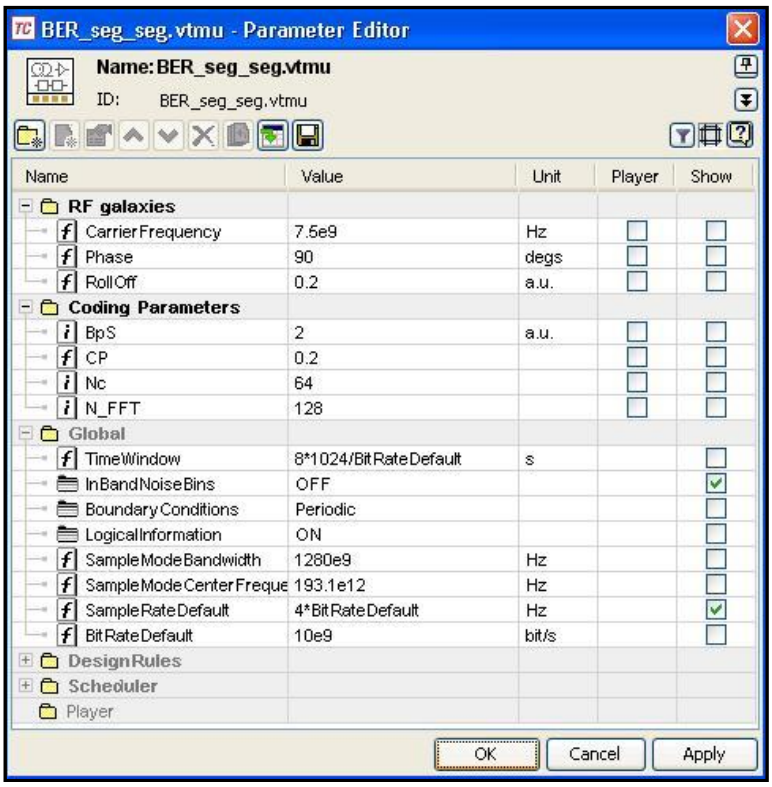

Fig. IV.23 Parameter editor of the universe schematic [VPI]

The quantity of cyclic prefix present in the sequence will also be modified in order to see the effects on the received constellation.

IV.3.2. Custom modules modifications

If the EVM and BER values are to be calculated, a logical channel has to be added to the scenario. This is why RF upconversion galaxy in Figure IV.22 has two input ports: one for the coded OFDM sequence and another for the original sequence coming from the PRBS generator.

As shown in Figure IV.24, a *LogicAddChannel* module has been inserted in the right bottom of the RF upconversion galaxy. The *ChannelLabel* parameter of this module must be the same for the modules in charge of performing the EVM and BER calculations.

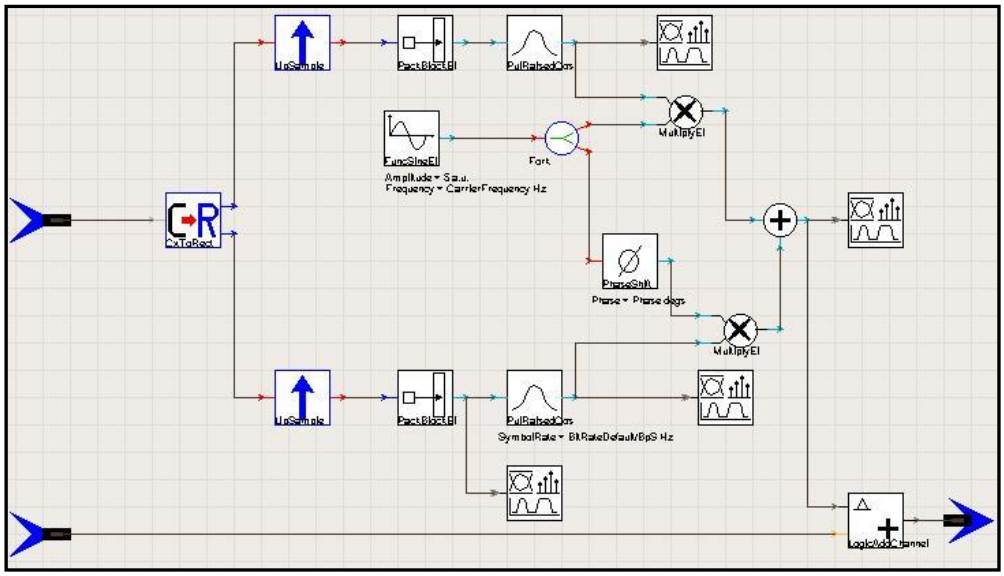

Fig. IV.24 RF upconversion module with a logical channel [VPI]

Another modification has been introduced in the OFDM decoder module in order to obtain the 5 output configuration mentioned in section IV.1.2.

Figure IV.25 shows the resulting schematic for the OFDM decoder galaxy, where the I and Q components of the downconverted OFDM signal at the input of the module give rise to 5 different sequences at its outputs:

- The symbol-rate-compensated I and Q components of the decoded OFDM signal (upper ports) are used to calculate the EVM
- The uncompensated parts (middle ports) are fed to a 2-dimension numerical analyzer to plot the received constellation diagram (see Figure IV.26)
- The bitrate-compensated decoded sequence (lower port) will be used for the BER calculation

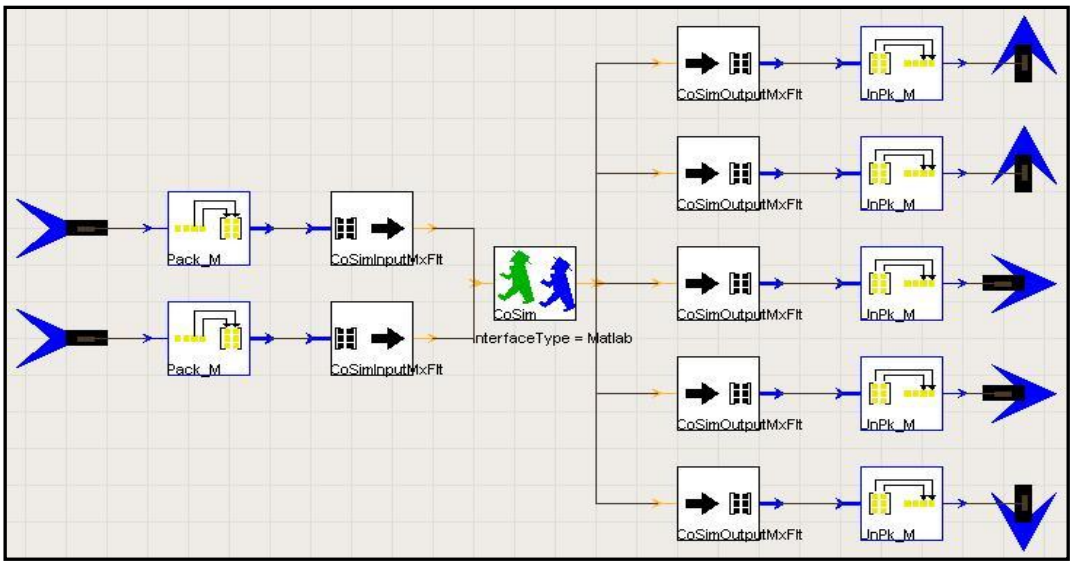

Fig. IV.25 OFDM decoder galaxy schematic: 5 output configuration [VPI]

IV.3.3. Error Vector Magnitude and Bit Error Rate measuring

Figure IV.26 is a zoomed version of the universe schematic, where modules taking part in the EVM and BER measuring are viewed in detail.

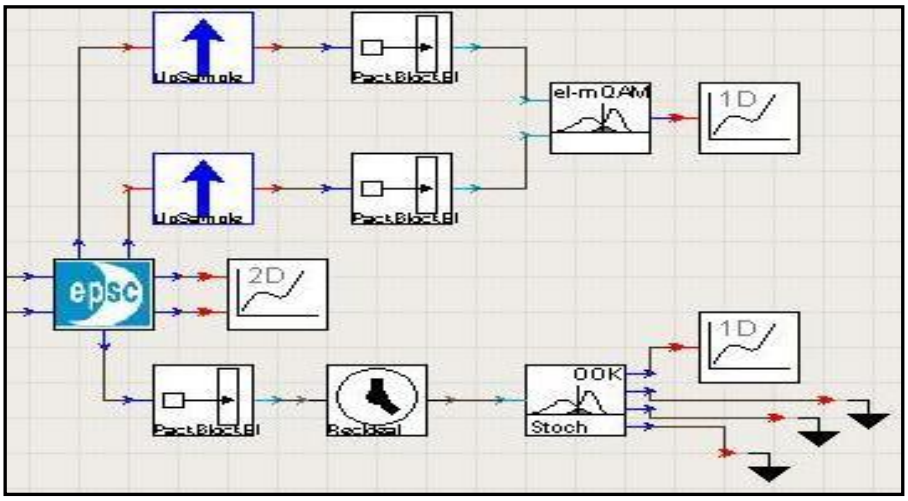

Fig. IV.26 EVM and BER measuring [VPI]

As in VPI's demo, the *BER_El-mQAM* module is used to calculate the EVM of the received constellation. This module expects I and Q sequences of electrical samples with length TimeWindow*Bitrate, so the received information symbols have to be first compensated in Matlab (adding zeros to the sequence) and then upsampled by a factor equal to the *BpS* parameter before converting them into electrical samples.

Despite offering clock recovery and amplitude and phase correction of the received symbols, the EVM calculation performed by the *BER_El-mQAM*

module would not be correct if the compensating symbols were taken into account. For that purpose, the I*gnoreSybols* parameter of this module should be set to *ApplyOnce*, and then the *NumberOfSymbolsToIgnore* and *StartTimeToIngore* parameters should be set to:

$$NumberOfSymbolsToIgnore = TimeWindow \cdot \frac{BitRate}{BpS} - \left(N_c \cdot floor\left(TimeWindow \cdot \right.\right.$$

BitRateBpS/ceil(N_FFT(1+CP))

$$StartTimeToIgnore = 1/BitRate \cdot BpS \left(N_c \cdot floor\left(TimeWindow \cdot \frac{BitRate}{BpS} / ceil(N_{FFT} \cdot (1 + CP)) \right) \right)$$

(IV.11)

This way, the number of symbols to ignore is indicated to the module, as well as the time when it should start ignoring them. By giving these parameters the values in expression (IV.12), the zero-valued symbols used for the symbol rate compensation are going to be omitted from the calculations

The module in charge of performing the BER calculations is the *BER_OOK_Stoch* star. As shown in Figure IV.22, this module has 4 outputs and just one of them is connected to a numerical analyzer. This output corresponds to the bit error rate value for the received sequence, and is the only one which will be represented in this simulation.

As this module also expects a TimeWindow*Bitrate sequence of electrical samples at its input, the compensated sequence of demodulated bits is needed. However, this time the upconversion stage is not needed, because the bitrate compensation is enough to provide the expected sequence length.

As in the EVM case, the module offers the possibility to ignore the compensating bits, so the following values are given to the IgnoreBits and Start TimeToIgnore parameters:

$$NumberOfBitsToIgnore = TimeWindow \cdot BitRate - \left(N_c \cdot BpS \cdot floor\left(TimeWindow \cdot \frac{BitRate}{BpS} / ceil(N_{FFT} \cdot (1 + CP)) \right) \right)$$

$$StartTimeToIgnore = 1/BitRate \cdot N_c \cdot BpS \cdot floor\left(\frac{TimeWindowBitRate}{BpS} / ceil(N\_FFT(1 + CP)) \right)$$

(IV.12)

These parameters will appear in the Parameter editor as long as the *IgnoreBits* parameter is set to *ApplyONce*. In order to assist the BER calculations, a clock recovery module is previously inserted.

The customized sequence comparer module presented in section IV.1.6 can be also used to perform the BER calculations, allowing the possibility to see which of the information bits has been wrongly received.

IV.3.4. Reference frequency choice and cyclic prefix extraction

IV.3.4.1. Reference frequency choice

In order to simulate the chromatic dispersion effect in a fibre, the simulator takes the following Taylor expansion (which is analyzed in Chapter II) up to the fourth term centred in a user-specified reference frequency f_{ref}.

$$\begin{aligned}\beta(\omega) &\approx \beta(\omega_0)+(\omega-\omega_o)\frac{\partial\beta}{\partial\omega}+\frac{(\omega-\omega_o)^2}{2}\frac{\partial^2\beta}{\partial\omega^2}+\frac{(\omega-\omega_o)^3}{6}\frac{\partial^3\beta}{\partial\omega^3}+\dots \\ &= \beta_o+\Delta\omega\beta_1+\frac{\Delta\omega^2}{2}\beta_2+\frac{\Delta\omega^3}{6}\beta_3+\dots\end{aligned} \quad \textbf{(IV.13)}$$

That sets a limit on the total bandwidth around f_{ref} that can be correctly approximated and that is why it is important to choose it carefully.

The first term in the expansion is then a constant phase for all signals travelling through the fibre and as such it is neglected since it represents a change in the phase reference, which is set to zero at the reference frequency.

The second term is the group delay and it is set to zero in the f_{ref}. In the simulator this is equivalent to setting the clock to zero at the time when the f_{ref} is expected at the fiber's receiver end, that is, it sets the time where the temporal simulation window starts. The delays of the rest of the frequencies are then set accordingly. The Taylor expansion is therefore only left with two terms which are respectively quantified by the user-defined parameters D (chromatic dispersion) and S (dispersion slope).

The slope will be considered negligible even when in the simulations is set to the typical value in third window ($0.08 \cdot 10^{-3} s/m^3$).

Here the attention will be focused on focused on the 2nd order term. According to the model for chromatic dispersion described in section II.1, the fibre transfer function has the form:

$$H(\omega) = e^{j\chi(\omega-\omega_{ref})^2} \quad , \quad \chi = \frac{\beta_2}{2}L \qquad \textbf{(IV.14)}$$

Where ω_{ref} is the angular reference frequency for which the Taylor expression is considered, *L* is the fibre length ω depends on the evaluated frequency.

Within the performed simulations, there are basically two natural choices for this reference frequency (f_{ref}): one is the optical carrier frequency (f_o) and the other one is the frequency where the optical OFDM spectrum is centred ($f_o + f_{RF}$). While VPI's *Long Haul* demo uses the latter, several tests have been performed in order to understand the reason why this is done and the implications behind the choice of one or the other.

The tests have revealed a rather symmetric behaviour of either one of the natural choices:

- For $f_{ref} = f_o$, the constellation is not phase shifted, but the received temporal sequence is delayed with respect to the emitted temporal sequence. This delay is longer the higher is the optical carrier frequency, or the longer the optical fibre.
- For $f_{ref} = f_o + f_{RF}$, the constellation suffers a phase shift which also grows proportionally to the fiber length and f_{RF}, though no delay in the temporal received sequence is observed.

For a better understanding of these concepts, a mathematical model has been developed. If the spectrum of the input signal to the fibre is expressed as:

$$X_{IN}(\omega) = \delta(\omega - \omega_o) + Y(\omega - (\omega_o + \omega_{RF})) \quad \textbf{(IV.15)}$$

Where $Y(w)$ represents the spectrum of the OFDM signal. Thus, the spectrum of the output signal is:

$$X_{OUT}(\omega) = H(\omega)\, X_{IN}(\omega) = \delta(\omega - \omega_o)e^{j\chi(\omega_o - \omega_{ref})^2} + Y(\omega - (\omega_o + \omega_{RF}))e^{j\chi(\omega - \omega_{ref})^2} \quad \textbf{(IV.16)}$$

If the reference frequency is set to the optical carrier frequency ($\omega_{ref} = \omega_o$):

$$X_{OUT}(\omega) = \delta(\omega - \omega_o) + Y(\omega - (\omega_o + \omega_{RF}))e^{j\chi(\omega - \omega_o)^2} \quad \textbf{(IV.17)}$$

On the other hand, if the RF frequency is considered as the reference frequency ($\omega_{ref} = \omega_{RF}$), the output signal is:

$$X_{OUT}(\omega) = \delta(\omega - \omega_o)e^{j\chi(\omega_{RF})^2} + Y(\omega - (\omega_o + \omega_{RF}))e^{j\chi(\omega - (\omega_o + \omega_{RF}))^2} \quad \textbf{(IV.18)}$$

The delay for the pulse in (IV.17) is given by $e^{j\chi(\omega - \omega_o)^2}$, and the phase shift in (IV.18) appears due to the $e^{j\chi(\omega_{RF})^2}$ term. In order to provide these values, the temporal expressions should be calculated.

The photodetected current can be described as a function of its responsivity multiplied by the square of the received signal modulus:

$$i_D = R|x_{out}(t)|^2 \quad \textbf{(IV.19)}$$

Thus, the delay τ_g for the pulse and the phase shift affecting the constellation can be calculated from the estimation of the temporal expressions for each of the above choices of the reference frequency respectively as:

$$|x_{out}(t)| \sim \left|1 + Y_D(t - \tau_g(f_{RF}))\right|, \quad \tau_g = \frac{DLcf_{RF}}{2f_0^2}$$

$$|x_{out}(t)| \sim \left|1 + Y_D(t)e^{j\Delta\emptyset(f_{RF})}\right|, \quad \Delta\emptyset[rad] = -\frac{\pi DLc}{f_0}f_{RF}^2 \quad \textbf{(IV.20)}$$

Where *D* is the amount of CD to be compensated [s/m], *L* is the fibre link distance, *c* is the speed of light and Y_D is the OFDM dispersed spectrum.

It has been checked that the simulation results match the theoretical values of the calculated delay and phase shift for the simulated parameters. In this case, a delay of nearly $0.5\,ns$ has been observed when setting $f_{ref} = f_o$ though no phase shift has affected the signal. On the other hand, no delay was observed when $f_{ref} = f_o + f_{RF}$, but a phase shift of 55º appeared. This will be seen in the simulation results section.

In any case, while a phase shift can be compensated at the receiver, it is not that easy to try to compensate for a time delay in the simulator. Thus, it has been concluded that in this matter it is best to follow the example set by the VPI demo and set $f_{ref} = f_o + f_{RF}$ in the performed simulations.

IV.3.4.2. Cyclic prefix extraction

Once that it has been seen that the best choice for the reference frequency is the centre of the optical OFDM spectrum, this section analyzes which is the best cyclic prefix extraction strategy.

In Figure IV.27, the transmission and reception simulation window in VPI for three optical OFDM symbols with their corresponding cyclic prefix are represented. They consist of a temporal sequence of length *Time Window*. For simplicity, each OFDM symbol is composed by just three subcarriers, where number 1 will be the lower frequency subcarrier, number 2 will be the subcarrier centred in the middle of the OFDM band and number 3 represents the highest frequency subcarrier.

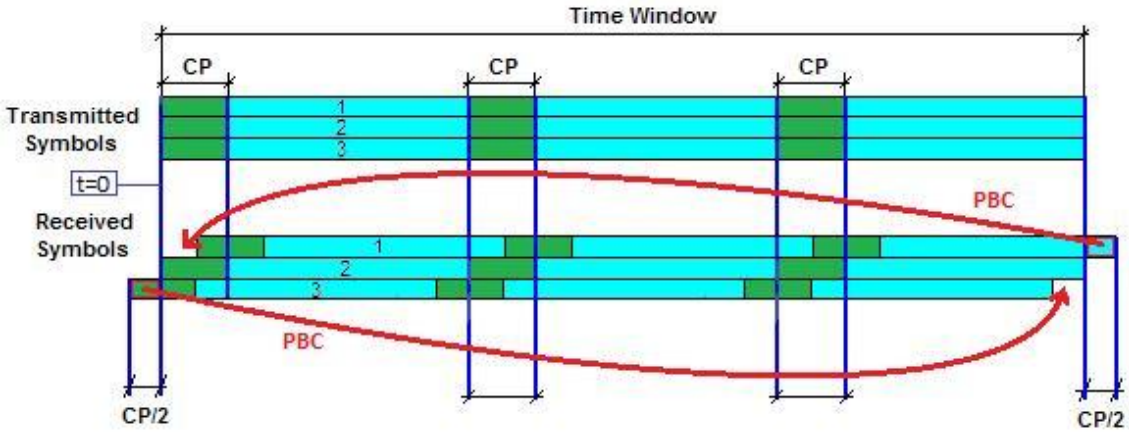

Fig. IV.27 Transmission and detection temporal simulation window for 3 optical OFDM symbols

It can be seen that the subcarriers experience different delays due to chromatic dispersion and therefore have different arrival times. In the figure, a positive dispersion coefficient D has been represented so that the higher frequency subcarriers are the first to arrive. Since the reference frequency is set to the central frequency, this is where the temporal simulation window begins (zero group delay considered) and therefore the higher frequency subcarriers should be out of the temporal window. Owing to the Periodic Boundary Conditions (PBC) characteristic of VPI, it will appear at the end of the temporal window.

Likewise, the last part of the slower frequency stream falls outside the temporal window and is moved to the beginning of the temporal simulation window, as it can be seen from Figure IV.27.

From the received symbols stream the part where information coming from different OFDM symbols overlap should be removed in order to avoid ISI problems. This part, as shown graphically in Figure IV.28, is found CP/2 to the left with respect to the CP part in the emitter and therefore for a correct CP extraction a CP/2 shift to the right of the FFT window should be taken into account.

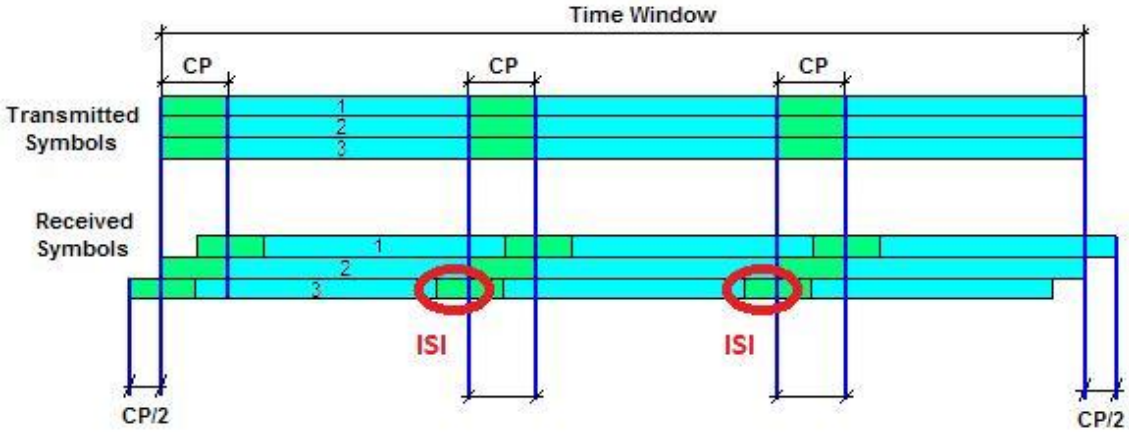

Fig. IV.28 Periodic Boundary Conditions and ISI affecting the third subcarrier

The figure shows that if the CP is extracted at the same point where it was inserted we will have some unavoidable ISI no matter how big this CP could be. This is something that was seen in the simulations and solved it by the CP/2 shift to the right explained above. In practice a correct FFT window synchronization is critical [P4].

Since every subcarrier experiences a different phase shift due to the CP/2 temporal shift a phase correction needs to be included in the equalizer.

The following expression shows the programming sentence which has been inserted in the OFDM decoder Matlab code in order to move half cyclic prefix to the beginning of every OFDM symbol:

```
yy1=[yy1(NTS_QAM_CP-ceil(N_FFT*CP/2)+1:NTS_QAM_CP),
        yy1(1:NTS_QAM_CP-ceil(N_FFT*CP/2))];
```
(IV.21)

After that, the symbols corresponding to the CP are extracted:

```
yy1_SP=reshape(yy1,ceil(N_FFT*(1+CP)),NTS_OFDM)

yy1_CP=yy1_SP((ceil(N_FFT*CP)+1):size(yy1_SP,1),:
```
(IV.22)

Moreover, an additional equalization has to be performed on the *ephase* coefficients resulting from the ideal equalization in expression (IV.8) to compensate for the CP/2 extraction, as each subcarrier will change its phase in a different way:

```
ephase=ephase.*exp([0:1:(Nc/2)-1,-Nc/2:1:-1]*i*2*pi*
  ceil((CP/2)*N_FFT)/N_FFT);
```
(IV.23)

IV.3.5. Simulation results I: OFDM signal spectrum

The main interest of this section is to monitor the OFDM signal spectra through the most significant stages of the transmission, so it can be noticed how the main modules participating in the simulation affect the signal.

First, the electrical OFDM signal spectra is plotted for different stages inside the RF upconversion module, as it can be seen by the positions of the signal analyzers in Figure IV.24. After that, the optically modulated OFDM signal is represented before and after the transmission link, and finally the received electrical spectrum will be compared to the one originated in the transmitter.

The first representation corresponds to the spectra of the coded OFDM signal before the pulse shaping module, just after being sampled to convert the floating numbers representing the analogue values of the signal into electrical samples. In a real OFDM system, this point would correspond to the digital to analogue conversion stage, once the sampling is completed but the filtering has still to be done.

The resulting spectrum is the same as in the Electrical OFDM Generation and Detection simulation, where no negative frequencies are represented so the main OFDM signal spans from 0 to 2.5 GHz, though the alias have not been filtered out yet, so they appear together in a periodic sequence. This time only one component of the signal will be represented (in this case, the quadrature).

Figure IV.29 shows the mentioned spectrum, where the upper graph shows the resulting signal when no oversampling is used. Note that the aliases are right next to the main OFDM signal and also very close between them, which would require the use of an ideal filter to eliminate them.

If *2x*oversampling is applied, the spectrum's bandwidth is halved. Thus, the OFDM signal aliases can easily be filtered out, as shown in the lower graph in Figure IV.29. As the used sampling rate is 4 times the bitrate, 4 signal spectrums are represented in each figure, where only the first half (or the first 2.5 GHz of the spectrum) has to be recovered.

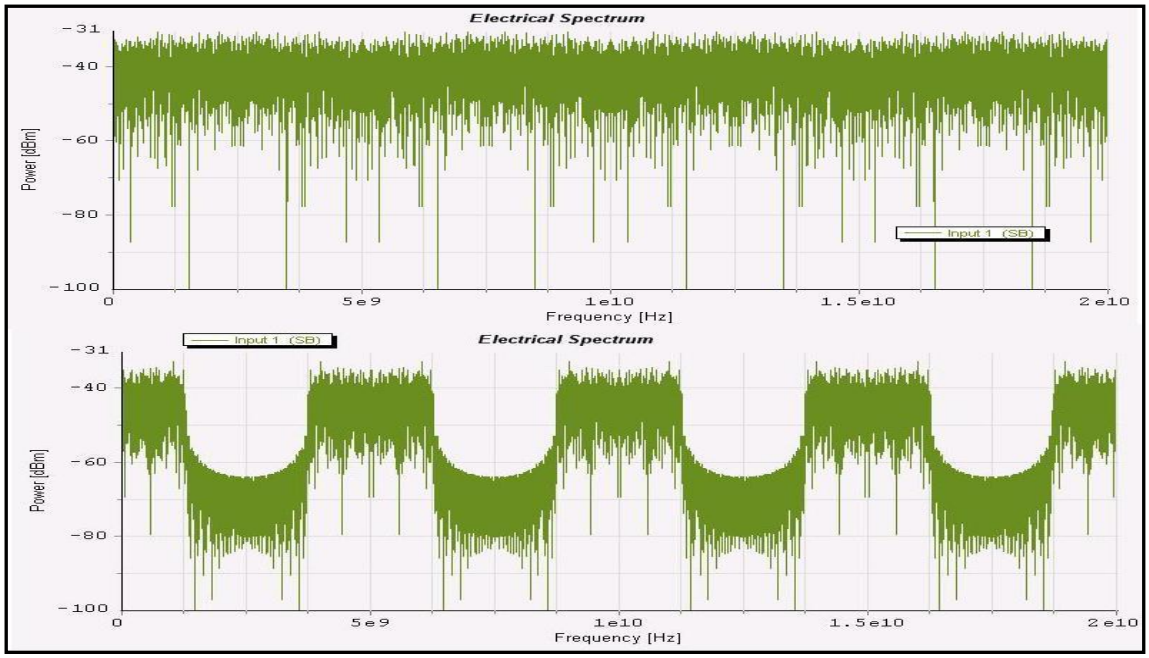

Fig. IV.29 OFDM spectrum before the DAC's filter [VPI]

All of the following figures in this section will represent the case where no oversampling is applied in the upper part and the *2x*oversampling case in the lower one.

Next, the *PulseRaisedCosQAM* module filters the aliases out, preserving the main OFDM signal. As in previous simulations, a roll-off factor of 0.2 has been used to simulate a close to real OFDM system. Figure IV.30 shows the resulting spectrum with and without the use of zero padding.

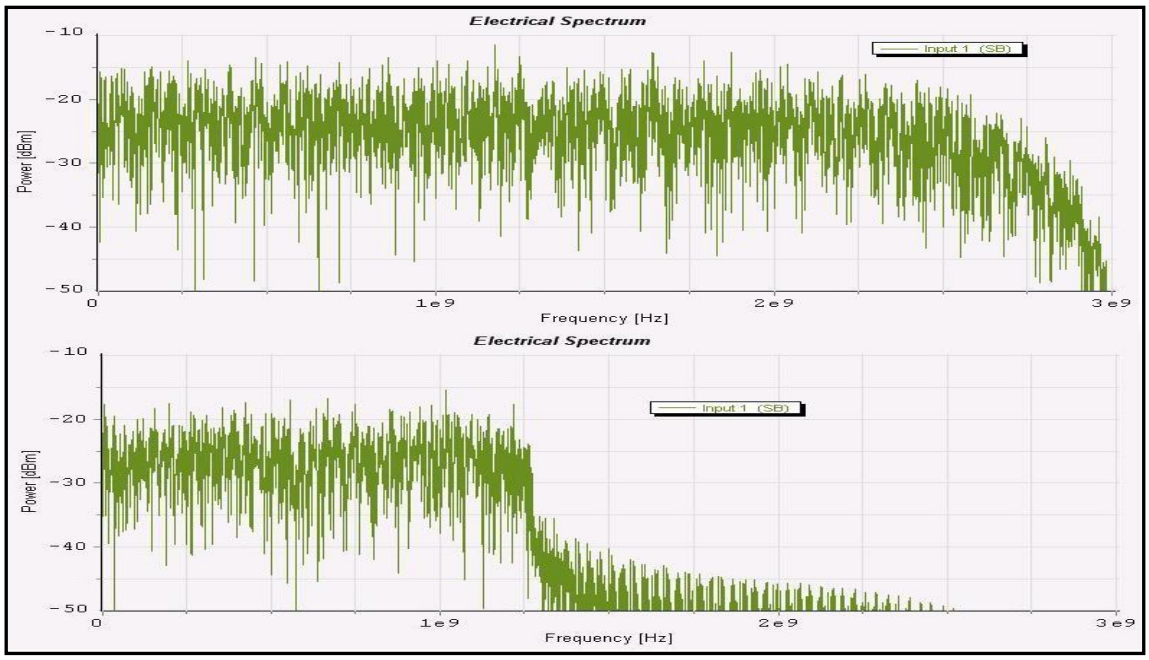

Fig. IV.30 OFDM spectrum after the DAC's filter [VPI]

The last signal analyzer in the RF upconversion galaxy will represent the upconverted OFDM signal spectrum. Here, the I and Q components have been multiplied by a 7.5 GHz carrier and added with a 90º phase shift for the quadrature component.

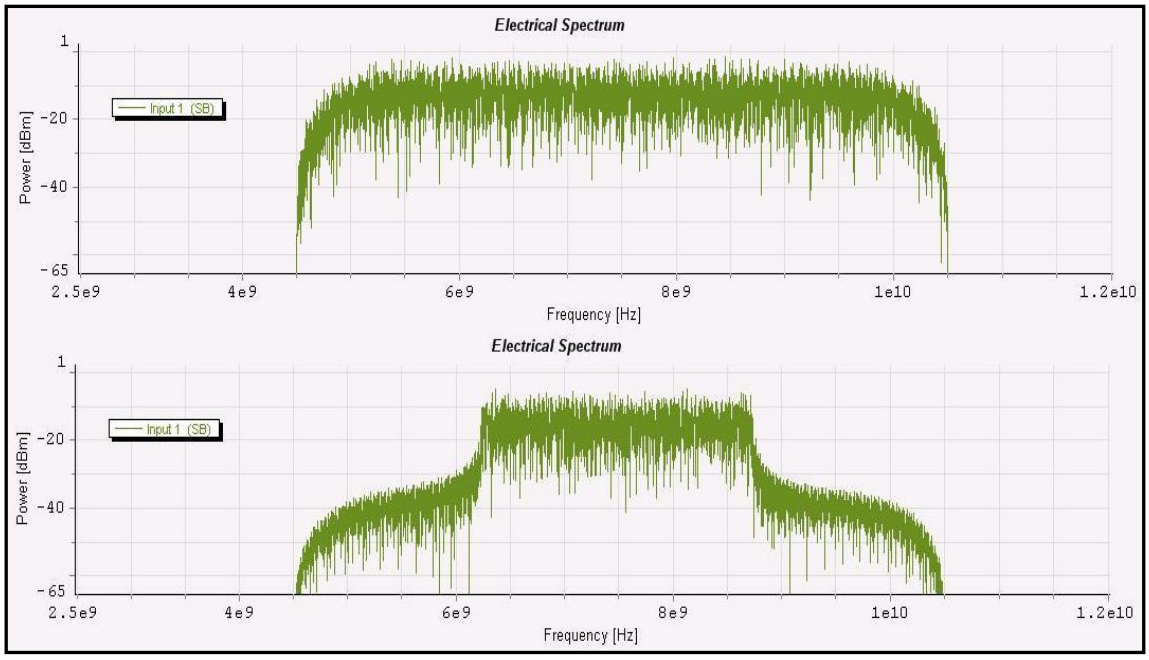

Fig. IV.31 Upconverted OFDM signal [VPI]

Once the coded OFDM signal is upconverted, it has to be optically modulated by a MZM. As explained in Chapter II, the resulting spectrum will consist of an optical carrier (which in this case is centred at 193.1 THz) and two sidebands of the optical OFDM signal, as shown in Figure IV.32:

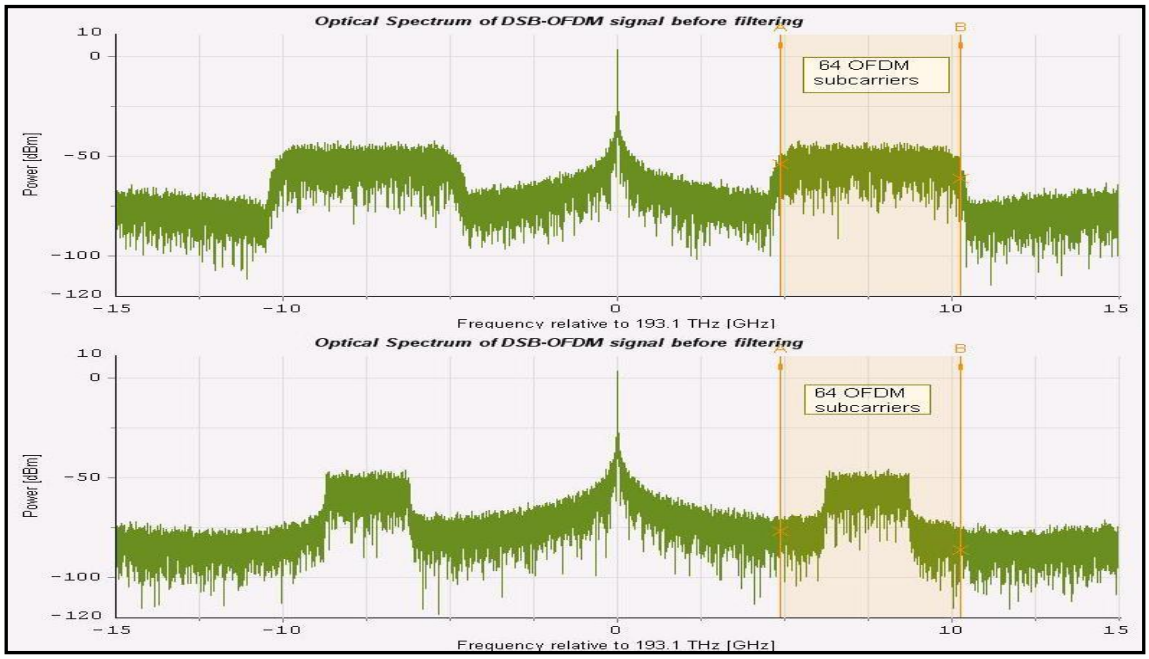

Fig. IV.32 Double sideband optical OFDM signal [VPI]

An optical filter will be then in charge of removing the lower sideband, so the single sideband (SSB) transmission configuration is achieved. The resulting spectrum is represented in Figure IV.33:

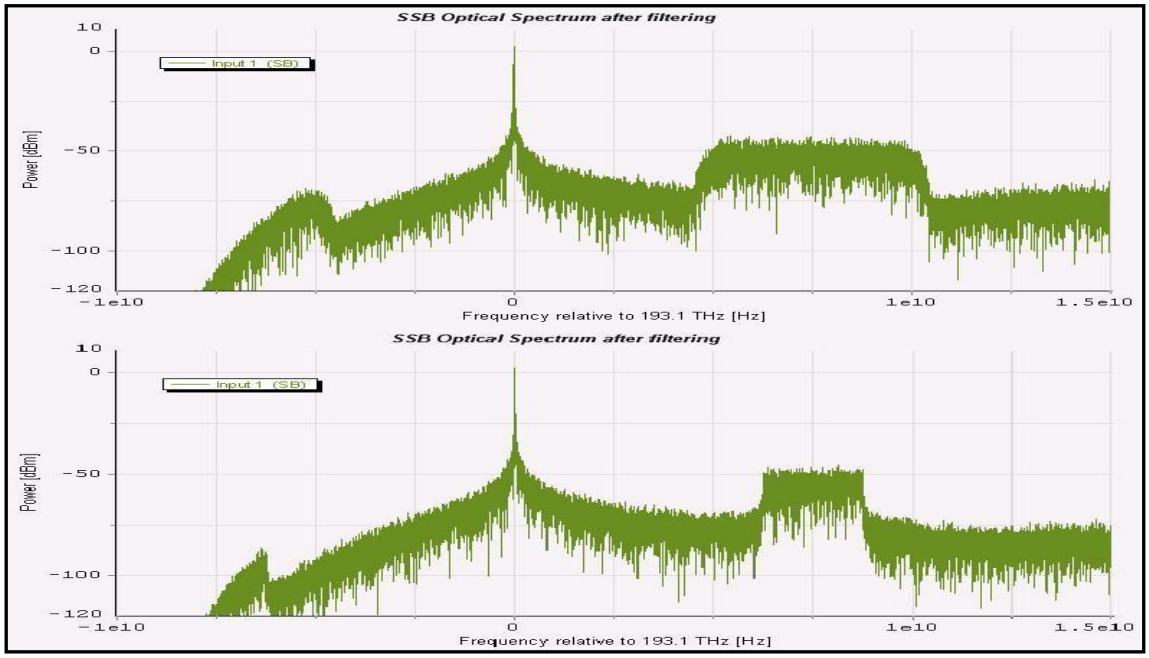

Fig. IV.33 Single sideband optical OFDM signal [VPI]

The following step is to transmit the optical OFDM signal through the fibre link. Figure IV.34 shows the spectrum of the received signal after a 1000 km transmission (10-loop circuit), where a slight out-of-band power growth can be appreciated with respect to the last figure.

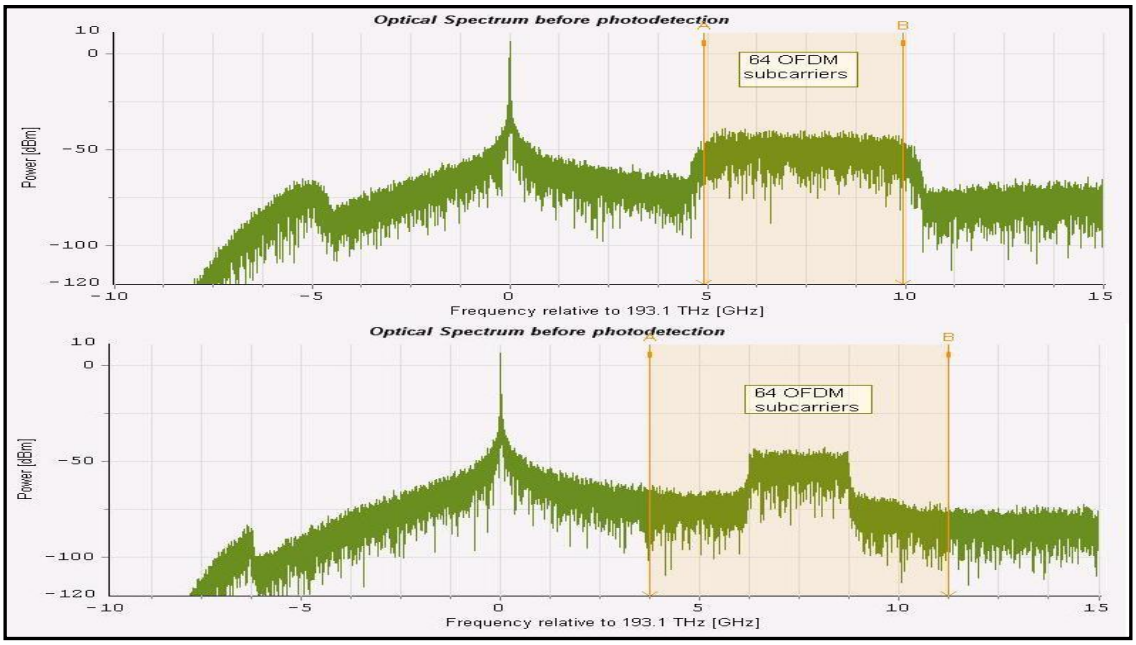

Fig. IV.34 Optical OFDM signal after the fibre link [VPI]

The electrical spectrum of the received OFDM signal can be represented once the signal is photodetected. In Figure IV.35, the noise component composed by the mixing products appearing due to direct detection can be easily distinguished, falling off in the created gap ranging from 0 to near 5 GHz.

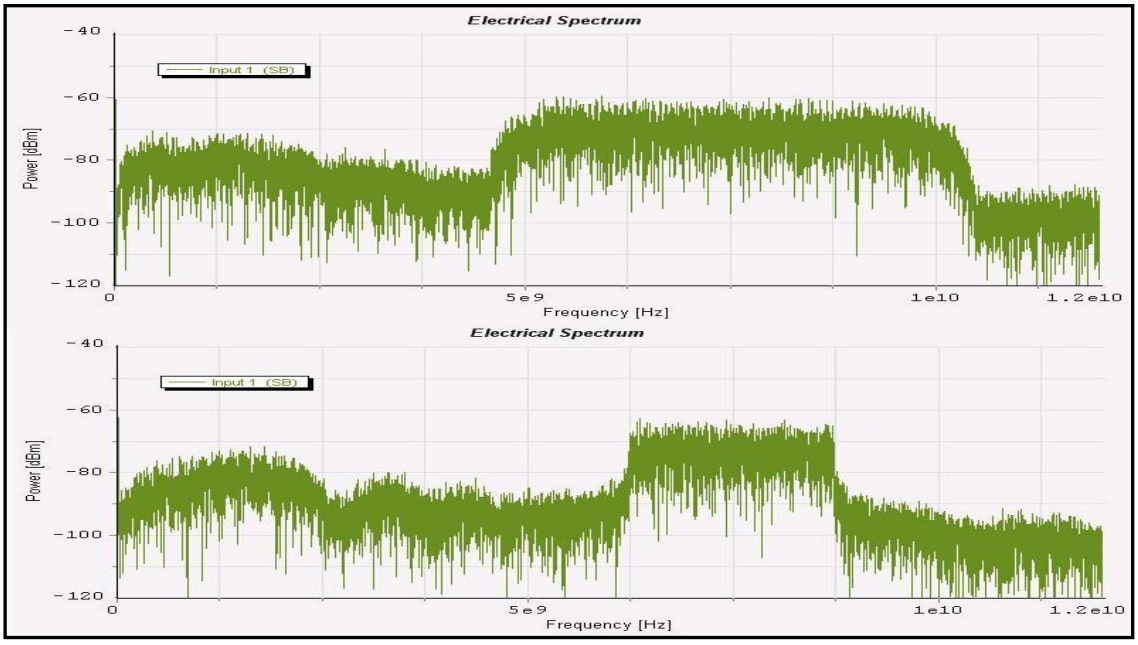

Fig. IV.35 Electrical OFDM signal after photodetection [VPI]

The obtained photocurrent representing the received OFDM signal will then go through an RF downconversion stage, where (ideally) the transmitted OFDM signal is recovered. Figure IV.36 shows the recovered quadrature component spectrum, which should be similar to the one represented in Figure IV.30.

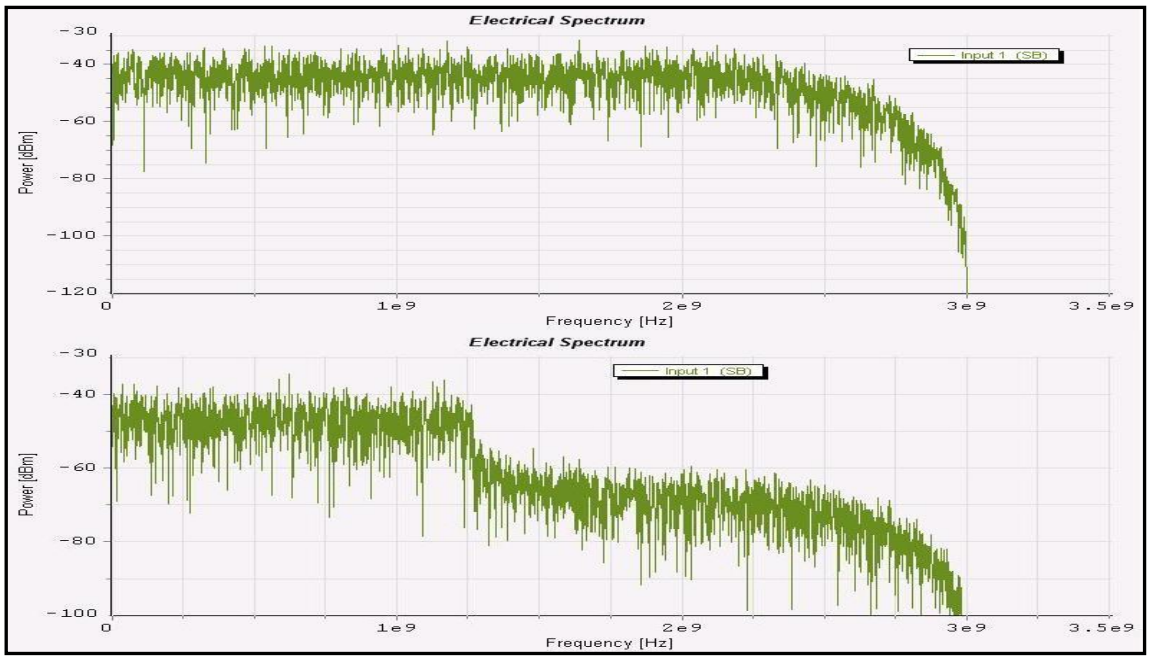

Fig. IV.36 Downconverted electrical OFDM signal [VPI]

However, by comparing Figures IV.30 and IV.36, a considerable decrease in the received power level can be observed. This is why an amplification stage is usually placed at the receiver, so an amplifier module has been inserted at the input of the RF downconversion galaxy (see Figure IV.11).

After the RF downconversion stage, the resulting OFDM signal is fed to the OFDM decoder, where the representation of the received constellation diagram and the calculation of the EVM and BER values will account for the quality of the transmission. These parameters are dealt with in the following section.

IV.3.6. Simulation results II: Decoded signal

In this section, the results of the received constellation diagram, EVM and BER values are going to be described for different transmission parameters, such as the use of cyclic prefix or the fibre link distance.

First, the reliability of the system has been tested without the optical link (and also without the optical modulation and demodulation stages, so the RF up/downconversion modules were linked with VPI wires). The squared constellation in Figure IV.37 proves that the OFDM decoder is able to recover the original transmitted symbols after going through frequency upconversion and downconversion stages.

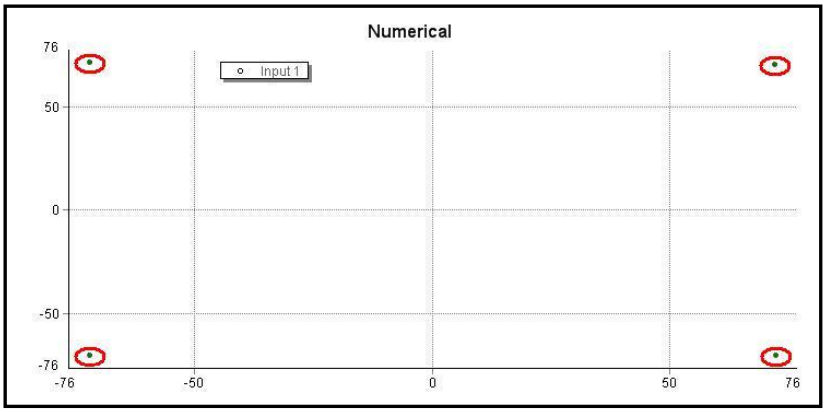

Fig. IV.37 Received constellation without optical channel [VPI]

The next step is to run a simulation with the same parameters as in the *OFDM for Long-Haul Transmission* demo. Thus, the optical channel has been added again as in Figure IV.22, for a 1000 km fibre link without using equalization:

The received constellation depicted in Figure IV.38 is very similar to the one obtained with VPI demos, as it was shown in Figure III.27 in Chapter III. Although the EVM value is not relevant for a case in which no equalization is applied, its value was 0.715.

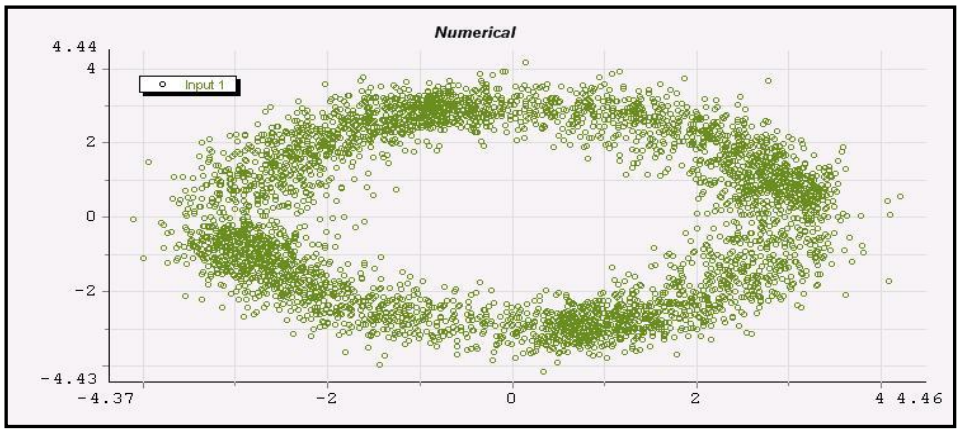

Fig. IV.38 Received constellation diagram without equalization [VPI]

When equalization is applied, though cyclic prefix and zero padding are still not used, the left constellation in Figure IV.39 is received, where a constant phase error makes it different from the equalized constellation in VPI demos (shown in Figure III.25).

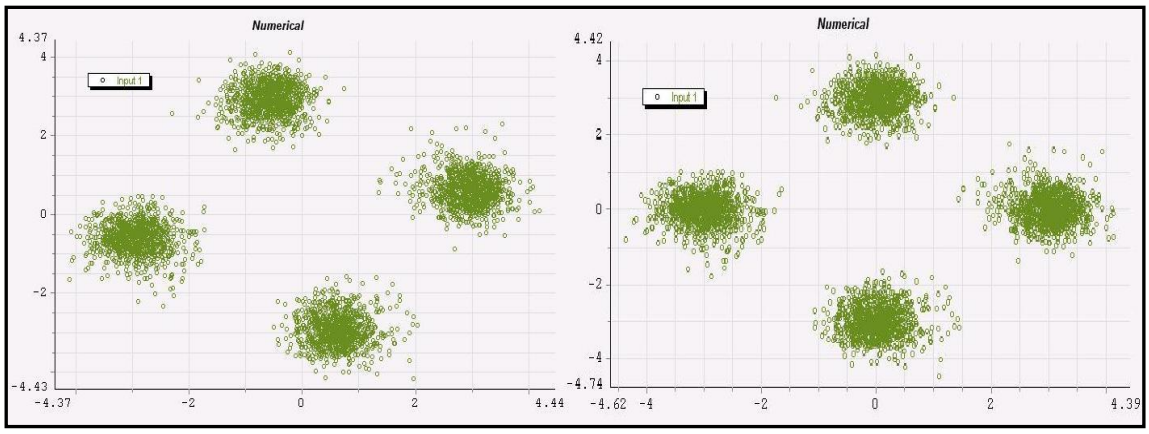

Fig. IV.39 Equalized constellation with and without constant phase error (left and right, respectively) [VPI]

This phase shift appears because the reference frequency has been set to the middle of the OFDM band ($f_0 + f_{RF}$), so the expected difference of 55º over the squared constellation (see section IV.3.4) can be appreciated in the figure.

By correcting the equalizer code in Matlab by (45º-55º = -10º) the same constellation form as in the *Long-Haul* demo is obtained, as shown in the right graph in Figure X.A. The EVM for this case is 0,186.

For the next figures, a - 55º phase shift has been applied in the equalizer code in order to show a squared constellation. Thanks to it, the obtained BER values for all of them are approximated to 0 by VPI, as all of the symbols fall within the corresponding quadrant of the diagram.

If the cyclic prefix is used for the transmission and extracted as in expression (IV.24), a notorious improvement in the symbol dispersion is obtained. This is shown in the next figure, where the right graph represents the constellation diagram when a CP of 20% has been added to the transmission over another one where no CP was used (left).

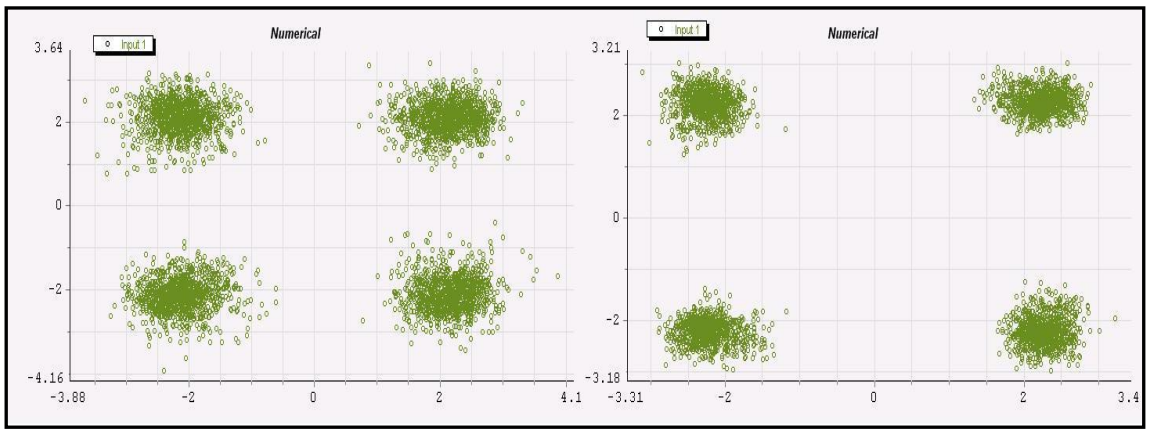

Fig. IV.40 Dispersion improvement by using CP [VPI]

In this case, the EVM improves from 0.186 to 0.115, even going beyond the 0.177 EVM value obtained in the VPI demo with the same parameters.

Figure IV.41 shows how the use of oversampling by means of zero padding also achieves an improvement in the received constellation form. The left graph shows the resulting constellation when a *2xoversampling* configuration is used without CP (128 IFFT inputs for 64 information subcarriers).

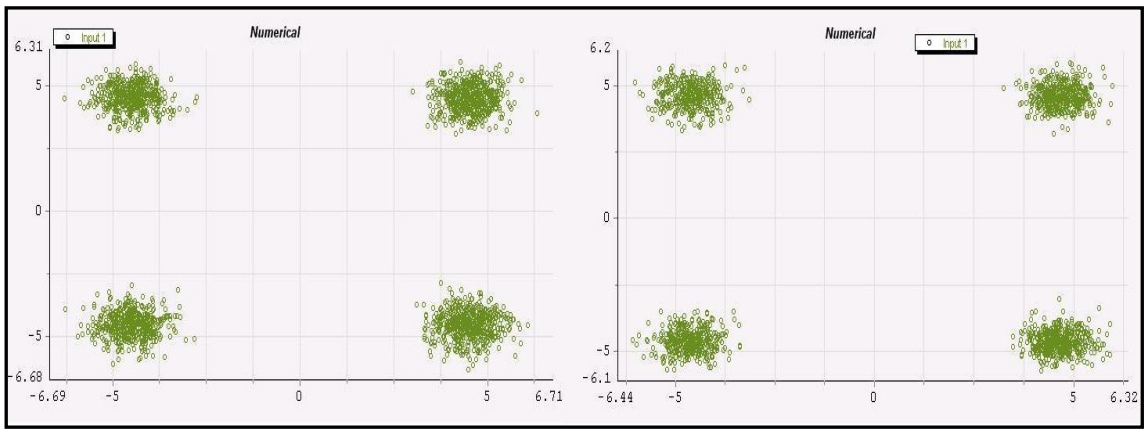

Fig.IV.41 Constellation with zero padding: without (left) and with (right) CP [VPI]

This configuration allows a slight improvement in the calculated EVM, giving a value of 0.112 at the cost of reduced transmission efficiency.

If a CP of 20% is added to this configuration, the best value of EVM is achieved: 0.095, though less than 30% of the bits are used to represent information.

Note that fewer points are represented as more overheads are used. This is because the OFDM coder discards information bits in order to allocate the desired CP and zero padding quantity, as explained in section IV.1.

The following figure represents the received constellation diagrams for two different link distances. In the left side, the constellation after a 500 km transmission is shown, while in the right graph the OFDM signal has been transmitted over a 2000 km loop.

In the used configuration, oversampling and a CP of 10% have been applied. The phase shifts due to the selected reference frequency are not compensated.

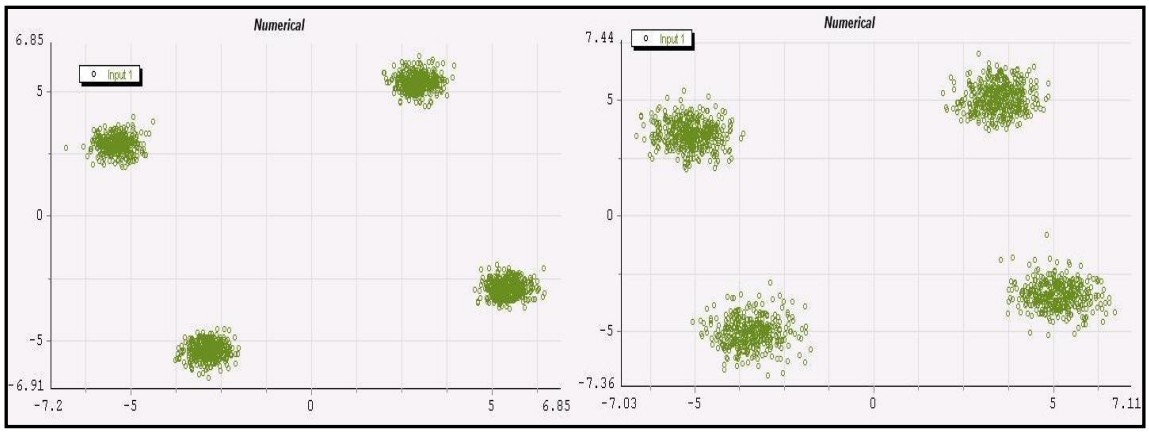

Fig. IV.42 Received constellations for 500 km (left) and 2000 km (right) [VPI]

Although the phase shift is not compensated, the EVM value is worse as the distance increases, and less dispersion can be appreciated by looking at the graphs. In this case, EVM values are 0.076 for 500 km and 0.131 for 2000 km.

CHAPTER V – CONCLUSIONS AND FUTURE LINES

V.1. Conclusions

In this Master Thesis, a revision of basic concepts regarding orthogonal frequency division multiplex (OFDM) has been carried out. The goal of this study has been the adaptation of these concepts into the special characteristics offered by optical systems.

Thus, the following step has been to study the most relevant features of optical communications, such as the type of modulation and demodulation systems and the optical filter and fibre parameters.

Some of these concepts are not usually referred in the current bibliography of optical OFDM, though they are the basis for creative contributions to the subject. Hence, this has been the main reason why the first two chapters of this document have been dedicated to highlight the main aspects concerning the use of OFDM in optical transmissions, hoping that they serve as a reference for future studies of the subject.

The different combinations of electrical generation of the OFDM signal and the optical modulation and reception categories give rise to several transmission systems able to implement an optical OFDM communication. The most relevant ones for this work's purpose have been described in detail before introducing the simulation environment.

The software Virtual *Photonics Inc. - Transmission Maker* (VPI) has been used as the tool to contrast all the acquired knowledge on optical OFDM in a simulation scenario. Two built-in demonstration simulations offered by VPI have been tested in order to understand the role of each parameter within the system and the effects resulting from changing their value.

However, after several tests some limitations have been observed. This has been the reason why new simulation scenarios have been developed in order to overcome these limitations. Previously, an introduction to the simulation environment offered by VPI has been done, emphasizing the required techniques to create a customized simulation.

For that purpose, a Matlab code implementing the OFDM coder and decoder functions has been programmed and implemented in VPI to execute the modulating and demodulating functions for the OFDM signal in the optical OFDM system.

Two different simulation scenarios have been created to implement the same functions as the VPI demos. This time, though, the transparency of the customized modules allows the user to fully explore and understand the working principle of the system in order to relate them with the theoretical concepts described in the first chapters.

Different tests on the customized simulation scenarios have allowed to select the optimum parameters in order to obtain the desired results.

The theoretical model for the optical channel considering chromatic dispersion as the most relevant effect has proven to be a useful approximation to design an equalizer for the custom simulations and to understand the role played by the reference frequency parameter in the fibre simulator's model in order to make a good choice for its value.

Moreover, some modifications with respect to the coding and decoding functions of the VPI demos have been applied to correct the observed limitations.

One of the main improvements that have been achieved with the realization of our own simulation scenarios is to see the effect of adding a cyclic prefix relative to an OFDM symbol into the transmitted sequence.

This effect could not be seen in the simulation results offered by the VPI demos, but after a methodical study it has been observed that the chromatic dispersion inherent to the fibre requires a different procedure for the cyclic prefix extraction at the decoder.

This modification has been applied on the customized simulations, and it has been checked that the addition of cyclic prefix provides the expected results. The Accordance project has been interested in this strategy, implementing it on their studies and simulations.

Moreover, the oversampling technique has been implemented in the coder functions by means of zero padding the central positions of the IFFT input sequence. This technique was not applied in the demos, and allows the use of conventional filters in a practical OFDM system.

V.2. Future lines

As future lines, the work carried out in this project can be continued by applying the optical OFDM concepts in other kinds of systems, such as multiuser environments.

Also, some modifications can be included at a lower level in the optical modulation scheme, for instance by using an IQ MZM or coherent detection at the receiver.

Another option to consider is to continue improving the customized simulations presented in this Master Thesis. As ideal equalization has been used to compensate for the phase errors at the receiver, one of the proposed improvements is to use a training sequence with pilot subcarriers in the OFDM symbols in order to compensate for these errors.

Moreover, other configurations can be implemented for the optical system scenarios presented in Chapter IV, for instance the use of zero padding to generate the frequency gap (already implemented in the Matlab code) to avoid using the upconversion and downconversion stages.

Currently, a practical implementation of an optical OFDM system is under way in the TSC Optical Communications Group Labs. The obtained results from the simulations performed in this work have also contributed to its development.

REFERENCES

Books

[B1] William Shieh and Ivan Djordjevic, *Orthogonal Frequency Division Multiplexing for Optical Communications* (1st edition, 2010)

[B2] Godvind P. Agrawal, *Nonlinear fiber optics* (1st edition, 1989)

[B3] Eduard Bertran Albertí, *Procesado digital de señales: Fundamentos para comunicaciones y control – II* (1st edition, 2006).

[B4] Richard Van Nee and Ramjee Prasad, *OFDM for wireless multimedia communications* (1st edition, 2000)

[B5] Ye Li and Gordon L. Stüber, *Orthogonal Frequency Division Multiplex for Wireless Communications* (1st edition, 2006)

[B6] Edward A. Lee and David G. Messerschmitt, Digital Communication (2nd edition, 1999)

[B7] A. Artés Rodríguez (et al), "Comunicaciones Digitales", ed. Pearson Prentice Hall, 2007

[B8] John G. Proakis and Dimitris G. Manolakis, *Digital Signal Processing: Principles, Algorithms, and Applications* (3rd edition, 1996).

Papers and tutorials

[P1] Jean Armstrong, *OFDM for Optical Communications* (Journal of Lightwave Technology, vol. 27, 2009)

[P2] Fred Buchali, Roman Dischler and Xiang Liu, *Optical OFDM: A Promising High-Speed Optical Transport Technology* (Bell Labs Technical Journal, 2009)

[P3] Louis Litwin and Michael Pugel, The *principles of OFDM* (RF Signal Processing Magazine, 2001)

[P4] Sander L. Jansen, *SC341 OFDM for Optical Communications* (Short Course OFC, 2010)

[P5] Wang Hongwei, FFT Basics and Case Study using Multi-Instrument (Virtins Technology, 2009)

[P6] Arthur Lowery and Jean Armstrong*, Adaptation of OFDM to Compensate Impairments in Optical Transmission Systems* (Monash University, 2007)

[P7] Arthur Lowwery, Du L. and Jean Armstrong, *Orthogonal frequency division multiplexing for adaptive dispersion compensating in long haul WDM systems* (Opt. Fiber Commun. Conf., 2006)

[P8] I.B. Djordjevic and B. Vasic, *Orthogonal frequency division multiplexing for high-speed optical transmission* (Optics Express, 2006)

[P9] D.F. Hewitt, *Orthogonal frequency division multiplexing using baseband optical single sideband for simpler adaptive dispersion compensation* (Opt. Fiber Commun. Conf., 2007)

[P10] W.R. Peng, . Wu, V.R. Arbab et al., *Experimental demonstration of a coherently modulated and directly detected optical OFDM system using an RF-tone insertion* (Opt. Fiber Commun. Conf., 2008)

[P11] W.R. Peng, . Wu, V.R. Arbab et al., *Experimental demonstration of 340 km SSMF transmission using a virtual single sideband OFDM signal that employs carrier suppressed and iterative detection techniques* (Opt. Fiber Commun. Conf., 2008)

[P12] Arthur Lowery, L.B. Du and Jean Armstrong, *Performance of optical OFDM in ultralong-haul WDM lightwave systems* (Journal of Lightwave Technology, 2007)

[P13] B.J. Schmidt, Arthur Lowery and Jean Armstrong, *Experimental Demonstrations of Electronic Dispersion Compensation for Long-Haul Transmission Using Direct-Detection Optical OFDM* (Journal of Lightwave Technology, 2008)

[P14] Ivan B. Djordjevic, *PMD compensation in fiber-optic communication systems with direct detection using LDPC-coded OFDM* (Optics Express, 2007)

[P15] J. Zhang et al., *A novel automatic PMD compensation scheme based on DSP in optical fiber communication systems* (IEEE International Conference on Information, Communications and Signal processing, ICICS 2009)

[P16] J.M. Kahn and J. R. Barry, *Wireless infrared communications* (Proc. IEEE, vol 85, 1997)

[P17] Jean Armstrong, Brendon J.C. Schmidt, Dhruv Kalra, Himal A. Suraweera and Arthur J. Lowery, *Performance of Asymmetrically Clipped Optical OFDM in AWGN for an Intensity Modulated Direct Detection System* (Monash University, 2007)

[P18] Charan Langton, *Orthogonal Frequency Division Multiplex (OFDM) tutorial* (Intuitive Guide to Principles of Communications, 2004)

[P19] C. Liu and F. Li, "*On spectrum modeling of OFDM signals for digital broadcasting*", in Proc. ICSP, 2004, pp. 1886–1889.

[P20] S. Talbot and B. Farhang-Boroujeny, "*Spectral Method of Blind Carrier Tracking for OFDM*", IEEE transactions on signal processing, vol. 56-7, 2008.

[P21] M. Ivrlac and J. Nossek, "*Influence of a Cyclic Prefix on the Spectral Power Density of Cyclo-Stationary Random Sequences*", ed. Springer, Multi-Carrier Spread Spectrum, 2007.

Websites

[W1] Wikipedia

[W2] EE Times: http://www.eetimes.com/electronics-news/4139996/IEEE-802-11a--Speeding-Up-Wireless-Connectivity-in-the-Home

[W3] Blinkdagger (Matlab blog): http://blinkdagger.com/matlab/matlab-fft-and-zero-padding/

[W4] Wikitel http://es.wikitel.info/wiki/OFDM

[W5] Intuitive Guide to Principles of Communications: http://www.complextoreal.com/

[W6] VPI Photonics official website: http://www.vpiphotonics.com/

ACRONYMS

- ADC - Analogue-to-digital converter
- ASE - Amplified spontaneous emission
- BER – Bit error rate
- CO-D - Coherent detection
- CP - Cyclic prefix
- DAC - Digital-to-analogue converter
- DD- Direct detection
- DFT - Discrete Fourier transform
- DMT - Discrete multitone
- DTFT - Discrete-time Fourier transform
- EVM - Error vector magnitude
- FDM - Frequency division multiplexing
- FFT – Fast Fourier transform
- GDD - Group Delay Dispersion
- GUI - Graphical user interface
- ICI – Intercarrier interference
- IDFT - Inverse discrete Fourier transform
- IF - Intermediate frequency
- IFFT - Inverse fast Fourier transform
- IM - Intensity modulation
- ISI - Inter-symbol interference
- LO – Local oscillator
- MZM - Mach-Zehnder modulator
- OFDM – Orthogonal frequency division multiplexing
- OSSB – Offset single sideband
- PEW - Parameter editor window
- PRBS - Pseudo-random bit sequence
- QP - Quadrature point
- SER - Symbol error rate
- SSB - Single sideband
- QAM – Quadrature amplitude modulation
- VPI - Virtual Photonics Inc.

Escola Politècnica Superior de Castelldefels
UNIVERSITAT POLITÈCNICA DE CATALUNYA

ANNEXES

TITLE: Fiber-based Orthogonal Frequency Division Multiplexing Transmission Systems

MASTER DEGREE: Master in Science in Telecommunication Engineering & Management

AUTHOR: Eduardo Heras Miguel

DIRECTOR: Concepción Santos Blanco

DATE: October 27th 2010

INDEX

ANNEX A: INSIGHT INTO THE OPERATION OF AN OFDM SYSTEM

In Chapter I it has been said that the output of an IFFT operation results in an approximately bandlimited signal s(t), consisting of sinusoids of the baseband subcarrier frequencies. Because of the nature of this procedure, this signal will consist of both real and imaginary components [P3], which in wireless OFDM systems results in a complex signal feeding an IQ modulator for upconversion to the carrier frequency.

On the other hand, in baseband systems such as ADSL, s(t) is a real signal, so the input vector to the IFFT is constrained to have Hermitian symmetry. By using this technique, the imaginary component of the IFFT output is canceled.

Because the IFFT simultaneously performs modulation and multiplexing, there is no point in the transmitter or receiver where an individual time domain subcarrier can be observed, as they are only present in the frequency domain. Still, in a linear channel this approach would be very useful to describe the overall system, hence a single subcarrier will be tracked through the processing of the IFFT operation for some different cases, so it can be seen how to achieve Hermitian symmetry for baseband systems. In order to simplify the explanation, only one symbol will be considered, without the use of cyclic prefix (CP).

Also from Chapter I, it can be deduced that the *m*th discrete time domain component associated with the *k*th subcarrier of a given OFDM symbol is

$$x_m = \frac{1}{\sqrt{N}} c_k exp\left(\frac{j2\pi km}{N}\right) \quad \text{for} \quad 0 \leq m \leq N-1 \qquad \textbf{(A.1)}$$

Thus, fixing values for the symbol c_k and the number of subcarriers N, the discrete signal can be plotted for each subcarrier *k*. A symbol value of $c_k = 1$ for 32 subcarriers has been chosen in [P1] to represent individual discrete time domain subcarriers, as it can be seen on Figures A.1 and A.2, where the real and imaginary components of the OFDM signal are represented in the upper and lower parts of each graph, respectively.

For k = 0 (the top subcarrier in the parallel inputs of the IFFT), the samples have a constant value. This can be easily deduced from Expression A.1, where the exponential will not change its value through any discrete index *m*. This will represent the DC term in the baseband signal and the component at the carrier frequency in wireless and optical systems, where the OFDM signal is upconverted to a higher frequency.

For k = 1, the sequence represents the samples of one cycle of a sinusoid of frequency $1/T_s$, where T_s is the symbol period not considering the CP. For k = 2, the (baseband) frequency has been doubled and the samples now give two cycles of a sinusoid.

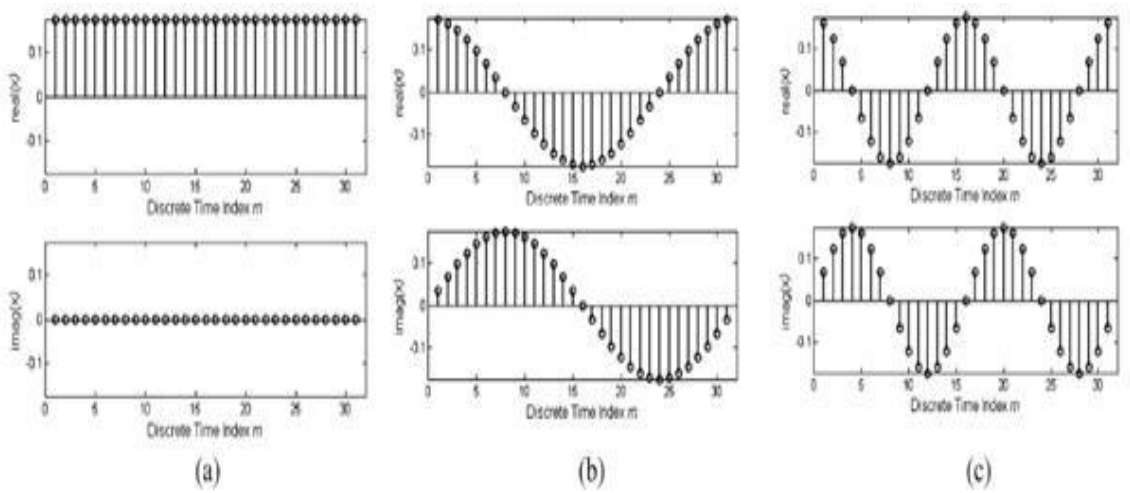

Fig. A.1 Discrete time domain signal for individual subcarriers for (a) k = 0, (b) k = 1 and (c) k = 2 [P1]

It can also be observed that the imaginary component has a constant phase delay over the real one, which will be the key to eliminate it from the signal so a real valued signal can be transmitted.

Because of the circular property of the FFT and IFFT [P1], the represented sinusoid will increase its number of cycles for each subcarrier (increasing *k*) until the *N/2*th term (also called the Nyquist term, where the signal is critically sampled). From there, the number of cycles starts decreasing until one cycle for the last subcarrier (k = N - 1). Such property is represented in figure A.2:

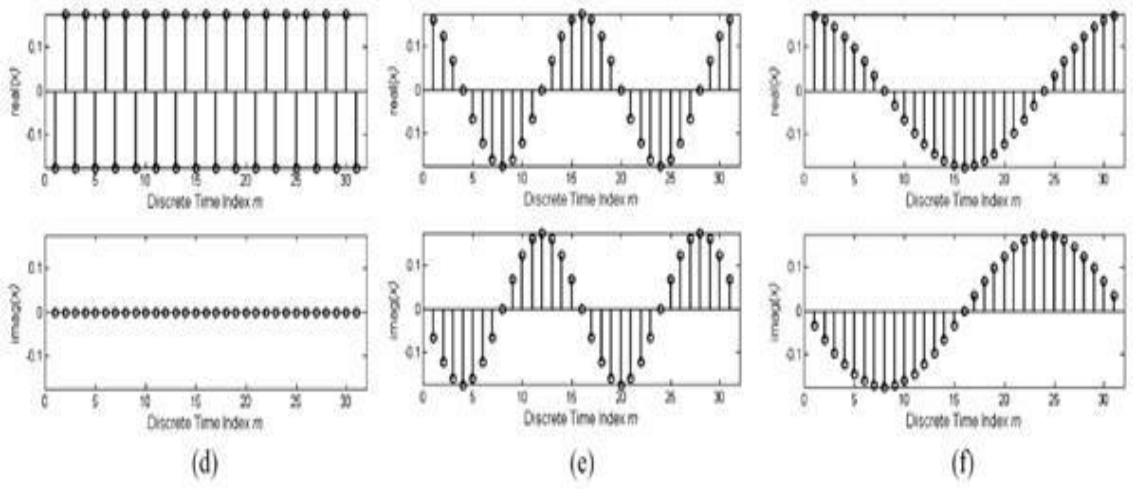

Fig. A.2 Discrete time domain signal for individual subcarriers for (d) k = N/2 (Nyquist term), (e) k = N-2 and (f) k = N-1 [P1]

In mathematical analysis, a Hermitian function is a complex function with the property that its complex conjugate is equal to the original function with the variable changed in sign:

$$f(-x) = \overline{f(x)} \quad \textbf{(A.2)}$$

For all x in the domain of *f*. This definition extends also to functions of two or more variables. For instance, in the case that *f* is a function of two variables, it will be Hermitian as long as:

$$f(-x_1, -x_2) = \overline{f(x_1, x_2)} \quad \textbf{(A.3)}$$

For all pairs (x_1,x_2) in the domain of *f*. Taking this and the basic properties of the Fourier transform, it follows that:

- The function *f* is real-valued if and only if the Fourier transform of *f* is Hermitian
- The function *f* is Hermitian if and only if the Fourier transform of *f* is real-valued

Now, knowing that in a complex valued IFFT the first half of the rows corresponds to the positive frequencies while the last half corresponds to negative frequencies, it can be deduced that Hermitian symmetry will be achieved by inserting the complex conjugate of the first half of the IFFT rows into the second half, as depicted in Figure A.3:

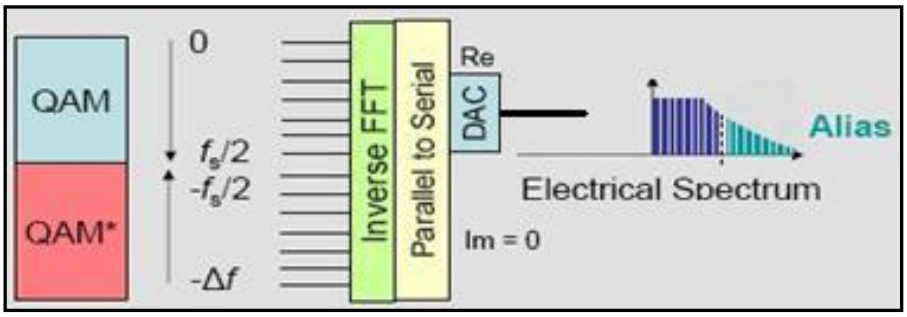

Fig. A.3 Use of Hermitian symmetry at the IFFT input sequence [P6]

This way, the imaginary component is cancelled and the output values of the IFFT will represent a real-valued OFDM signal.

ANNEX B: CYCLIC PREFIX EFFECT ON THE OFDM SIGNAL SPECTRUM

One answer to the question “What’s the cyclic prefix used for?” could be: to “deceive” the channel. Evidently, a linear convolution operation is carried out in the channel; however, a circular convolution would be of more interest, because this would provide a purely multiplicative effect in the transformed domain, eliminating inter-carrier interference (ICI), as explained in [B7].

Apart from that, the cyclic prefix incorporation avoids block to block (or OFDM symbol) interferences, which means null inter-symbol interference (ISI). As long as the cyclic prefix duration is equal or longer than the channel’s impulse response, the effect of one block over the previous one will be limited to its cyclic prefix corruption, without damaging the information part. The introduction of any temporal guard interval would achieve this null ISI characteristic, but only the cyclic prefix can guarantee null ICI.

However, this elegant way of avoiding ISI comes, of course, at the price of reduced bandwidth efficiency, since the cyclic prefix adds redundancy to the signal. Besides this loss in efficiency, the cyclic prefix is responsible for another loss in performance, because it also affects the spectral power density of the transmitted signal, such that a ripple is introduced inside the main frequency band, as shown in one of the simulated results depicted in Figure B.1:

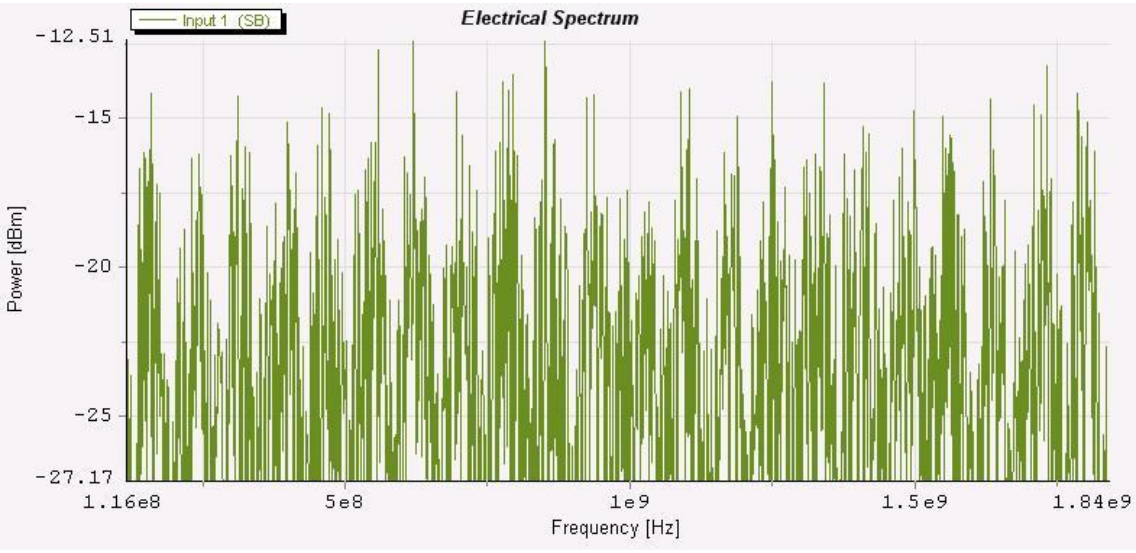

Fig. B.1 Zoomed ripple in the OFDM band for a high quantity of CP [VPI]

This ripple is originated due to an increase of the temporal duration of the transmitter functions when using CP: the sincs forming the OFDM spectrum are narrower in frequency than before, so their maximums don’t match up exactly with their neighbours’ nulls and the resulting spectrum is not plain any more, but it suffers from rippling.

In [P19] it is mathematically demonstrated that the power spectrum density (PSD) of an OFDM subcarrier is only affected by the symbol rate and the pulse shaping window, no matter what other parameters are in the system.

Thus, a single subcarrier's PSD can be plotted as a function of different OFDM symbol lengths (T) in number of samples, as it is done in Figure B.2. Note that as T increases, the spectrum becomes narrower.

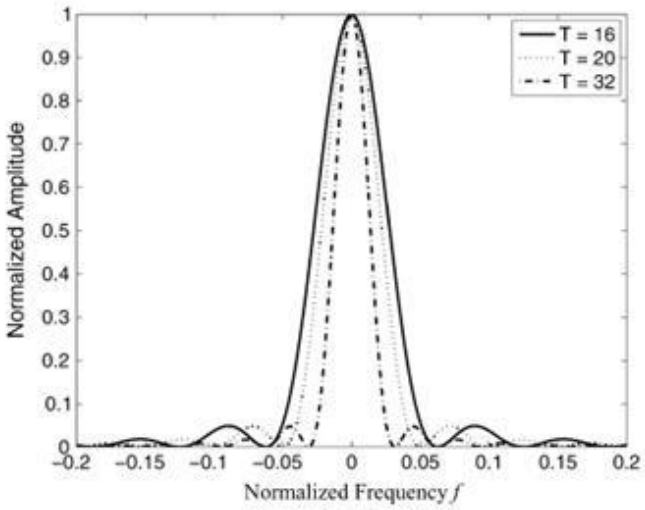

Fig. B.2 Subcarrier PSD for different symbol periods [P20]

If T is increased by increasing the cyclic prefix length with a fixed IFFT size N, the subcarrier spacing remains constant. Taking this into account, since the individual subcarrier spectrum decreases in width, an increase in the cyclic prefix length induces ripples with larger amplitudes in the in-band region of the OFDM PSD. This is shown in the next figure for the cases where the cyclic prefix length C takes values of 0, 4 and 16 samples.

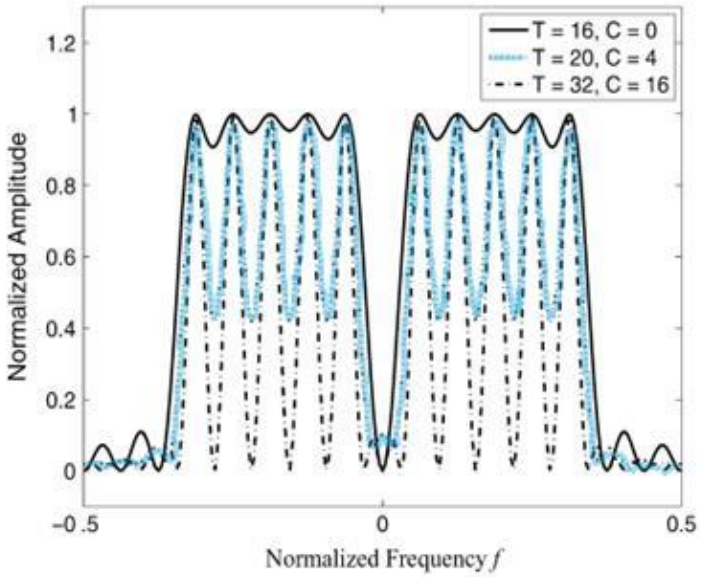

Fig. B.3 OFDM PSD for different symbol periods T and CP length C [P20]

This ripple may require a reduction of the transmitted power in order to obey regulatory spectrum masks, that is, the transmitted power cannot be made as large as it potentially could, because of the “overshoot” in the power density. This power reduction may lead to a loss in the signal to noise ratio at the receiver, since the transmitted power usually has to stay inside regulatory spectrum masks.

On the other hand, in [P20] a spectral method of carrier tracking is presented, where the mentioned ripple is used in order to provide an estimate of the carrier offset.

ANNEX C: DIRECT DETECTION OPTICAL OFDM TRANSMITTER CONFIGURATIONS

Many different transmitter configurations can be designed for a DD-OOFDM system depending on the subcarrier modulation, input sequence of the IFFT, complexity of the used components, etc. In [P6], various experimental demonstrations have been performed, giving rise to four basic transmitter configurations that mainly depend on the input sequence of the IFFT. Thus, each transmitter will have different degrees of optical complexity depending on the required components, though a single photodiode DD photoreceiver is used in all the scenarios, so no laser is required. A colourless transmitter is also introduced, where there is no need of optical filter to suppress one optical sideband. The CP insertion is not considered in the figures, but it should be added to all of them at the output of the IFFT, before the data serialization.

In all of the upcoming scenarios, an optical single sideband (OSSB) OFDM signal and a component at the optical carrier frequency are transmitted. Usually, a frequency guard band separates the OFDM signal from the optical carrier, and the signal is received by detecting the carrier signal mixing products described in Chapter II.

To provide the optimum noise performance, the transmitter optical modulator should be biased for equal carrier and sideband powers as this provides the peak electrical SNR and lowest BER for a given OSNR.

C.1. Real drive signal

This is a simple configuration, where half of the input sequence of the IFFT is formed by the QAM symbols, and the other half are the conjugates of each of the symbols. As explained in Annex A, this technique is called the Hermitian symmetry and provides a real valued OFDM signal that will be formed after a serialization of the IFFT outputs and the subsequent digital to analogue conversion. Figure C.1 shows the transmitter scheme.

Note that only one DAC is needed after the data serialization, as the imaginary component of the signal has been removed due to the Hermitian symmetry technique.

The resulting electrical spectrum is shown as in inset in figure C.1. Because no zero padding has been used, there is no gap between the DC component (0 Hz frequency) and the OFDM subcarriers, and the alias is very close to it. The following configurations may suffer one of these problems, but not both at the same time.

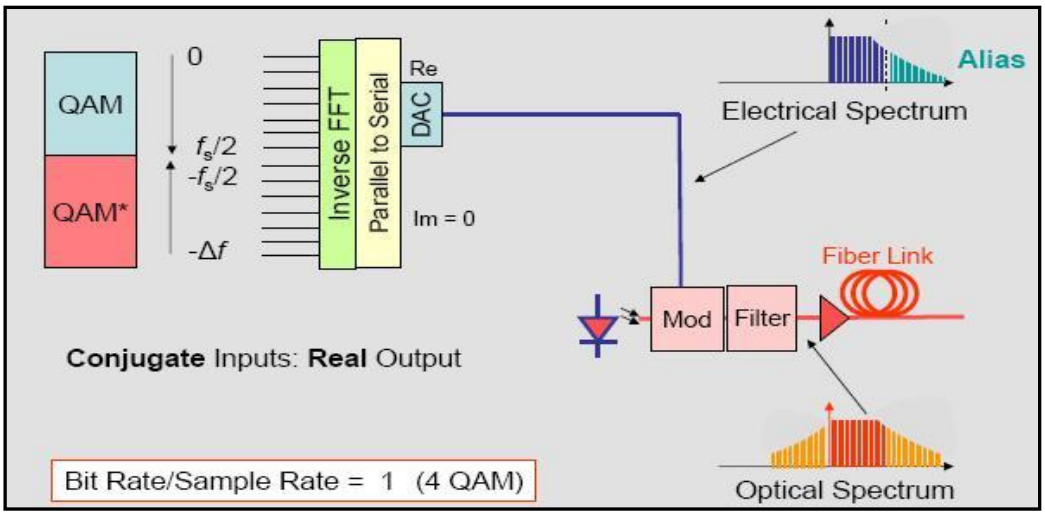

Fig. C.1 Real drive signal configuration [P6]

A single input optical modulator is used to generate a double sideband optical signal, and then an optical filter is used to suppress one of the two optical sidebands. The resulting optical signal (lower inset in figure C.1) is transmitted to the fibre link.

C.2. Trigonometric interpolation (oversampling)

This configuration is similar to the previous one, as it uses the conjugate of the input symbol sequence of the IFFT to form a real valued OFDM signal. In this case, though, zero padding is used in the middle of the sequence to shift the alias away from the useful signal, as depicted in figure C.2:

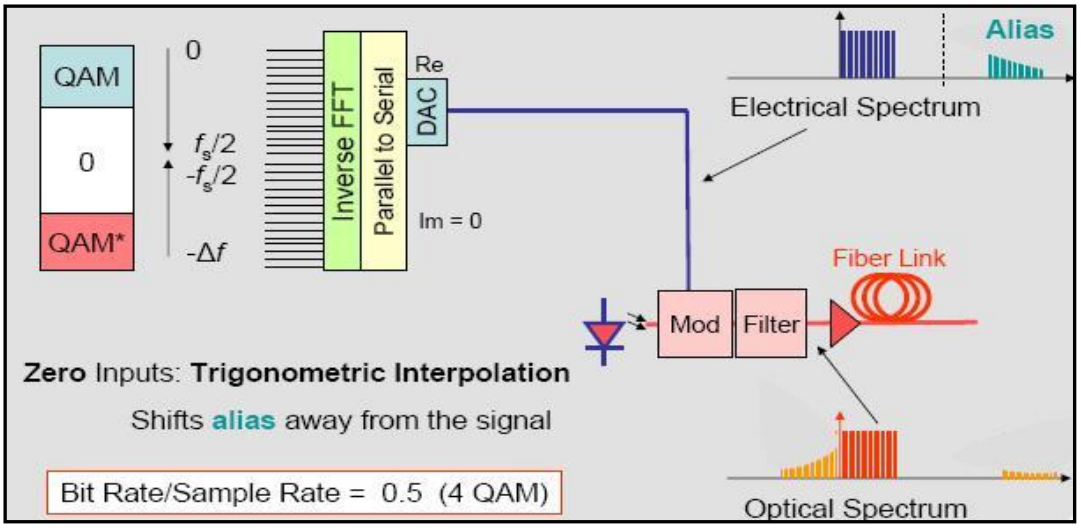

Fig. C.2 Trigonometric interpolation configuration [P6]

As explained in Chapter I, this technique can be translated into a trigonometric interpolation in the discrete time domain, achieving a narrower spectra for the signal and its aliases and thus allowing the use of cheaper filters for a real system. Note that the bit per sample rate has been halved with regard to the previous configuration, as usually half of the input IFFT sequence is used for zero padding.

C.3. Band shifted from DC

The purpose of this configuration is to create a gap between the DC component and the OFDM subcarriers, so that the unwanted mixing products generated due to the square law detection of the photodiode at the receiver fall on it, as described in Chapter II. This is achieved by using the same quantity of zero padding as in the trigonometric interpolation configuration, though this time the zeros are not inserted in the middle of the IFFT input sequence but at its edges, as shown in figure C.3.

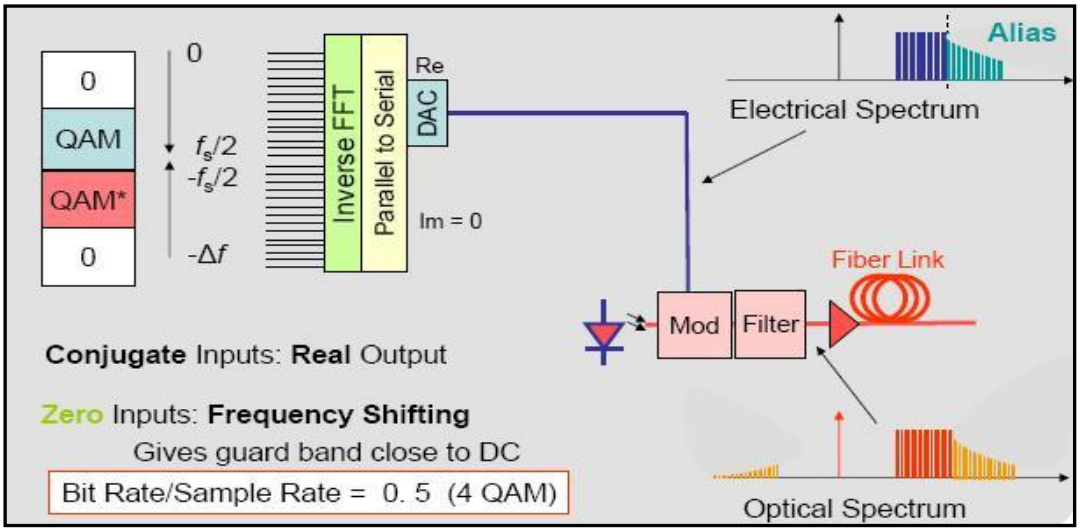

Fig. C.3 Band shifted from DC configuration [P6]

The remaining half of the input sequence is formed by the QAM symbols and their conjugates to achieve a real OFDM signal at the DAC output. As in the real drive configuration, the alias is close to OFDM spectra because there are no zeros in the middle of the IFFT sequence. However, it is common to set the IFFT input corresponding to the Nyquist frequency to zero. In a vector of N inputs ranging from X_0 to X_{N-1}, the Nyquist frequency would correspond to the $X_{N/2-1}th$ input, representing the highest frequency component.

If the guard band width is equal to the bandwidth used for the OFDM signal, then only N/4 independent complex values can be transmitted per OFDM symbol. This means that only 128 data subcarriers can enter a typical IFFT stage consisting of 512 points.

Again, a single input optical modulator and an optical filter are used before transmitting the signal into the fibre link.

C.4. RF upconversion

This time, the gap between the DC component and the OFDM subcarriers is created through a frequency upconversion stage previous to the e/o conversion. This allows the complex baseband OFDM signal to be mixed with an RF carrier before driving the single input optical modulator, though another DAC is required after the IFFT output serialization stage. Because of the frequency upconversion, there is no need to use Hermitian symmetry to cancel the imaginary component of the signal, so one DAC is needed to process the real part of the OFDM signal and another for the imaginary part (that is, inphase and quadrature, respectively). Figure C.4 shows the scheme for this configuration:

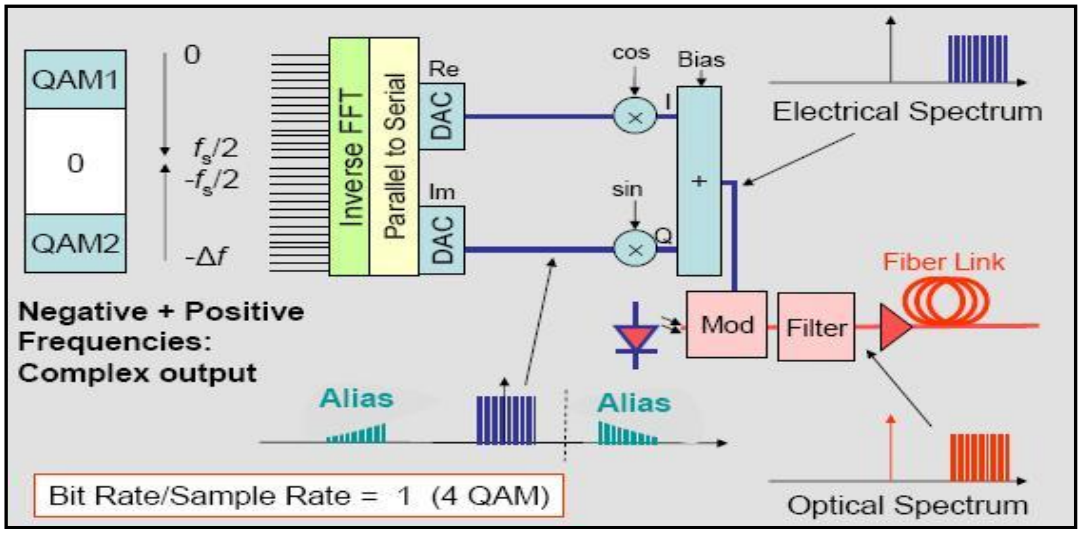

Fig. C.4 RF upconversion configuration [P6]

Thus, the width of the guard band is not determined by nulling the OFDM inputs, but by the RF frequency, and so all subcarriers except the dc subcarrier can be used to carry data if the DAC filter is good enough. However, in the scheme depicted in figure C.4, trigonometric interpolation is used in order to shift the alias away.

The analogue upconversion allows flexible placement of the signal spectrum relative to the optical carrier and the RF frequency is independent of the DAC sample rate. As in the previous designs, an optical filter is used to suppress one sideband. For a given data rate, this design requires a DAC sample rate of approximately one quarter that of the first design, but the addition of analogue mixers with such high frequency and bandwidth requirements could cause problems with frequency synchronization and inphase (I) and quadrature (Q) balance in a real system.

As this is the configuration that has been performed in the simulations presented in Chapter IV, it is interesting to know the theoretically expected form of the spectra at each point, so it can be compared with the experimental results. From left to right, Figure C.5 shows the obtained spectra at the following points of the scheme:

1. Baseband OFDM signal and its aliases after the DACs. The dotted line represents the subsequent RF filtering used to remove images
2. OFDM signal after the RF upconversion stage
3. Filtering the optical lower sideband after the e/o conversion

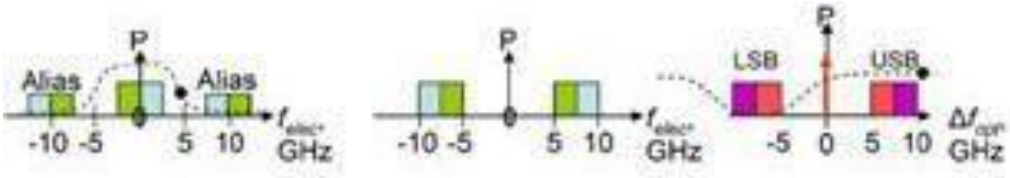

Fig. C.5 Spectra at each point of the scheme [P6]

C.5. Colourless transmitter

Another option would be to use the scheme depicted in figure C.6, where a complex IQ modulator is the input of the I and Q components of the OFDM signal. Only one optical single sideband is generated by using a signal and its Hilbert transform to drive the optical I/Q modulator.

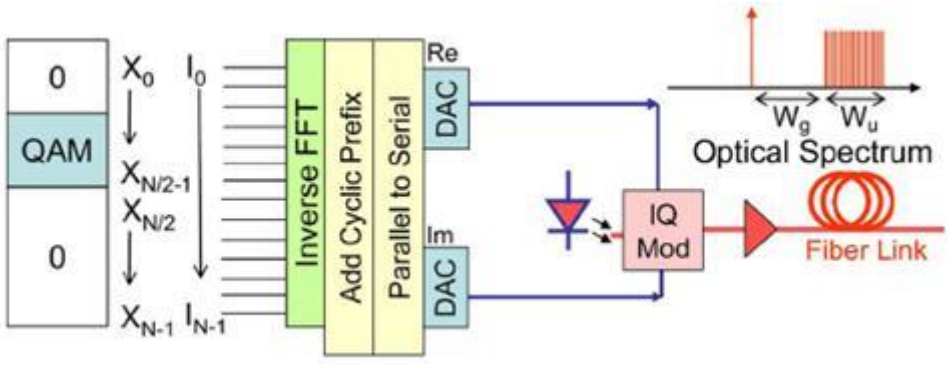

Fig. C.6 Colourless transmitter configuration [P6]

A Hilbert transform can be generated simply in an OFDM transmitter, by setting half of the IFFT inputs to zero. In this case the input vector to the IFFT is given by $I_0 \dots I_{N-1} = X_0 \dots X_{\frac{N}{2}-1}, 0 \dots 0$. The IFFT output is then a single sided, analytic signal and its real and imaginary components are used for the I and Q inputs of the complex optical modulator for OSSB transmission without an optical filter.

Here, the frequency guard band is created by setting the corresponding inputs to zero. This design requires two DACs, each with the same sample rate as the Band shifted from DC design in section C.3.

ANNEX D: MATLAB CODE

D.1. OFDM coder

```
% OFDM coder

function[y]=ofdm_coder(prbs,TimeWindow,BitRate,BpS,Nc,N_FFT,CP)


%%%INPUT VARIABLES

% x Number of prbs bits, x1 Data input vector
% length(x)=Time window* Bitrate. It must be an integer multiple of
BpS
% N_FFT number of total carriers (for FFTs). It must be a power of two
% Nc number of info carriers (N_FFT-ZP). It must be an integer
multiple of 2 because half of the zeros are located in the middle of
the input sequence of the IFFT (Oversampling)
% BpS Bits per symbol (QAM)
% CP Cyclix prefix


%Global variables are defined

%NTS_OFDM NTS_INFO NTB_INFO Ignore_Bits;

%%%%% x1=prbs(x);
x1=prbs(1:TimeWindow*BitRate);

% identify the info bits to send and how many to discard

NTS_OFDM=floor(length(x1)/(BpS*ceil(N_FFT*(1+CP)))); %Total number of
OFDM symbols

NTS_INFO=NTS_OFDM*Nc; %Total number of QAM inforamtion symbols

NTB_INFO=NTS_INFO*BpS; %Total number of information bits

NTS_ZP=(N_FFT-Nc)*NTS_OFDM; % Total number of symbols due to zero
padding

NTS_CP=NTS_OFDM*ceil(N_FFT*CP);% Total number of symbols due to CP

NTS_casados=NTS_INFO+NTS_ZP+NTS_CP;% Total number of symbols to
transmit. Ideally it should be TimeWindow*BitRate/BpS, but it may not
cover the whole sequence

xx1=x1(1:NTB_INFO) % Vector containing the information bits to
transmit

% The QAM symbol sequence is built with the information bits to
transmit(a vector xx1_QAM of size NTS_INFO)
```

```
    xx1_QAM=qammod(bi2de(reshape(xx1,BpS,NTS_INFO)'),2^BpS)

% The OFDM INFO symbol sequence is built with the previous QAM
sequence

    xx1_OFDM_INFO=reshape(xx1_QAM,Nc,NTS_OFDM)
% Zero padding is inserted to obtain a matrix of size (N_FFT x
NTS_OFDM)

    if(mod(N_FFT,2)== mod(Nc,2))

        %xx1_OFDM_ZP=[zeros((N_FFT-
Nc)/2,NTS_OFDM);xx1_OFDM_INFO;zeros((N_FFT-Nc)/2,NTS_OFDM)] %Gap
generation by means of zero padding
        xx1_OFDM_ZP=[xx1_OFDM_INFO(1:Nc/2,:);zeros(N_FFT-
Nc,NTS_OFDM);xx1_OFDM_INFO((Nc/2)+1:Nc,:)] % Oversampling

    else
        disp('Both N_FFT and Nc must be even or odd integers')
    end

% IFFT is applied

    xx1_IFFT=ifft(xx1_OFDM_ZP,N_FFT)

%     %border ofdm symbols change to zero
%
%      mk=diag([0, zeros(1,NTS_OFDM-2), 0 ]);
%
%      xx1_IFFT=xx1_IFFT*mk;

% Cyclic prefix is added to each OFDM symbol

    xx1_CP=[xx1_IFFT(1+N_FFT-ceil(N_FFT*CP):N_FFT,:);xx1_IFFT]

     y=[(xx1_CP(:).'),zeros(1,((TimeWindow*BitRate/BpS) -
NTS_casados))]; % As the effective bitrate will be smaller than the
original bitrate (if ZP or CP have been used)we add zeros to
compensate for this bitrate difference(TimeWindow*BitRate/BpS -
NTS_casados)


    if ((NTB_INFO/(BpS*Nc))*ceil(N_FFT*(1+CP))==length(y))% test of
symbol rate before and after IFFT

        disp('CHECK OK')

    else

        disp('CHECK NOK')

    end

% (Upsampler * LPF in VPI )
% y is a complex number
```

D.2. OFDM decoder

```
%OFDM decoder z=ofdm_decoder(y,BpS,Nc,N_FFT,CP)

function [I Q I_EVM Q_EVM zz]=ofdm_decoder_simu
(y_real,y_imag,BitRate, TimeWindow,BpS,Nc,N_FFT,CP)

yrx=complex(y_real,y_imag);

NTS_OFDM=floor(length(yrx)/(ceil(N_FFT*(1+CP)))); %Total number of
OFDM symbols that it must be integer
NTS_QAM_CP=NTS_OFDM*ceil(N_FFT*(1+CP));
NTS_INFO=Nc*NTS_OFDM;
NTB_INFO=NTS_INFO*BpS; %Total number of information bits

NTS_ZP=(N_FFT-Nc)*NTS_OFDM;
NTS_CP=NTS_OFDM*ceil(N_FFT*CP);
NTS_casados=NTS_INFO+NTS_ZP+NTS_CP;


%yy1=adc(y,Qbits);
yy1=yrx(1:NTS_OFDM*ceil(N_FFT*(1+CP))) % Compensating seros are
extracted


%%%%%%%%%%%%%%%%%%%%%%%%%%%%%%%%%%%%%%%%%%%%%%%%%%%%%%%%%%%%%%%%%%%%%%%%%%%%%%%%
%%%%%%%%%%%%%%%%%%%%%%%%%%%%%%%%
%ADC
%yy1 is the parameter of analog signal
%Qbits indicates the paramater of number of quantification bits
%Qmax maximum level of input signal
%Qmin minimum level of input signal
%A amplification

Qbits=32;
QbitsQ=Qbits;
QbitsI=Qbits;
y_I=real(yy1);
y_Q=imag(yy1);

%REAL_PART%

QmaxI=max(y_I);
QminI=min(y_I);

DRI=QmaxI-QminI;

if DRI==0 %if input signal is a constant, the adc doesn't act
    dI=y_I;
else
    dqI=DRI/(2^QbitsI);
    FI= y_I-(floor(y_I/dqI))<(0.5);
    bI=[FI.*floor(y_I/dqI)+(1-FI).*ceil(y_I/dqI)];
    AI=2/(max(bI)-min(bI));

end
```

```
%IMAGINARY_PART%

QmaxQ=max(y_Q);
QminQ=min(y_Q);

DRQ=QmaxQ-QminQ;

if DRQ==0 %if input signal is a constant, the adc doesn't act
    dQ=y_Q;
else
    dqQ=DRQ/(2^QbitsQ);
    FQ= y_Q-(floor(y_Q/dqQ))<(0.5);
    bQ=[FQ.*floor(y_Q/dqQ)+(1-FQ).*ceil(y_Q/dqQ)];
    AQ=2/(max(bQ)-min(bQ));

end
A=median([AQ AI],2);
dI=bI*AI;
dQ=bQ*AQ;

%Plots
% figure()
% Subplot(1,2,1)
% plot(1:50,dI(1:ceil(N_FFT*(1+CP)))) %optional: draw the figure of a
quantificated OFDM symbol, real data
% Subplot(1,2,2)
% plot(1:50,dQ(1:ceil(N_FFT*(1+CP)))) %optional: draw the figure of a
quantificated OFDM symbol, imaginary data

yy1_adc=dI+(dQ.*i);

%ADC end
%%%%%%%%%%%%%%%%%%%%%%%%%%%%%%%%%%%%%%%%%%%%%%%%%%%%%%%%%%%%%%%%%%%%%%%%%%%%
%%%%%%%%%%%%%%%%%%%%%%%%%%%%%%%%%%%%

yy1=[yy1_adc(NTS_QAM_CP-
ceil(N_FFT*CP/2)+1:NTS_QAM_CP),yy1_adc(1:NTS_QAM_CP-
ceil(N_FFT*CP/2))];   % The last half CP is moved to the start of the
string
yy1_SP=reshape(yy1,ceil(N_FFT*(1+CP)),NTS_OFDM)%

yy1_CP=yy1_SP((ceil(N_FFT*CP)+1):size(yy1_SP,1),:)%CP symbols are
extracted
yy1_FFT=fft(yy1_CP,N_FFT) %The FFT is performed


% Zero Padding removal
%yy1_QAM=yy1_FFT((N_FFT-Nc)/2+1:size(yy1_FFT,1)-(N_FFT-Nc)/2,:)
yy1_QAM=[yy1_FFT(1:Nc/2,:);yy1_FFT((size(yy1_FFT,1)-
Nc/2)+1:size(yy1_FFT,1),:)]% Mod Edu

    %Equalization
        D=17e-6;  %Dispersion
        BW=5e9;   %Signal Bandwidth
        c=3e8;    %Speed of light
        frf=7.5e9 %Reference frequency
        L=1000e3; %Fibre link distance
        fo=193.1e12; %Optical carrier frequency
        lambda=c/fo; %Wavelength
```

```
       %Lowery_coefs=[-2.1203982e-001 -2.1805440e-001 -1.9621803e-001
-2.1203336e-001 -2.6253623e-001 -2.8899551e-001 -2.8514322e-001 -
3.3394620e-001 -3.7314924e-001 -4.0120419e-001 -4.2135611e-001 -
5.1788445e-001 -5.6894703e-001 -6.2998440e-001 -7.3253757e-001 -
7.8296186e-001 -8.9312601e-001 -9.5320192e-001 -1.0216461e+000 -
1.1529878e+000 -1.2464763e+000 -1.3586995e+000 -1.4649820e+000 -
1.5616805e+000 -1.6995038e+000 -1.8490457e+000 -1.9557745e+000 -
2.0796425e+000 -2.4095242e+000 -2.5301500e+000 -2.6837541e+000 -
2.7322297e+000 -2.8382730e+000 -2.8455154e+000 -2.7563871e+000 -
2.6329964e+000 -2.3774626e+000 -2.1575748e+000 -1.9194399e+000 -
1.7613838e+000 -1.6535138e+000 -1.5558741e+000 -1.4912738e+000 -
1.3888316e+000 -1.2861190e+000 -1.1495645e+000 -1.0487200e+000 -
9.3607302e-001 -8.4476346e-001 -7.6078367e-001 -7.2272519e-001 -
6.5489735e-001 -5.8596704e-001 -5.2277312e-001 -4.3974641e-001 -
4.0816652e-001 -3.5987323e-001 -3.3098928e-001 -3.0215140e-001 -
2.6586525e-001 -2.5848681e-001 -2.2973098e-001 -2.0955423e-001 -
2.1413641e-001]
       %ephase=exp(-(pi/4)*i).*exp(Lowery_coefs.*i)
       %ephase=exp(Lowery_coefs.*i)

        %ephase=exp((-(lambda^2)*D*pi*((5e9.*[0:(Nc/2)-1,-Nc/2:1:-
1]./Nc).^2)*L)*i/(4*c));
        %ephase=exp(-(pi/4)*i).*exp((-
(lambda^2)*D*pi*((5e9.*[0:(Nc/2)-1,-Nc/2:1:-1]./Nc).^2)*L)*i/(4*c));
        %ephase=exp(-((lambda)^2/c*D*pi*(7.5e9+(5e9.*[0:1:(Nc/2)-1,-
Nc/2:1:-1]./N_FFT)).^2)*L*i); % Ultima para fref =193
        ephase=exp(-(pi/4)*i)*exp(((lambda)^2/c*D*pi*
((BW.*[0:1:(Nc/2)-1,-Nc/2:1:-1]./N_FFT)).^2)*L*i); % For fref = 193.1
THz + 7.5 GHz
        ephase=ephase.*exp([0:1:(Nc/2)-1,-Nc/2:1:-
1]*i*2*pi*ceil((CP/2)*N_FFT)/N_FFT);
        %ephase=exp(-((lambda)^2/c*D*pi*(-2.5e9+(5e9.*[0:1:(Nc/2)-1,-
Nc/2:1:-1]./N_FFT)).^2)*L*i); %Eq con fref 193.1 THz +10 GHz
        %ephase=exp((-(lambda^2)*D*pi*((5e9.*[(Nc/2)-1:-1:0,Nc-1:-
1:Nc/2]./N_FFT).^2)*L)*i/c);
        %ephase=exp(-(pi/4)*i).*exp((-
(lambda^2)*D*pi*((5e9.*[0:(Nc/2)-1,-Nc/2:1:-1]./N_FFT).^2)*L)*i/c); %%
Mod Edu

      yy1_QAM=(diag(ephase)*yy1_QAM);
     %yy1_QAM=exp(1.6023e4*1000e3*i)*yy1_QAM;
    %fin eq

% parallel to serial

yy1_QAM_serial=yy1_QAM(:)

%I=real(yy1_preQAM);
%Q=imag(yy1_preQAM);

%I=[real(yy1_QAM_serial)',zeros(1,(BitRate*TimeWindow/BpS)-
length(yy1_QAM_serial))];
%Q=[imag(yy1_QAM_serial)',zeros(1,(BitRate*TimeWindow/BpS)-
length(yy1_QAM_serial))];
%Isalida=[I,zeros(1,BitRate*TimeWindow-length(I))];
%Qsalida=[Q,zeros(1,BitRate*TimeWindow-length(Q))];

I=real(yy1_QAM_serial)';
Q=imag(yy1_QAM_serial)';
I_EVM=[I(:)',zeros(1,(TimeWindow*BitRate/BpS)-length(I))]; % Para EVM
```

```
Q_EVM=[Q(:)',zeros(1,(TimeWindow*BitRate/BpS)-length(Q))]; % Para EVM

yy1_bits=de2bi(qamdemod(yy1_QAM_serial,2^BpS))' %Demodulation
z=yy1_bits(:)';%just output bits info
zz=[yy1_bits(:)',zeros(1,BpS*(length(yrx)-length(yy1_bits)))] %zero
padding to complete the starting size
```